Impacts of Climate Change on Wastewater Systems in Reykjavík

Ásta Ósk Hlöðversdóttir

Faculty of Civil and Environmental Engineering
University of Iceland

Impact of Climate Change on Wastewater Systems in Reykjavík

Ásta Ósk Hlöðversdóttir

60 ECTS thesis submitted in partial fulfillment of a
Magister Scientiarum degree in Environmental Engineering

Advisors
Brynjólfur Björnsson
Hrund Ólöf Andradóttir
Jónas Elíasson
Philippe Crochet

Faculty Representative
Gunnar Guðni Tómasson

Faculty of Civil and Environmental Engineering
School of Engineering and Natural Sciences
University of Iceland
Reykjavik, December 2010

Impacts of Climate Change on Wastewater Systems in Reykjavík
Impacts of Climate Change on Wastewater Systems
60 ECTS thesis submitted in partial fulfillment of a *Magister Scientiarum* degree in Environmental Engineering

Faculty of Civil and Environmental Engineering
School of Engineering and Natural Sciences
University of Iceland
VR II, Hjarðarhaga 2-6
107, Reykjavik
Iceland

Telephone: 525 4000

Bibliographic information:
Ásta Ósk Hlöðversdóttir, 2010, *Impacts of Climate Change on Wastewater Systems in Reykjavík*, Master's thesis, Faculty of Civil and Environmental Engineering, University of Iceland, pp. 99.

Printing: Prenttorg
Reykjavik, Iceland, December 2010

Abstract

Due to climate change, precipitation is projected to increase in Northern Europe (Bates et. al., 2008). Such changes can influence the design and management of wastewater systems. Most of the current climate change studies have not analyzed short duration precipitation which is needed for wastewater system design. The objectives of this project are first to investigate whether changes in short duration extreme precipitation have occurred in Reykjavík in the past decades, then to assess increased flood risk in the wastewater system in downtown Reykjavík using the Mike Urban simulation program.

No significant precipitation trends were found on an annual basis. A positive significant trend of 0.12mm/decade, was found in August (10 minutes duration) and a negative trend of -0.08 mm/decade was found in November. The times series analysis also revealed the presence of decadal to multi-decadal variations related to natural climate variability, which may have counteracting effects on long-term trend detection, as the variations could be larger in magnitude than potential trends. By updating the 1M5 method, used for Icelandic wastewater system design, with new data (1985-2008), 10 minutes design intensity increased by 16%.

Flooding in downtown Reykjavík was analyzed using both an 11 year long time series from a digital rain gauge, and Chicago design storms with intensity with a 5 year return period. Three scenarios were analyzed, firstly current design practice, secondly current situation, and thirdly a 20 % increase. Number of sensitive areas were identified, and already 20% of the system is under pressure for an event with a 5 year return period. The effects of densifications were also investigated, revealing that a 10% increase in runoff coefficient could increase floods by 35%.

Table of Contents

List of Figures

List of Tables

Abbreviations

1M5: Precipitation with duration of one day and return period of 5 year

CDS_1: Chicago Design Storm with precipitation intensity with a 5 year return period found using the original 1M5 method.

CDS_2: Chicago Design Storm with precipitation intensity with a 5 year return period found using the updated 1M5 method.

CDS_3: CDS_2 scaled by 20 %

IMO: Icelandic Metrological Office

IMO_1: Time series from IMO from 1998-2008 scaled down by 16%

IMO_2: Time series from IMO from 1998-2008

IMO_3: Time series from IMO from 1998-2008 scaled up by 20%

KS: Kolmogorov Smirnov

M. Number of flooded manholes

M_{-1m} : Number of manholes with water level 1 m below ground

MK: Mann Kendall

MT: Precipitation with return period T

MW: Mann-Whitney

P: Number of full flowing pipes

R_{tot}: Total monthly precipitation

S: Standard deviation

T: Return period

$\bar{T}$: Average temperature

T_d: Temperature at the day of precipitation maxima

T_{wet}: Average temperature on wet days

t_r: Duration

V: Volume of water flowing up from manholes

$\bar{X}$: Mean

Acknowledgements

This work is supported by the Reykjavík Energy Environment and Energy Research Fund.

I would like to thank all my advisors for their time, help and advises for the past year: Brynjólfur Björnsson, Hrund Ólöf Andradóttir, Jónas Elíasson and Philippe Crochet.

I would like to thank the Icelandic Metrological Office, especially Trausti Jónsson and Þóranna Pálsdóttir for access to and help with data.

I would like to thank Reykjavík Energy for their cooperation, especially, Íris Þórarinsdóttir, Kristján Helgi Tómasson and Pétur Þór Kristinsson.

1 Introduction

Extreme weather events have recently been happening with great frequency and intensity, causing major urban flooding events such as the 2007 United Kingdom floods (Lane, 2008) and the 2005, 2002 and 1997 European Floods (Kundzeqicz et al., 2005; Ulbrich et al., 2003). These events are having a great economical impact in the western world and have sparked a greater interest in the extreme aspects of global warming. Increases in temperature and mean precipitation have already been observed around the globe, although decreases have also been seen (Bates, et al., 2008). Most of the current studies have not analyzed the more extreme short duration precipitation which is typically needed for wastewater system design, and only a handful of studies have looked at possible impacts on wastewater systems.

1.1 Observed changes in precipitation

Climate change is affecting the hydrologic cycle in various ways. Precipitation patterns are changing, snow and ice is melting, and atmospheric water vapour and evaporation is increasing. Evaporation increases because of surface heating and with increased temperature the water-holding capacity of the atmosphere increases. As atmospheric moisture content directly affects precipitation, stronger rainfall events are expected with climate change (Trenberth K. E., 1999).

1.1.1 Annual Precipitation

The natural variability, both in space and time, of hydrologic variables poses a great challenge in monitoring changes, and therefore there is still a great uncertainty of the scale of these changes. Figure 1 shows the decadal variability of the global annual precipitation, using anomalies (mm) with respect to the 1981-2000 base period, i.e. the columns are difference between annual precipitation and the mean annual precipitation in 1981-2000. Interestingly, no statistically significant trend can be found for the global average precipitation from 1951 – 2005 (Bates, et al., 2008), and in general the greatest annual precipitation was in the period 1940-1970. The lines on Figure 1 are curves where fluctuations on less than decadal time scale have been removed by smoothing (Trenberth, et al., 2007). These lines clearly show 10-20 years oscillations.

Although no trends are seen when looking at annual precipitation on a global level, changes can be seen on regional and local levels. Figure 2 shows trends in annual precipitation at local levels, firstly for the entire 20th century (upper panel) and secondly for the last part of the century, 1979 – 2005 (lower panel).

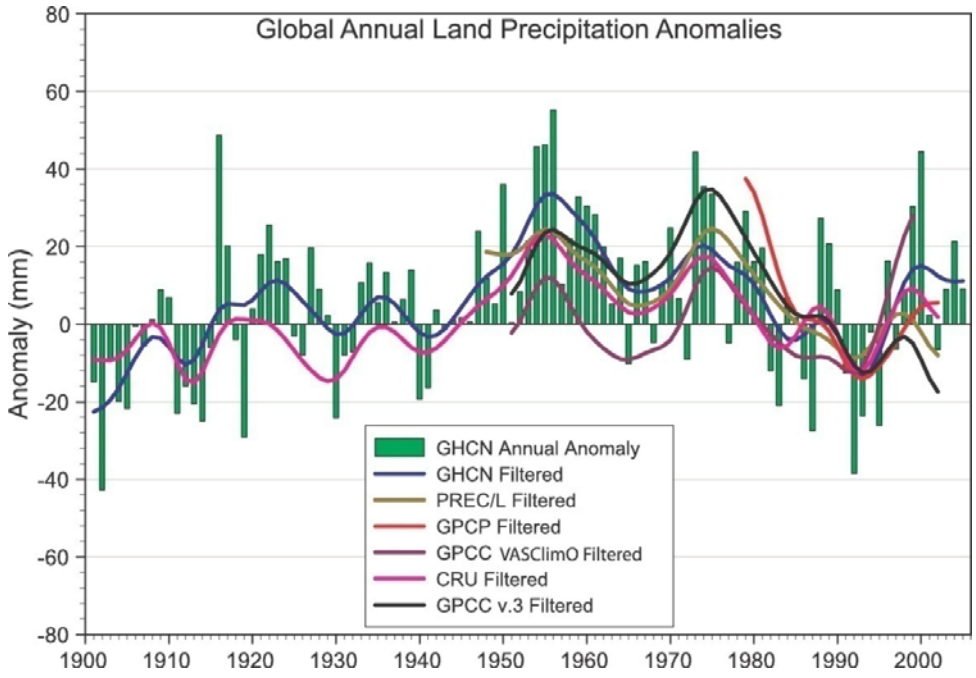

Figure 1: Time series for 1900-2005 annual global land precipitation anomalies (mm) from Global Historical Climatology Network (GHCN) with respect to the 1981 – 2000 base period. Smoothed decadal-scale values are also given for 6 other data sets (IPCC, 2007).

As can be seen by the large prominence of green shading in the upper panel of Figure 2, annual precipitation has generally increased over the 20th century between 30°N and 85°N. In comparison, the lower panel of the figure shows decreases have occurred in the past 30-40 years from 10°N to 30°N. The increasing trend is evident for all grid boxes in Northern Europe when looking at the 1901-2005, but when looking at the 1979-2005 period, grid-boxes with decreasing trends can be seen for example north of Britain.

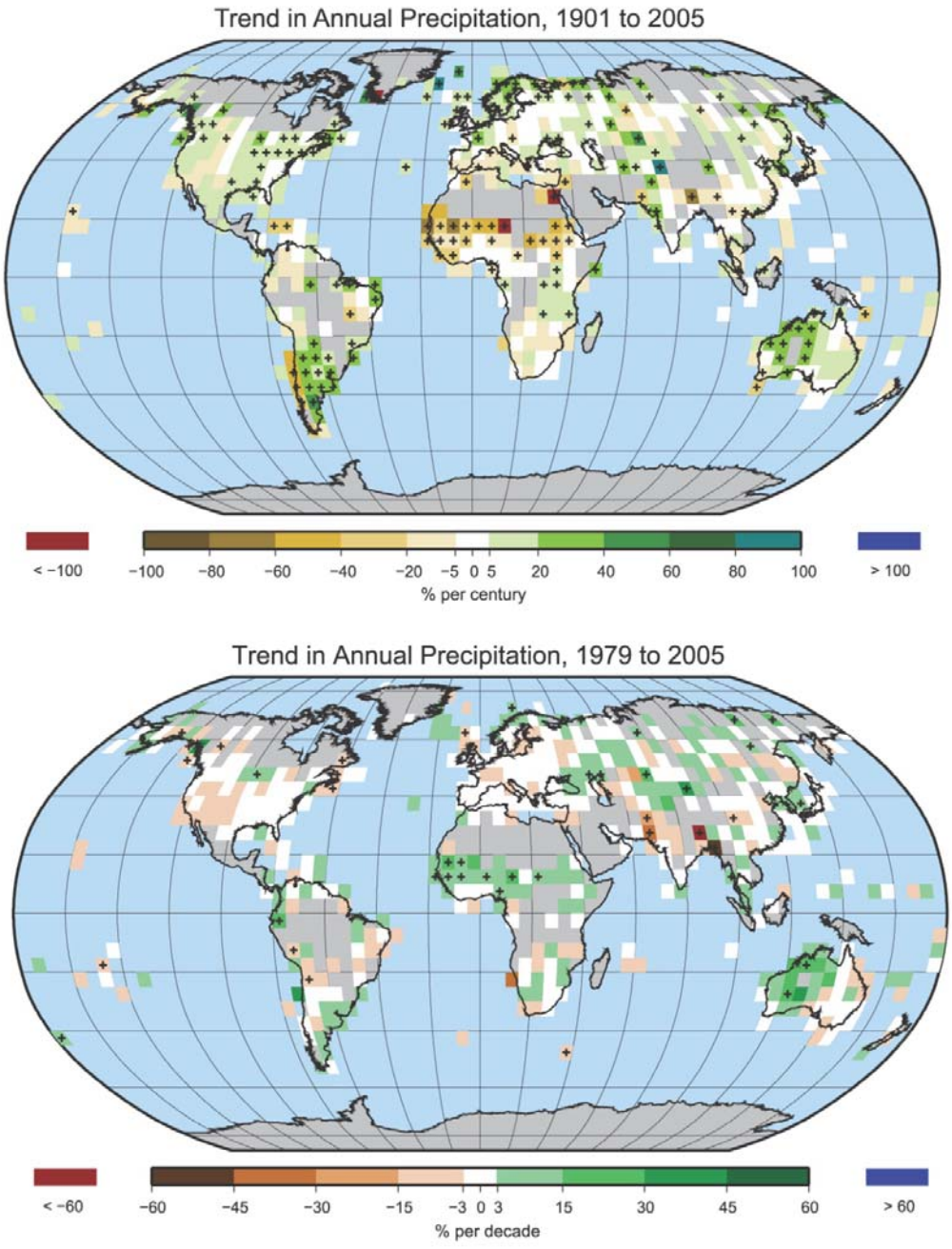

Figure 2: Trend of annual land precipitation amounts for 1901 to 2005 (top, % per century) and 1979 to 2005 (bottom, % per decade), using the GHCN precipitation data set from NCDC. The percentage is based on the means for the 1961 to 1990 period. Areas in grey have insufficient data to produce reliable trends. Trends significant at the 5% level are indicated by black + marks (IPCC, 2007).

1.1.2 Extreme precipitation

According to Bates et al. (2008) extreme or heavy precipitation, often defined as above the 95th percentile, is increasing even in places where total amounts have decreased. Table 1 shows results from various researches on extreme precipitation with 1 day duration in Europe and North- America.

Table 1: Observed trends in extreme precipitation, with duration of 1 day.

Country	Annual	Winter	Spring	Summer	Autumn	Indicator	Source
Canada (1900-1998)	No changes.	Increase in snowfall in Northern Canada	No trend	Increase in Eastern Canada	Increase in snowfall in Northern Canada	90th percentiles annual maxima, 20-yr return	(Zhang, et al., 2001)
US (1910-1996)	1.6% of the mean per century	2% of the mean per century	0.6% of the mean per century	2% of the mean per century	1.6% of the mean per century	95th percentiles of precipitation intensity	(Karl & Knight, 1998)
Poland (1951-2006)	Decreasing trends	Decrease	Some increasing trends	Decrease	Some decreasing trends	90th and 95th percentiles	(Lupikasza, 2009)
Czech Republic (1961-2005)		Increase	Insignificant decrease	Insignificant increase	Decrease	90th and 95th percentiles	(Kyselý, 2008)
Germany (1950-2004)		+5-13% per decade	-3-9% per decade	+5-13% per decade	+5-13%	95th and 99th percentiles (per decade)	(Zolina, et al., 2008)
Belgium (1898-1997)	No significant trends	NA	NA	NA	NA		(Vaes, et al., 2002)
Norway (1900 – 2004)	Significant trends in the south western region	NA	NA	NA	NA	Annual maxima	(Alfnes & Førland, 2006)
UK (1961-1995)	No significant trends	Increase	No significant trends	Decrease	No significant trends	90th percentiles	(Osborn, et al., 2000)

Zhang et al. (2001) analysed 68 stations all over Canada and looked at three indicators; 90th percentiles of daily precipitation, the annual maximum daily value and the 20 year return values. They found increase in snowfall in Northern Canada in autumn and winter and increase in rainfall in Eastern Canada in the summer. They pointed out that the

observed increase in mean precipitation in Canada over the past century is due to increases in the number of days with small precipitation but there is no trend in annual extreme precipitation. Moreover, their study revealed that precipitation extreme exhibit a marked decadal-scale variation.

Karl and Knight (1998) analysed daily precipitation dataset consisting of 182 stations across the United States for the period 1910-1996. They found that precipitation had increased by about 10% in the United States, and that this increase was mostly due to an increase in heavy daily precipitation events, both their magnitude and frequency had increased. Table 1 shows increase in terms of percent of the mean per century for one indicator, 95^{th} percentiles of precipitation intensity.

Lupikasza (2009) studied daily precipitation from 48 rain gauges within Poland using 5 indicators; maximum 5 day precipitation and 90^{th} and 95^{th} percentiles for both precipitation magnitude and frequency. She only found positive trends in spring, but all other seasons showed negative trends. Kyselý (2008) used a dataset from 175 rain-gauge stations covering the period 1961-2005 to analyse seasonal trends in the Czech Republic. Using 90^{th} and 95^{th} percentiles precipitation he found significant increasing trends in winter and decreases in autumn. Zolina et al. (2008) analysed daily precipitation from more than 2000 stations in Western Germany for 1950-2004, both using 95^{th} and 99^{th} percentiles. The largest increase, 13% per decade was in Central and Southern Germany in the winter, spring and autumn, while mostly negative trends were found for the summertime. Osborn, et al. (2000) analysed 110 UK stations over the period 1961-1995. They found an increase in the heaviest events in winter, but decline in the summer.

Different methodology makes it impossible to directly compare the numbers or trends presented in Table 1, so it is only possible to deduce general assumptions. It should be pointed out that different tests of significance are used, so what is deemed significant in one research may be insignificant in another. The table shows that the seasonal trends can vary greatly, and in places where no overall trends can be detected, seasonal trends can be seen. It seems that the most prominent increasing season is winter, but increasing trend is found in all the research (except for Lupikasza (2009)).

The quality of historical precipitation data differs greatly on a global level. As can be seen in Table 1, only about half of the countries featured seem to have data before 1950, and the other datasets start around 1900. Kunkel (2003) used a U.S. dataset starting in 1895 and found out that the extreme precipitation around 1900 was actually just as high as it was around 1990, which shows that care needs to be taken when making assumptions based on short datasets. Because of the great natural variability of precipitation it can be difficult to rely on the current historical precipitation data (series ranging from 20-100 years) to discover if the precipitation patterns are really changing, or if we are observing natural fluctuations.

The lack of solid data becomes even a greater problem when precipitation with shorter durations is analysed, needed for wastewater system design, since only in a few places long enough time series exist. Table 2 provides an overview of research from Denmark, Canada and Italy dealing with duration from 5 minutes to 6 hours. While the time series in Table 1 typically have 50-100 years of data, the time series in Table 2 have down to 20 years of data.

Table 2: Overview of research of trends in annual maximum precipitation with shorter duration than 1 day. Trend magnitudes are examples given in mm/h/year

	5 min	10 min	15 min	30 min	1 h	2 h	3 h	6h	
Denmark (1979 – 2000)		Significant positive trend						Not significant trend	(Arnbjerg-Nielsen, 2006)
Northern Ontario, (1952-1994)	0.07	0.08	0.15	0.19	0.18				(Adamowski, et al., 2009)
North Vancouver (1964-1997	1.02		0.61	0.30	0.13	0.08			(Denault, et al., 2006)
Tuscany (1935-1992)					0.30		0.10	0.05	(Pagliara, et al., 1998)

Arnbjerg-Nielsen (2006) used the 41 existing rain gauges that exist in Denmark with high resolution and 20 years of observation period to examine 10 min and 6 h intensity. He used a test that assumes that trend is due to random fluctuation, and if rejected on a 5% significant level, a significant trend was found. For the 10 min intensity a statistically significant trend was found which was more pronounced for the eastern part of the country, but the 6 h trends are less significant.

Adamowski et al. (2009) chose 15 stations of the 65 available for Ontario, Canada, with high resolution and a 20-30 year record length. They used Mann-Kendall test for trend and linear regression to determine the trend for durations from 5 min to 1 h. Only 16% of the tests were found to be significant at the 5% level. Table 2 shows the average results for the stations in the northern part of Ontario, but in that area, only 5 tests were significant, one 5 min, one 10 min and two 15 min.

Denault et al. (2006) used one gauge in North Vancouver. Using linear regression on annual maximum time series, the significant trend slopes shown in Table 2 were found. For comparison, three other gauges in the region were analysed but, only one of them showed prominent trends.

Pagliara et al. (1998) looked at two rain gauges in Tuscany, Italy, but found only a significant trend for one (shown in Table 2). They used Kendall's test to determine if there was a trend and an ARIMA model to quantify it.

It can be seen from the research referenced above, that although trends are frequently found for short duration precipitation, they are not always statistically significant. One of the reasons could be too short precipitation measurements, showing the need for better long term data.

1.2 Projected changes in precipitation

To predict the weather of the future, different emission scenarios for the 21st century have been defined, based on international political development, as shown in Figure 3 (Nakićenović & Swart, 2000). The A1 storyline has the fastest economic growth, regional interactions, and the maximum world population will be reached in 2050. In scenario A2 there is a continuously increasing population, less interaction and integration of economies and the focus is on local solutions. The A2 scenario has the least economic growth and technological advancement. The B1 storyline has the same population development as A1 but faster globalisation. The economy is service and information based, and thus less use of resources. The B2 storyline the focus is on environmentally friendly and local solutions. The population growth is steady throughout the century but slower than A2. The economic growth is slower than in A1 and B1.

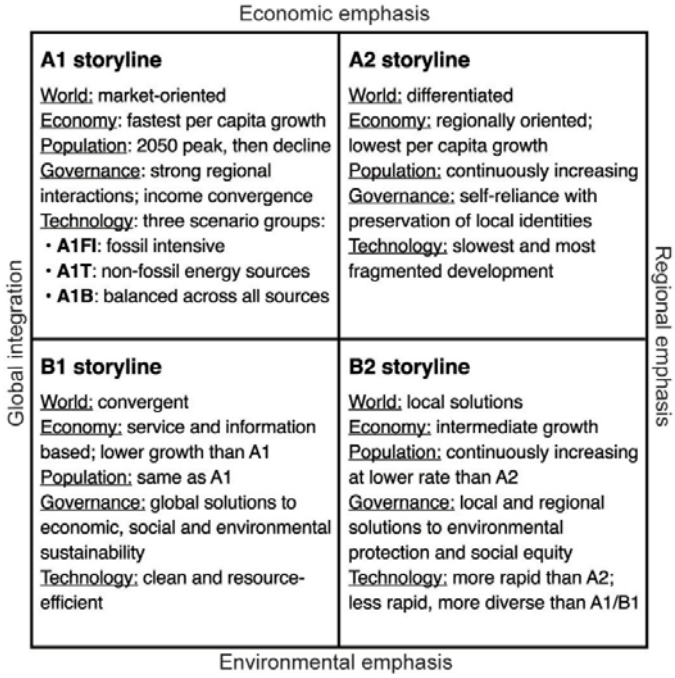

Figure 3: Summary of the characteristics of the four SRES storylines (IPCC, 2007)

Based on these scenarios, Global Climate Models (GCM) have been developed from numerical weather forecasting models, which simulate the development of the climate. Figure 4 shows the average projected changes of 15 models in mean precipitation over the 21st century. For all scenarios, annual mean precipitation is expected to increase in Northern Europe and decrease further south, with great seasonal variations (Bates, et al., 2008). According to Figure 4, less change in mean precipitation should be expected for Iceland, or 0 – 0.2 mm/day, which is similar as for the UK, while for example Norway could expect more changes. The mean precipitation in Europe increases in winter due to both increased wet day frequency and increased mean precipitation for the wet day.

Figure 5 shows that projections also show increases in precipitation intensity almost everywhere, seen by the prominence of green and blue, particularly at mid and high latitudes where mean precipitation also increases. In Central Europe, the precipitation

decreases as the number of wet days decrease (Christensen, et al., 2007). In Europe extreme daily precipitation does increase in the summer although mean precipitation does decrease (Christensen, et al., 2007).

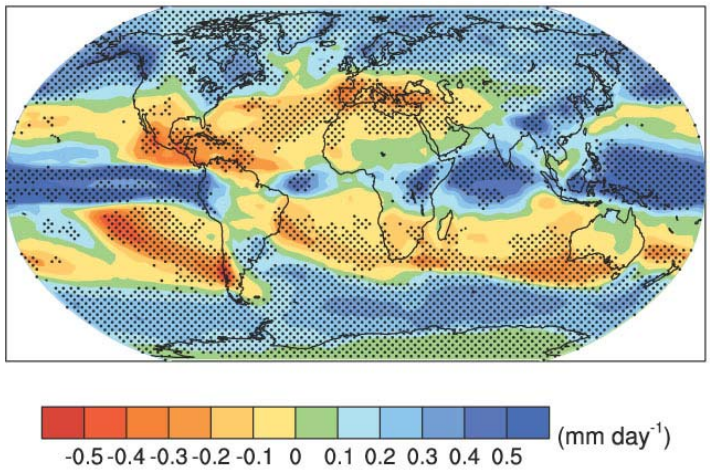

Figure 4: Fifteen-model mean changes in precipitation for the period 2080 – 2099 relative to 1980-1999 (IPCC, 2007)

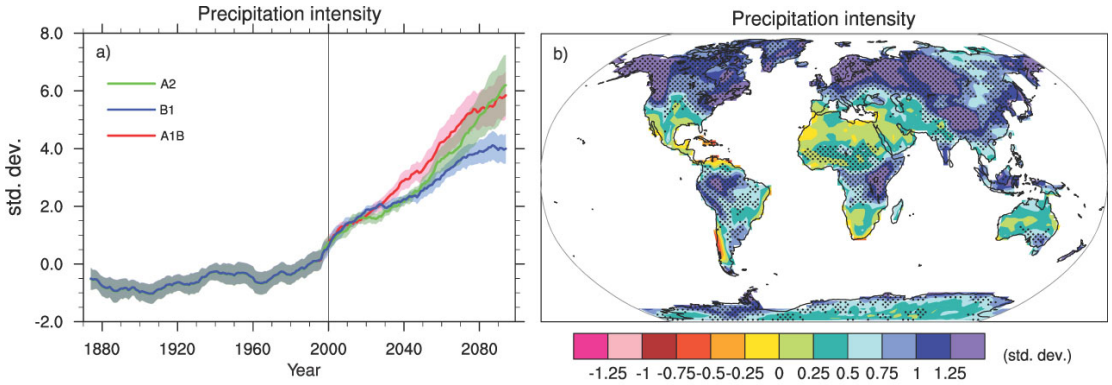

Figure 5: Changes in extremes based on multi-model simulations from nine global coupled climate a) Globally averaged changes in precipitation intensity (defined as the annual total precipitation divided by the number of wet days) for a low (SRES B1), middle (SRES A1B), and high (SRES A2) scenario. b) Changes in spatial patterns of precipitation intensity in 2080-2099 relative to 1980-1999 from AIB scenario (IPCC, 2007).

The Global climate models are grid-box models with relatively coarse spatial resolution, typically 300 x 300 km, which makes theme difficult to use for any hydrological purposes (STARDEX, 2005). Therefore downscaling techniques are being developed and tested, for example in the European STARDEX project (STARDEX, 2005). According to (STARDEX, 2005) downscaling should not be a simple linear interpolation, but rather describe the sub-grid scale processes that are lacking from global climate models.

There are two major approaches to downscaling, dynamical and statistical. Dynamical downscaling involves the nesting of a finer-scale regional model within the coarser global climate model (STARDEX, 2005). Based on dynamical downscaling, regional climate models have been developed, for example within the European PRUDENCE project (Christensen, et al., 2007). The current regional models have spatial resolutions up to 25x25 km (Grum, et al., 2006) and temporal resolutions up to 30 min (Olsson, et al., 2009).

Statistical downscaling involves the application of relationships identified in the observed climate, between the large and smaller-scale, to climate model output (STARDEX, 2005). According to Wilby and Wigley (1997) statistical downscaling techniques may be described using four categories, namely: regression methods, weather pattern-based approaches, stochastic weather generators and limited-area modelling.

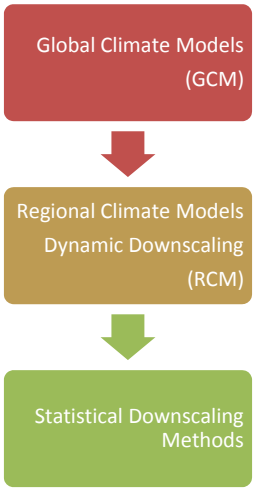

Figure 6 Flow diagram of how to get data with sufficient temporal and spatial resolution based on projections from Global Climate Models.

Data extraction as seen in Figure 6 can be seen widely in literature that deals with urban hydrology. Firstly, there is a global climate model (GCM); secondly a regional climate model (RCM) which dynamically downscales GCM data for a certain region; and thirdly RCM data is statistically downscaled to finally render data with high enough temporal and spatial resolutions. The Delta Change Method appears frequently in the literature when a simple method is needed to find future precipitation to use in urban drainage impact analyses (Grum, et al., 2006; Semadeni-Davies, et al., 2008; Olofsson, et al., 2007; Jónsdóttir, 2006). The method computes the differences between current and future GCM/RCM simulations and adds these changes to observed time-series (Hay, et al., 2000). It has been tested and has given tolerable results (Olsson, et al., 2006).

Grum, et al (2006) used time series from the HIRHAM regional climate model, based on A2 scenario. The model has a spatial resolution of 25x25 km and 1 h temporal resolution. They used a 3 step process where 1 h duration time series from 16 rain gauges in Copenhagen, within the chosen 25x25 grid box, were used to create a weighted average, which was then scaled using the present (1979-1996) and future (2071-2100) time series data from the climate model. Finally the future time series was transformed back to the 16

gauge point values. According to this method the current return period 2-4 year will increase in frequency by a factor of 2.

It has to be emphasised that the level of uncertainty at this stage is great, so the downscaled projections should not be looked at as a predictions of the future but rather simply a possible scenario. Some authors skip the imperfect process of downscaling, and simply assume a percentage increase (based on GCMs) in order to create a possible scenario for analysis of their local wastewater system (Waters, et al., 2003; Ashley, et al., 2005).

1.3 Precipitation in Iceland

The lack of long time series has limited the research done regarding trends in precipitation in Iceland. Three precipitation records exist that extend back to the late 1800s, Stykkishólmur (1857), Teigarhorn (1873) and Vestmannaeyjar (1881). Their locations can be seen in Figure 8. Hanna et al. (2004) analysed the total annual precipitation of these records and found a positive trend at all three stations, although only a significant trend at Vestmannaeyjar or 21% increase from 1881 to 2002. The precipitation records, along with their 10 years moving average can be seen in Figure 7. They also found that temperature and precipitation are weakly but significantly correlated, so warm periods are wetter than colder periods (Hanna, et al., 2004).

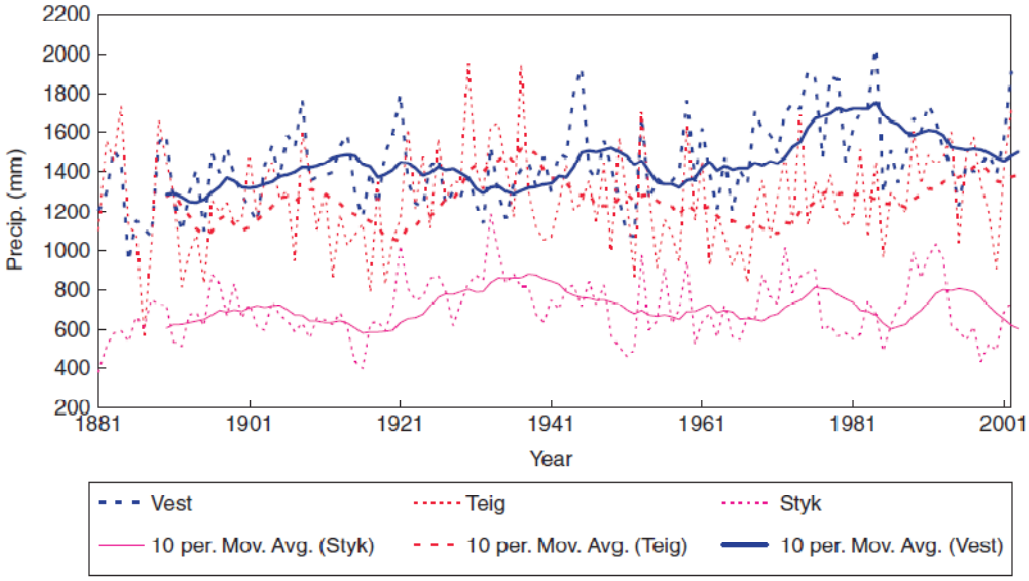

Figure 7: Annual precipitation at Vestmannaeyjar, Stykkishólmur and Teigarhorn, 1881-2002, with their 10 year running means. Reproduced with permission from Hanna, et al.(2004).

In Jónsdóttir et al. (2006) and Jónsdóttir et al. (2008) data from 28 rain gauges around Iceland was analysed, 12 of which having data from 1941, and the other 16 from 1961. Significant 4-15% positive trends per decade in annual precipitation were found for 5 stations using non-parametric methods (Jónsdóttir, et al., 2006) and 5-6 % per decade at six stations using parametric methods (Jónsdóttir, et al., 2008). They found mean daily

precipitation trends are positive in most seasons except for negative trends in the autumn in the south. They also analysed maximum one day precipitation in spring and autumn and found positive trends. In Table 3 the total number of significant and insignificant trends is shown. As can be seen there are no significant negative trends.

Table 3: Number of rain gauges with trends in mean precipitation and maximum 1 day duration precipitation in Iceland (Jónsdóttir, et al., 2008)

	Positive trends		Negative trends	
	Significant	Insignificant	Significant	insignificant
Mean total precipitation				
Annual	6	16		5
Autumn	4	12		11
Winter	2	22		3
Spring	1	17		9
Summer		16		11
Maximum 1 day duration				
Spring	2	18		7
Autumn	2	14		11

Crochet (2007) showed that there is a great decadal variability in annual and monthly precipitation, and that for example when shorter periods than in Jónsdóttir et al. (2008) are studied, such as the period 1991- 2000, negative trends can be found.

For wastewater system design, short duration precipitation measurements are needed. The Icelandic Meteorological office (IMO) has from 1951 had one analog rain gauge in Reykjavík with sufficient resolution. These precipitation measurements have not yet been analysed or tested for trends. In the past 10-15 years the IMO has been installing automatic rain gauges around the country as can be seen on Figure 8. If these stations will be properly maintained, it will hopefully be possible to carry out a country wide analysis in 10-15 years.

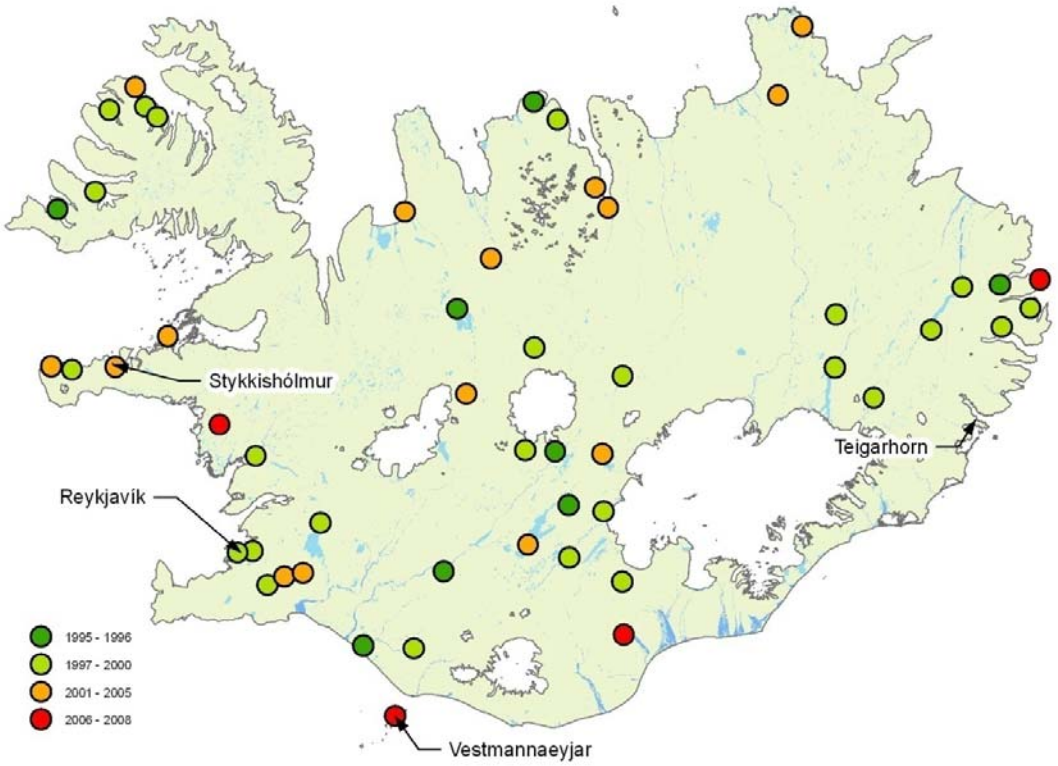

Figure 8: Installed automatic IMO rain gauges in Iceland that have been running for one year or more and are currently in service. The displayed year is the first whole measurement year

The Reykjavík road authorities (and affiliated bodies) have set up a few weather stations in the city. Hrafnsdóttir (2005) analysed two of them, which were set up in Breiðholt, Reykjavík in 1985. She did not perform any trend analyses of mean or extreme precipitation, but an interesting result was that the mean rain event was smaller in 1994-2001 than in 1985 – 2001.

The lack of high resolution data has created the demand for functions that can relate long duration (1 day) precipitation to short duration precipitation, but the IMO has a network all over the country of rain gauges that are read once or twice a day. The Wussow formula was recommended and used for many years (Bergþórsson, 1977). Elíasson and Thordarson (1996b) have shown that the Wussow formula overestimates short duration precipitation, and have recommended another function relating intensity duration and frequency, which is called the 1M5 method.

Table 4 shows the projected changes in mean annual precipitation in Iceland according to Global Climate Models (Björnsson, et al., 2008) for three climate change scenarios, A2, A1B and B2 (see chapter 1.2 and Figure 3) The projections are by seasons and two time frames. For the period 2046 – 2055 the greatest increase is expected in the autumn (for A scenarios), or around 5%, which is the opposite of what Jónsdóttir et al. (2008) found for southern Iceland. Here as before, the great uncertainties shown in Table 4 should be pointed out. For the later period, 2091-2100 the uncertainties are even greater, but for that

period the greatest changes are expected in the summer, 8-11 % for the A scenarios, but less for the B1 scenario.

Table 4: Projected changes (%) in mean annual precipitation per decade in Iceland (Björnsson, et al., 2008)

	2046-2055			2091-2100		
	Mean [%]	Conf. interval		Mean [%]	Conf. interval	
A2 storyline						
DJF	3,9	[-7,6	12,9]	3,7	[-11,0	16,5]
MAM	2,6	[-9,8	14,4]	5,6	[-5,1	17,1]
JJA	3,1	[-8,6	12,6]	11,0	[-1,6	25,3]
SON	5,1	[-1,8	13,9]	8,9	[-3,0	26,1]
A1B storyline						
DJF	3,1	[-7,3	17,4]	3,6	[-5,8	14,4]
MAM	2,8	[-5,4	9,6]	4,0	[-6,5	13,8]
JJA	4,0	[-9,8	17,4]	8,0	[0,0	19,0]
SON	4,7	[-0,8	12,2]	7,2	[-0,7	15,3]
B2 storyline						
DJF	-0,5	[-10,3	9,9]	1,3	[-8,7	11,7]
MAM	2,1	[-8,0	13,1]	5,6	[-3,2	16,4]
JJA	3,9	[-5,4	20,1]	6,0	[-4,7	17,2]
SON	2,0	[-4,2	7,4]	4,0	[-3,6	10,7]

1.4 Impacts of Climate Change on Urban Drainage

The underlying assumption for the design of stormwater and combined wastewater systems is that the precipitation and flooding events in the past can be used to predict events in the future. Climate change therefore challenges wastewater system design. Most of the literature about global warming and urban drainage is looking at possible future impacts, and little can be seen about already observed problems, except for extreme flooding events such as the European floods mentioned before. Already from that it is possible to deduce that global warming has not yet greatly affected the day to day running of sewer systems, which could be explained by that they are conservatively designed.

In her licentiate thesis, Karolina Berggren (2007) looked at the impacts of climate change on urban drainage. The main impacts that she defined can be seen in Table 5. If the intensity of precipitation increases and the capacity of the wastewater systems is too low, more floods should be expected. In a separate system this means surface flooding, but in combined systems basements can also be flooded, and more flow to be released through combined system overflows (CSO) which can lead to environmental problems in the receiving waters. Increased precipitation can lead to a higher ground water level, which can cause an extra stress on the system with greater infiltration. Also, a higher ground water level can decrease the initial infiltration capacity of the drainage area and thus cause more runoff in the wastewater system. Higher precipitation intensity can wash pollutants faster off the surface and thus increase the concentration of pollutants in the runoff (Berggren, et al., 2007).

Table 5: Examples of impacts of high intensity rainfall events on urban drainage systems (Berggren, et al., 2007)

Combined systems	Basement flooding Increased combined sewer overflow (CSO) More infiltration into pipes due to higher ground water
Stormwater systems	Surface flooding More infiltration into pipes due to higher ground water Rapid runoff with higher concentration of pollutants

Most of the found research that dealt with simulation of the impacts of global warming on an urban drainage system were analysing the capacity of the system, of both combined and separated systems. A preview of the main results of simulations for four different urban watershed studies is given in Table 6.

Table 6: Analyses of capacities of urban drainage systems

City/Country	Projected	Area (ha)	Runoff coefficient	Type	Impacts	Source
Mission/Wagg Creek watershed, Canada	Using linear trends found in the observed data– for years 2020 and 2050	440 steep	0,45	Separated	8% of pipes would have to be upgraded	(Denault, et al., 2006)
Ontario, Canada	15% increase 2050 (from literature review)	23 ha	0.34	Separated	24% of pipes surcharged	(Waters, et al., 2003)
Helsingborg, Sweden	Delta change 2081-2090	2914	0,05	Combined	10% increase of flow into WWTP	(Semadeni-Davies, et al., 2008)
Kalmar, Sweden	Delta change 2041-2070	54	0.37	Separated	50% increase in manhole flooding.	(Olofsson, et al., 2007)

Denault et al. (2006) analysed the small urban catchment Mission/Wagg Creek watershed in British Columbia, Canada. Interpolating trends that were found for a nearby rain gauge (see Table 2 for magnitude of trends), scenarios for 2020 and 2050 were found. By simulation it was found that 8% (515m out of 6200m) of the system would not be able to handle these scenarios.

Waters et al. (2003) did not perform a trend analysis of precipitation but instead used results from climate models to choose a scaling factor of 15% of rainfall depth of a one hour design rainfall with a return period of 2 years. They analyzed the Malvern district in Burlington, Ontario, Canada, which is a typical single family residential area. They found that 5 out of 21 pipe surcharged or 24%.

Semadeni-Davies et al. (2008) used the RCAO regional climate model developed by the Swedish Meteorological and Hydrological Institute which has a resolution of 6 hours and 49 km, to create scenarios for simulation of the period 2081-2090. The changes seen in the RCAO model, both increases and decreases, were used to scale the 1994-2003 precipitation time series, using the delta-change method described in chapter 1.2. They analyzed runoff in Helsingborg, Sweden, into the wastewater treatment plant, and found a 10% increase of flow into the WWTP.

Olofsson et al. (2007) used the Delta-Change method in the same manner as Semadeni-Davies et al. (2008) but analyzed a residential area in Kalmar, Sweden. They had climate model data from RCA3 with a resolution of 30 minutes and 50 km. They found a 50% increase of manhole flooding.

In many of the cases presented in Table 6, it has been deemed feasible/possible to exchange the problematic piping, since the problems are projected to start in a few decades, thus it should be possible to increase the capacity of the system within the framework of routine maintenance. This result gives an added incentive for simulating

local wastewater systems with projected precipitation data, in order to know already where capacity needs to be increased and thus be able to include these increases when pipes need to be replaced, be that this year or in 40 years.

Another factor increasing the flow in wastewater systems in colder regions is an increased frequency of snow melting periods. In the Oslo region, Plósz et al. (2006) showed that this could adversely influence wastewater treatment plant operation by simultaneously decreasing the influent wastewater temperature and the hydraulic retention times in the treatment unites.

Several guidelines for impact assessment and for both planning new systems and adapting old ones have been published, for example by the Swedish Water & Wastewater Association (Svenskt Vatten, 2007), the Danish Water and Waste Water Association (DANVA, 2007), New Zealand Climate Change Office (Shaw, et al., 2005), and by Hydro-Com Technologies (Arisz & Burell, 2006). Many of these sources state the importance of interdisciplinary approach, and the need for dialogue between policy makers and designers. One of the main suggestions, both for planning and adaption, is to minimize impermeable areas. Waters et al. (2003) looked at different adaptive measures for a watershed in Ontario and found out that by disconnecting half of roofs from the storm water system, the increased rainfall could be met.

1.5 Critical urban drainage issues in Icelandic urban areas

Reykjavík is the largest urban area in Iceland, and one of the first municipalities to start building up a wastewater system. In the past 20 years a great deal of work has been put into combining outlets and increasing wastewater treatment. Currently there are two wastewater treatment plants (WWTP) in Reykjavík, and two corresponding outlets, as can be seen in Figure 9. The first one, Skerjafjarðarveita services the southern part of Reykjavík as well as the neighbouring municipalities Garðabær, Kópavogur and Seltjarnarnes. The second, Sundaveita, services the northern part of Reykjavík and the municipality Mosfellsbær. Combined these systems serve 70% of the Icelandic population (Orkuveita Reykjavíkur, 2008).

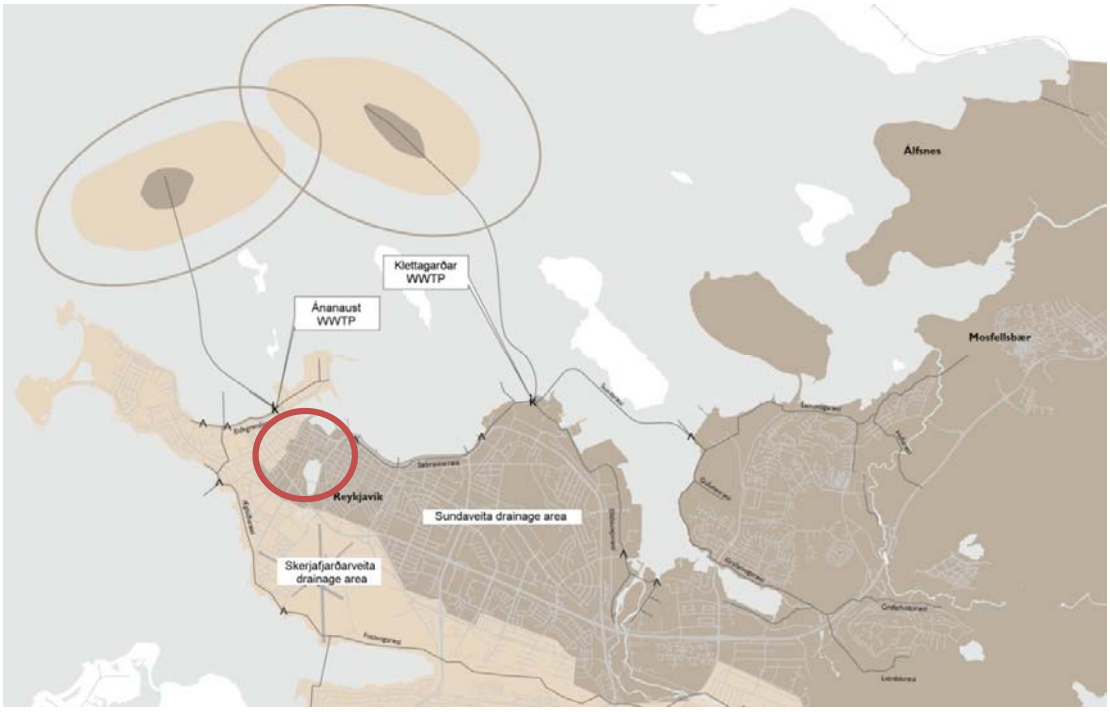

Figure 9: Reykjavík wastewater system (Orkuveita Reykjavíkur, 2007)

The oldest neighbourhood in Reykjavík, and where the first wastewater pipes were laid, is the downtown area, or the circled area in Figure 9. Figure 10-11 show how this area looked in the early 20th century. Figure 11 shows a typical open sewer solution, while Figure 10 shows the natural creek in Lækjargata which collected wastewater from a big part of Reykjavík at that time. Because of its foul smell and frequent flooding (once a year) it was closed in 1913 (Guðmundsdóttir & Gylfadóttir, 2007). This former creek is still an important part of the downtown wastewater system, although the density of the city has increased dramatically since the sewer in Lækjargata was originally constructed. The density in this area is only planned to increase. This is the area that will be modelled here, i.e. the area surrounding Lækjargata.

Figure 10: Lækurinn in Lækjargata, an open creek/sewer which was closed in 1913(Ólafsson, Lækurinn og Lækjargata, Lækjargata 2-14, 1907-1912)

Figure 11: Hafnarstræti, seen from east to west. An open wastewater drain can be seen in the centre of the photo (Ólafsson, 1910-1915)

1.5.1 Known flooding areas

When talking about flooding in this area, the first one that comes to mind is the infamous Básenda-flood which is an extreme case of floods caused by rise of sea level due to high tide combined with low pressure and wind in 1799 (Hjartarson, 2010). Such floods have been known to cause high water level in manholes in this area. Reykjavík Energy does not have registered incidents of floods in this area due to extreme precipitation. Insurance companies on the other hand do, as property damage due to extreme precipitation can fall under their insurances. As can be seen in Figure 12 floods due to extreme precipitation are categorized together with floods due to extreme snow melting. The map shows floods from 1997 until today, and as can be seen the incidents are not many, 13 out of the 309 incidents reported in the country (Sjóvá, 2010). These reports are though only from one insurance company.

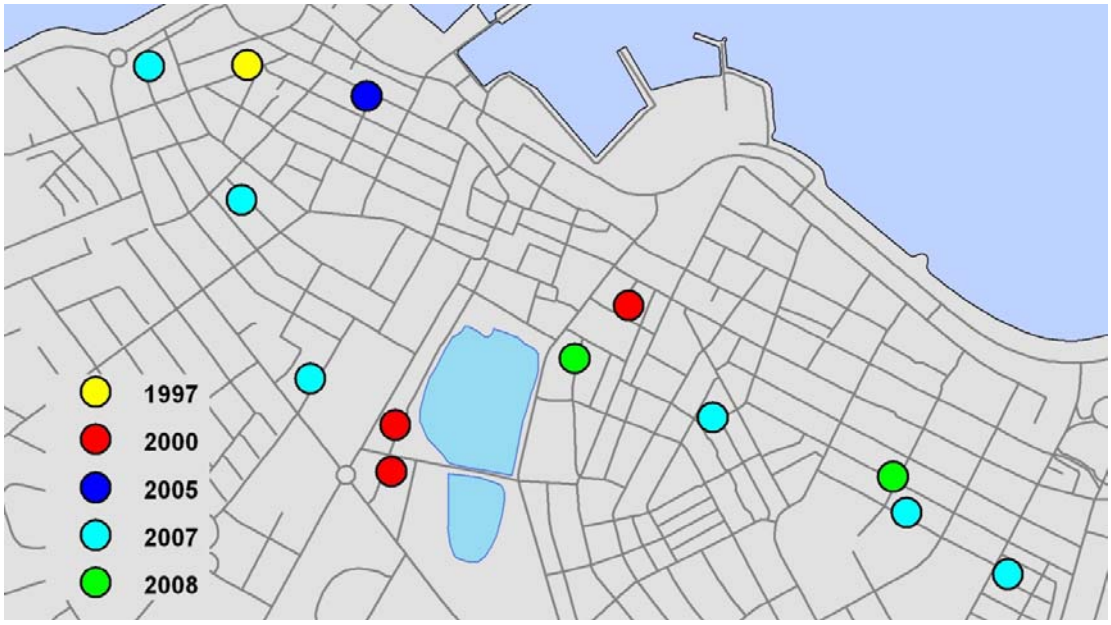

Figure 12: Property damage due to extreme precipitation or extreme snow melting reported to the Sjóvá insurance company (Sjóvá, 2010).

1.6 Thesis objectives and outline

The first objective of this study is to investigate whether changes have occurred in short duration extreme precipitation in Reykjavík in the past decades. This will be done by using various statistical methods to test both generally for changes, and if there is a trend. Until now only accumulated precipitation over longer periods, year (Hanna, et al., 2004), month and day (Jónsdóttir, et al., 2008) has been analysed to look for trends

The second objective is to analyse the impacts of such changes on the wastewater system of Reykjavík, and its design requirements, by modelling the old and sensitive downtown area, circled in Figure 9. Until now only a handful of areas in Iceland have been modelled using Mike Urban, mostly new neighbourhoods, and only using existing data or design values.

The thesis is divided into 4 parts: Firstly the introduction above, secondly methods, thirdly results, which are fourthly summarized in the last chapter, conclusions.

2 Methods

The analysis carried out in this thesis is threefold, as displayed in Figure 13. Firstly precipitation measurement data was statistically analysed. The precipitation data from IMO was then used to update the current design requirements. Design events (as well as precipitation datasets) were simulated in a flood model to create surface runoff, which finally was simulated into flow in pipes. All the methods shown in the small boxes in Figure 13 will be further explained in this chapter.

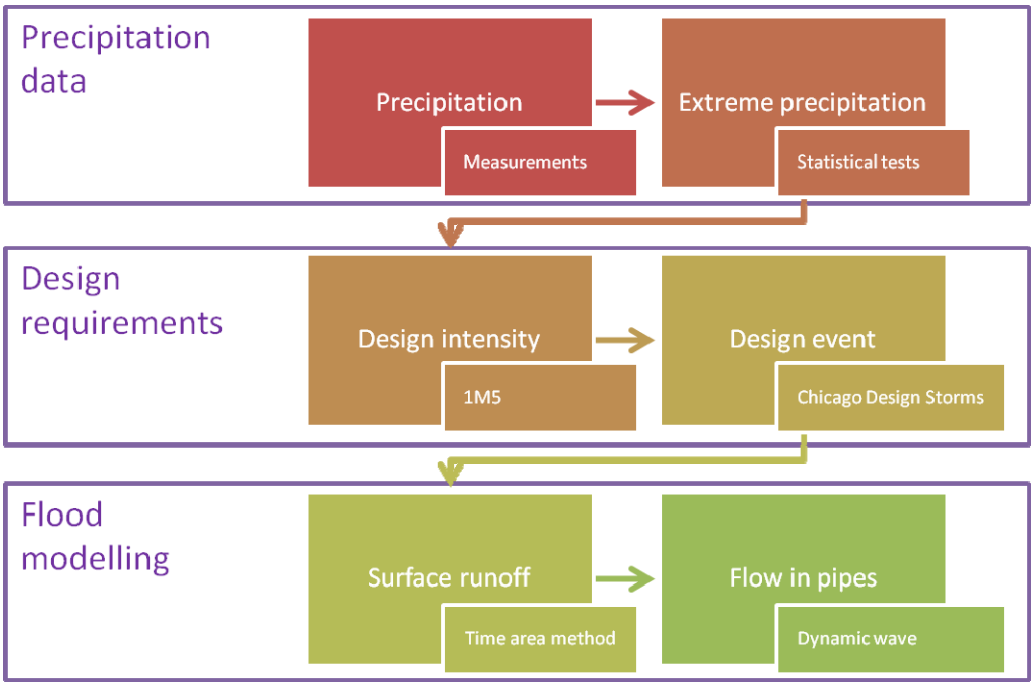

Figure 13: Overview of methods used in the thesis

2.1 Site description

The area that was picked for modelling is the old downtown area of Reykjavík, Kvosin. This site was selected as it is both one of the more sensitive areas, with parliament buildings and other important infrastructure as well as the oldest neighbourhoods where the first wastewater pipes in Reykjavík were laid. To make sure that all the drainage area would be included not only Kvosin was modelled but the surrounding neighbourhoods as well, as can be seen in Figure 14.

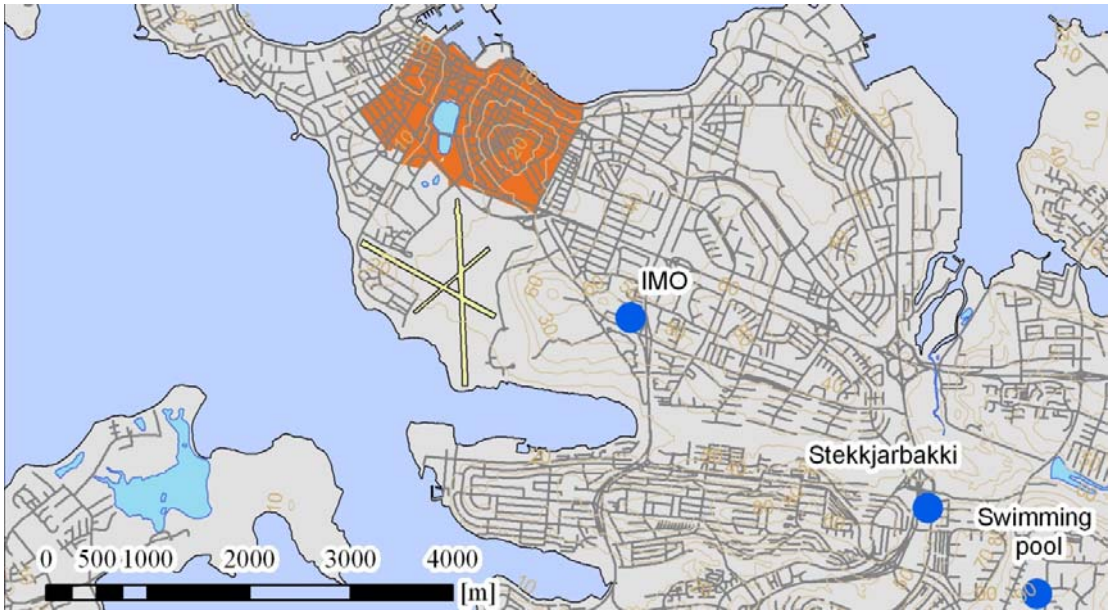

Figure 14: An overview of locations used in the thesis. The blue points are the rain gauges analysed and the orange area is the modelled area.

Figure 15 shows that majority of the system is built before 1950, but that most of Kvosin is relatively recent. Although the system is old most of the older parts have been lined in the past 10 years. Despite its age the system should therefore be in a reasonably good shape.

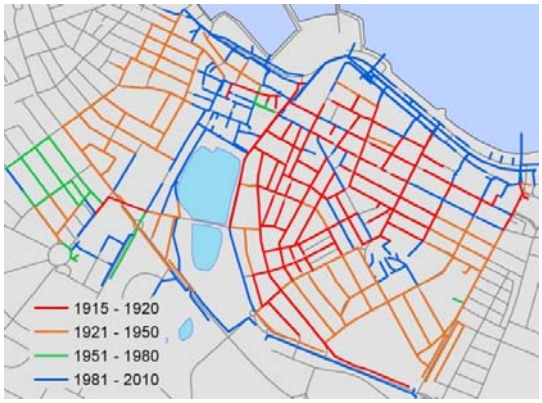

Figure 15: Map of the analysed area showing age of pipes

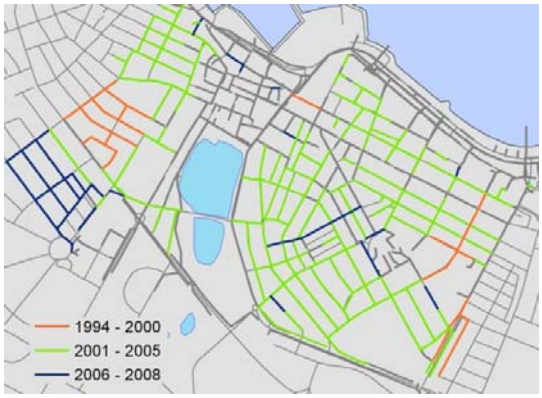

Figure 16: Map of the analysed area showing when pipes have been lined.

Reykjavík Energy has a GIS based database and with few modifications, pipe and manhole data could be imported into the Mike Urban GIS database. Figure 17 shows that the majority of the system is combined. Only a few pipes, or 19, are just sewage pipes. As they had parallel stormwater pipes they were generally discarded. Thus only combined and rain water pipes were imported and only main pipes, i.e. no home connections or swales. No information on manhole diameters was available so it was assumed to be 1m for all manholes. No modifications were made to count for possible pipe diameter loss due to lining, as lining should improve performance of the pipes. The diameter of pipes can be seen in Figure 18. As can be seen a large part of the system is smaller than the current minimum diameter of Reykjavík Energy, which is 250 mm (Orkuveita Reykjavíkur, 2009).

Figure 17: Map of the analysed area showing stormwater, sewage and combined system pipes

Figure 18: Map of the analysed area showing diameter of pipes

2.1.1 Densification

Although the modelled area is one of the oldest parts of town it is still a growing area. As can be seen in Figure 19 and 20 plans are to increase the density of both residential and commercial areas. In Figure 19 the areas numbered 4 (Mýrargata), 5 (Eimskip lot) and 6 (city centre) are within the defined drainage area, and in total 830 homes are planned in these areas. A big part of the drainage area falls under minor employment area densification, but within it is also the Austurhöfn area, where a concert and conference centre is rising. In a dense area such as this, increased density can increase domestic sewage flow, but it also matters for rainfall, as there are still some open spaces, lawns and unpaved areas.

Figure 19: Increasing density of residential areas. Circles indicate areas where plans are to build 50 or more homes (Skipulags- og byggingarsvið, 2008)

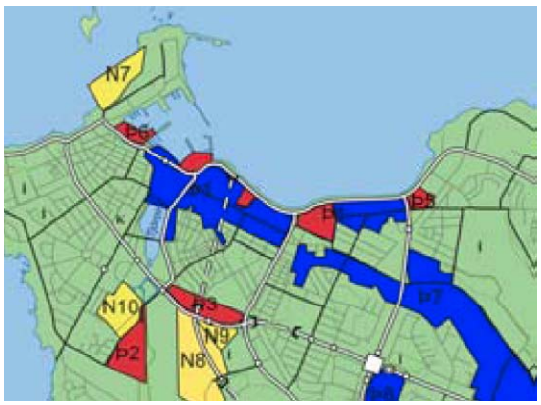

Figure 20: Increasing density of employment and commerce areas. Yellow areas are new areas, blue areas with minor densification and red with major densification or overall replanning (Skipulags- og byggingarsvið, 2008).

2.2 IMO rainfall data preparation

The IMO has the longest running precipitation series in Reykjavík. In 1951 an analog rain gauge was installed at the Reykjavík Domestic Airport. In 1973 it was moved to the new IMO headquarters at Bústaðavegur 9, see Figure 14. A new digital gauge was installed in 1997, and the analog gauge was discontinued in 2000. The data from the analog gauge has not yet been digitized, but the 10, 20, 30, 60 and 120 minute monthly maxima were regularly manually extracted.

To verify that the extractions were done in satisfying manner a new extraction was done for selected years. Unfortunately it was found that the extractions during the period 1986-2000 were systematically lower than the re-extractions. It was therefore decided to re-extract the 10 min maxima for the 1986-2000 period. Both the re-extracted data and the original data can be seen in Figure 21. The annual maxima of the original data is shown with a blue line, re-extracted data with red dots and green points represent data from the digital gauge (see below). By looking at the red points, it can be seen that they are clearly higher than the original points.

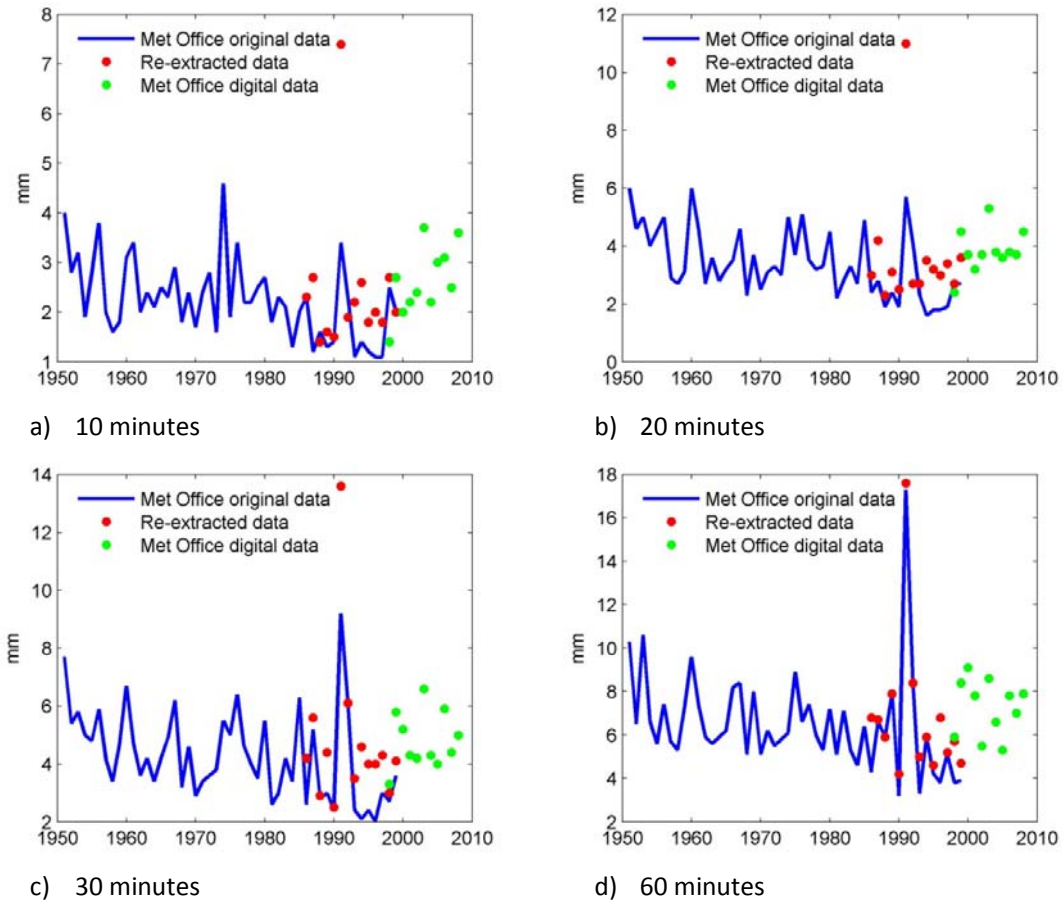

a) 10 minutes

b) 20 minutes

c) 30 minutes

d) 60 minutes

Figure 21: Annual maximum values from IMO

As 10 minute data was considered of the greatest importance and also easiest to extract, the same effort was not put into re-extracting for the other durations. Therefore only the days where 10 minutes maxima had been found were analyzed to look for 20, 30 and 60 minutes maxima. In Figure 21 it can be seen that just by looking at that one day many "new" maxima were found, but as to be expected, not as many as for the 10 minutes.

In 2000 the analog gauge was discontinued but a digital rain gauge has been in service at the same site since 1998. Despite the technical advancement, the data from the new gauge had a lot of noise, as can be seen in Figure 22. The black points represent the original records from the gauge. Under normal circumstances the black points should form an ever increasing line when it rains, but as can be seen several drops are observed. These could be everything from wind to snowmelt and evaporation from the gauge. The green line is the difference between two consecutive black points, discarding any drops. The blue line is then the cumulative function of the green line. Because of this noise, it was decided to manually verify every event for the monthly maxima. In Figure 21 the annual maxima of the digital data is represented with green points.

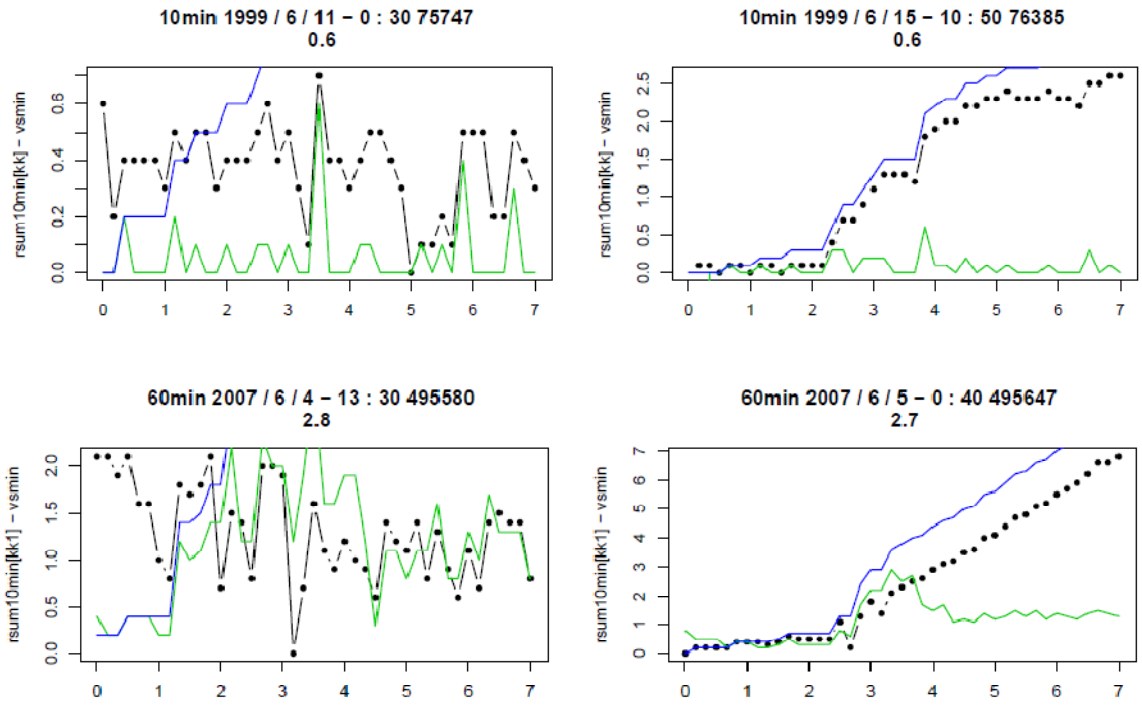

Figure 22: Examples of noise in the digital data from the IMO. The black points represent the original records from the rain gauge.

The data in Figure 21 thus came from three sources; firstly maxima manually extracted by the IMO, secondly data extracted by the author, and thirdly data from the digital rain gauge. This data was combined to form one time series, where the data extracted by the author was given precedence. It is this time series that the analysis in the following chapters is based on.

As can be seen in Figure 21 there is a very large precipitation event in 1991, which could be classified as an outlier. This downpour happened on the 16th of August 1991. Hundreds asked for help during the event all over the city, especially downtown. Property damage was estimated in millions (Morgunblaðið, 1991). It is difficult to determine if this was an event with a return period of 50, 100 or 1000 years, but as this was a significant very real event it will be included in most of the analyses.

2.3 Other high resolution precipitation data in Reykjavík

As mentioned in chapter 1.3, the Reykjavík road authorities operate four rain gauges in Reykjavík. In Breiðholt, there have been precipitation measurements at Stekkjarbakki and at the Breiðholt swimming pool since 1985, but the measurements at Stekkjarbakki were discontinued in 2003. The locations of these rain gauges can be seen in Figure 14. There are many complications with this data, as is thoroughly described and analyzed in Hrafnsdóttir (2005). One of her main results was the large amount of gaps in the data, ranging from hours to months.

Table 7: The resolution of the Breiðholt data

Period	Resolution
1985-1993	5 minutes
1994-1997	3 minutes
1996-1998	15 minutes
1999 -	10 minutes

The resolution of the measurement also differs, as can be seen in Table 7 which posed some problems for creating a 10 minutes series that could be compared to the IMO series. The 3 minutes series was accumulated into 9 minutes and linearly scaled up to 10 minutes. To find a scaling factor to scale 15 minutes down to 10 minutes the years 1996 and 1997 were analyzed, as both 3 minutes and 15 minutes data are available for those years. The scaling factor found was 0.84.

To create one usable time series, gaps in the Swimming pool series were filled by available data from Stekkjarbakki. Figure 23 shows the months that still did have gaps after the replacements. The months were almost no data was available are marked red, but those that are marked orange are missing the days were the maxima took place at the IMO. By looking at Figure 21 it can be seen that this data is not suitable for extreme value analysis, as many great events could be missing. These datasets could and have been used for stochastic modelling (Vatnaskil, 1995)

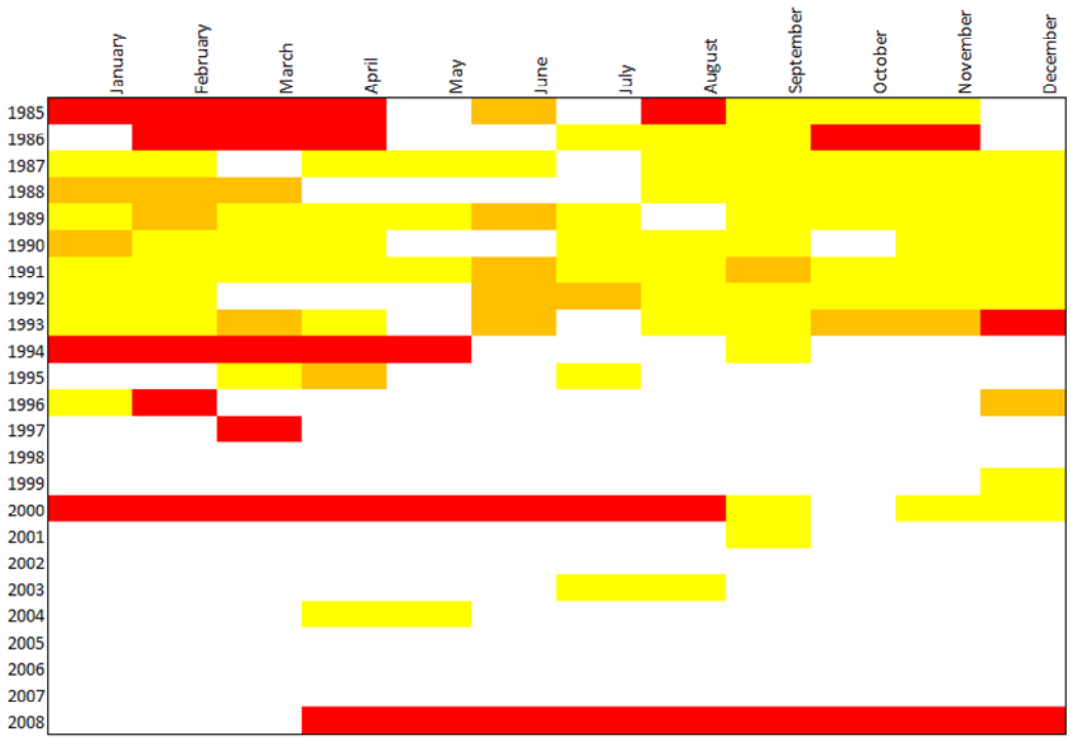

Figure 23: Gaps in the Breiðholt data. Red: No data available; orange: no data for a day with a maxima at the IMO; yellow: at least one day missing.

2.4 Precipitation data analysis

2.4.1 Methods for detecting changes

Only non-parametric tests were used, which do not assume any underlying distributions, and are less sensitive to outliers (Wang, et al., 2008). These tests only check if there is a significant change, and not for magnitude or direction. Thus the related Theil-Sen slope is introduced as well. Calculations were made for all durations, not only on an annual basis, but for all months as well.

Mann-Whitney Test

The Mann-Whitney (MW) test, also called the rank-sum test compares the distribution of samples A and B, of respective size, n_A and n_B. It has the test statistic WA which is the sum of the ranks of sample A within the combined sample. If the sample sizes are big enough it can be treated as normal and the mean and the variance of the rank-sum statistic WA are as follows

$$\mu_A = \frac{n_A(n_A + n_B + 1)}{2} \tag{3.1}$$

$$\sigma_A{}^2 = \frac{n_A n_B (n_A + n_B + 1)}{12} \tag{3.2}$$

The standardized form of WA, Z,

$$Z = \frac{WA - \mu_A}{\sigma_A} \tag{3.3}$$

is approximately N(0,1).

The null hypothesis is that both samples are drawn from the same population and have the same median. It is rejected on the α level if found p value is less than α (Helsel & Hirsch, 2002).

Kolmogorov-Smirnov Test

The two-sample Kolmogorov-Smirnov (KS) test compares the distributions of two samples. The null hypothesis is that the samples are drawn from the same distribution and the alternative is that they are drawn from different distributions. The test statistic for the two sided KS-test is (see for instance Wang, et al. (2008)

$$\tau = \max\left(F_A(x) - F_B(x)\right) \tag{3.4}$$

where $F_A(x)$ is the proportion of sample A that is less than or equal to x and $F_B(x)$ is the proportion of values in sample B that is less than or equal to x. The asymptotic p value is

$$p = Q\left(\tau \sqrt{\frac{n_A n_B}{n_A + n_B}}\right) \tag{3.5}$$

where

$$Q(t) = 2\sum_{k=1}^{\infty} (-1)^{k-1} e^{-2k^2 t^2} \tag{3.6}$$

The null hypothesis is rejected on the α level (for example 0,05) if the p-value is lower than α.

Mann-Kendall Test

The Mann-Kendall (MK) is a rank-based non-parametric test which checks for trend in a sample without assuming whether the trend is linear or nonlinear. The null hypothesis is that there is no trend. The MK-test statistic is

$$S = \sum_{i=1}^{N-1} \sum_{j=i+1}^{N} sgn(x_j - x_i) \tag{3.7}$$

Where x_j and x_i are sequential values and N is the sample size. A positive (negative) value for S indicates a positive (negative) trend.

The variance of S is given by

$$\sigma_S^2 = \frac{1}{18}(N(N-1)(2N+5) - \sum_{i=1}^{m} t_i(t_i-1)(2t_i+5) \quad (3.8)$$

where m is the number of tied groups in the data set and t_i is the number of data points in the i^{th} tied group.

The variable z,

$$z = \begin{cases} (S-1)/\sigma_s & if\ S > 0 \\ 0 & if\ S = 0 \\ (S+1)/\sigma_s & if\ S < 0 \end{cases} \quad (3.9)$$

is assumed to be normally distributed so the p values are found from the two sided normal distribution. The null hypothesis of no trend is rejected at α significant level if $p < \alpha$ (Wang, et al., 2008).

Theil-Sen slope

The tests above test only for the existence of a trend, or a change in distribution, not for the magnitude of the change. There are several estimators available to find the magnitude of a trend. The most commonly used is the simple least squares regression estimator, but since this data is not normally distributed, and the sample size is small other estimators have been shown to perform better, such as the Theil-Sen estimator (Wilcox, 2009).

The Theil-Sen slope is a non-parametric estimator of the slope of a trend line, thus a method of quantifying the trend. Conveniently it is related to the Mann-Kendall test for trend, so that the Theil-Sen slope is significant when the null hypothesis of no trend is rejected by the MK test.

The Theil-Sen slope is computed by first calculating the slope between all data points and then taking the median (Bonaccorso, et al., 2005):

$$b = median\left(\frac{y_j - y_i}{j - i}\right) \quad for\ i < j \quad (3.10)$$

To be able to plot the slope an intercept is needed, which can, according to (Peng, et al., 2008) be estimated by

$$q = median(y_i - b \cdot x_i) \quad (3.11)$$

To find the confidence interval for the Theil-Sen slope it is possible to use the percentile bootstrap method. A bootstrap sample is generated by resampling the dataset B times. The middle 95% of the resulting bootstrap estimates of the Theil-Sen slope is then the 95%

confidence interval. According to Wilcox (2010) sampling 599 times should be sufficient for finding 0,95 confidence interval.

Gaussian filter

To be able to see underling behaviour of the data, such as trends or oscillations, the data was smoothened with the following moving average filter six times.

$$Y_t = 0.25x_{t-1} + 0.5x_t + 0.25x_{t+1} \tag{3.12}$$

which is an approximation of the Gaussian filter (Elíasson D. J., 2009).

2.4.2 Precipitation with return period T

The most common distribution used to describe annual rainfall maxima is the Gumbel distribution. Its cumulative distribution can be stated as

$$F(x) = e^{-e^{-\alpha(x-\beta)}} \tag{3.13}$$

where α and β are parameters that can be estimated using a number of methods. To be able to directly compare, the methods outlined in Elíasson and Thordarson (1996b) based on the method of moments will be used:

$$\alpha = \frac{C1}{S_n} \tag{3.14}$$

$$\beta = \bar{X}_n - \frac{C2}{\alpha} \tag{3.15}$$

where C1 and C2 are constants depending on the size of the sample (

Table 8), and $\bar{X}_n$ and S_n are the mean and standard deviation of the sample.

Based on this Elíasson and Thordarson (1996b) have derived the following formula for precipitation with return period T

$$MT = \bar{X}_n - \frac{C2}{C1}S_n - \frac{1}{C1}S_n(\ln\left(-\ln\left(1-\frac{1}{T}\right)\right)) \tag{3.16}$$

Table 8: C1 and C2 constants (Elíasson & Thordarson, 1996b)

n	C1	C2	n	C1	C2
10	0,9497	0,4952	60	1,17467	0,55208
15	1,02057	0,5128	70	1,17536	0,55477
20	1,06283	0,52355	80	1,19382	0,55688
25	1,09145	0,53086	90	1,20073	0,5586
30	1,11238	0,53622	100	1,20649	0,56002
35	1,12847	0,54034	250	1,24292	0,56878
40	1,14132	0,54362	500	1,2588	0,5724
45	1,15185	0,5463	1000	1,26851	0,5745
50	1,16066	0,54854	∞	1,28255	0,57722

2.4.3 The 1M5 Method

For purposes of design of stormwater systems, as well as the design of combined wastewater systems, the precipitation intensity (rainfall per time unit) corresponding to a design event with a certain return period and duration needs to be found. The shorter the event (duration), and the longer the time that will pass between two events of this size (return period), the higher the precipitation intensity will be. Several methods have been used to create either curves or formulas that can easily be used by engineers to extract the intensity for the duration and return period needed for each application. When rainfall measurements close to the place of interest exist, with sufficient length and resolution, they should be used to statistically determine the needed precipitation intensity.

The 1M5 method, developed for Iceland by Elíasson and Thordarson (1996b) is the method recommended to find precipitation intensity for storm water system design in Reykjavík and is used all over the country. It was developed using the data that now has been re-extracted, and therefore the method should be updated.

The function is of the following form

$$I = \quad R(T_0, t_{r_0}) \quad f(T) \quad g(t_r) \tag{3.17}$$

Here T is return period (frequency), and t_r is duration. R is an index parameter which in the 1M5 method conveniently for Iceland is the 1 day precipitation with a 5 year return period, hereafter referred to as the 1M5 parameter. The 1M5 parameter can be easily extracted for most locations in Iceland, since precipitation measurements with resolution of 1 day are widely available.

The second part of the equation, the function f(T), is a multiplication factor to scale to the needed return period. When the index parameter 1M5, then there would be no need to scale and f would equal 1. In all other cases it could be written as

$$f(T) = \frac{MT}{1M5} = 1 + C_i(y - 1{,}5) \tag{3.18}$$

where the C_i parameter can be calculated using the following formula (Elíasson & Thordarson, 1996b) with mean value X_n and standard deviation S:

$$C_i = \frac{0{,}78}{\frac{\bar{X}}{S} + 0{,}72} \tag{3.19}$$

The final part of equation 3.17 is the function g which describes the relationship between intensity and duration, which is where high resolution data is needed:

$$R = \sqrt{R_a R_b}\, e^{-\sqrt{\left(\frac{\ln R_a - \ln R_b}{2}\right)^2 + C_3}} \tag{3.20}$$

where R_a and R_a are

$$R_a = 0{,}7642\ t_r{}^{0{,}5908} \tag{3.21}$$

$$R_b = 6{,}4722\ t_r{}^{0{,}25232} \tag{3.22}$$

t_r is duration (in minutes) and C_3 a factor to control the smoothing on the cross section of R_a and R_a, here 0,001 (Elíasson & Thordarson, 1996b).

These formulas have been hardcoded into a computer program which is the current design tool for most wastewater design in Iceland

2.5 Flood Modelling in Mike Urban

Today a number of different flood modelling software exists. For the past years Reykjavík Energy has required that the modelling software Mike Urban is used when new wastewater systems are being designed (Orkuveita Reykjavíkur, 2008). Therefore it was decided to use Mike Urban to model runoff and flow in pipes for the selected area. Mike Urban also offers many other possibilities that were not needed for this project such as modelling sediment and pollution transport, biological processes and real time control of flow regulators. It is possible to model the complete land phase of the hydrologic cycle.

Mike Urban is originally Danish, developed by DHI (formerly known as Danish Hydraulic Institute). It is widely used, especially in the Nordic region, but it has been tested all over the world. It is a GIS (geographic information system) based program.

2.5.1 Model details

The total area of the model is 21ha. No account of domestic wastewater was taken, as in most cases it is negligible compared to rain water. It should though be kept in mind that in extreme cases, at lower points in the system, it could intensify floods. Table 9 shows some statistics for the model.

Table 9: Model details

Manholes	862
Minimum level	-4,03 m
Maximum level	36,98 m
Manhole volume	1924 m^3
Pipes	946
Length	46332 m
Pipe volume	6225 m^3

2.5.2 Rainfall used for modelling

The rainfall that will be used for modelling will both be actual rainfall from the IMO automatic station (see chapter 2.2), and synthetic rain storms. The 1M5 method was used to derive precipitation intensity with the 1M5 parameter as 38mm (the value for the IMO station see Elíasson and Thordarson (1996a)) and C_i of 0,21 (the value recommended in Reykjavik by Elíasson and Thordarson (1996b)). When doing computer modelling it is not enough to know design intensity, time distribution of the rainfall (hyetograph) must also be defined. With more high resolution rainfall data available every year it may be possible to analyse storm patterns in Iceland, but that is far beyond the scope of this study. The storm pattern that has been used and recommended in Iceland (Orkuveita Reykjavíkur, 2008) is the Chicago Design Storms. This is a simple method that has been used, for example in Denmark (Spildevandskomiteens Regnudvalg, 2008), but it was derived by Keifer and Chu in 1957 for the city of Chicago. The main concept of the CDS is that the integrated precipitation for a given duration, t, measured from the time of maximum intensity, is equal to the precipitation for duration of t.

To be able to compare the current design practice (CDS combined with the 1M5 method), the available 11 years (1998-2008) from the IMO digital rain gauge at Bústaðavegur was as well used for simulation. That also allows for comparison with experienced floods during this time period.

2.5.3 Runoff

For surface runoff modelling the Time-Area method in MOUSE was used which is a simple synthetic unit hydrograph routing method. The time-area method, is, as the name implies, based on a time –area curve which expresses the curve of the fraction of drainage area contributing runoff to the drainage outlet, in this case manholes, as a function of time (Straub, et al., 2000). To develop a time-area curve the catchment's time of concentration is divided into equal time intervals, which are used to divide the catchment into zones delimited by isochrome lines (Ponce, 1989). Mike Urban characterizes each catchment as rectangular, divergent or convergent, based on its shape, and uses the corresponding time-area curve (see Figure 24). The drainage area was split into 845 sub-catchments, corresponding to each unsealed manhole. Each of these catchments was then characterized as rectangular, divergent or convergent. An example of such classification is shown in Figure 25.

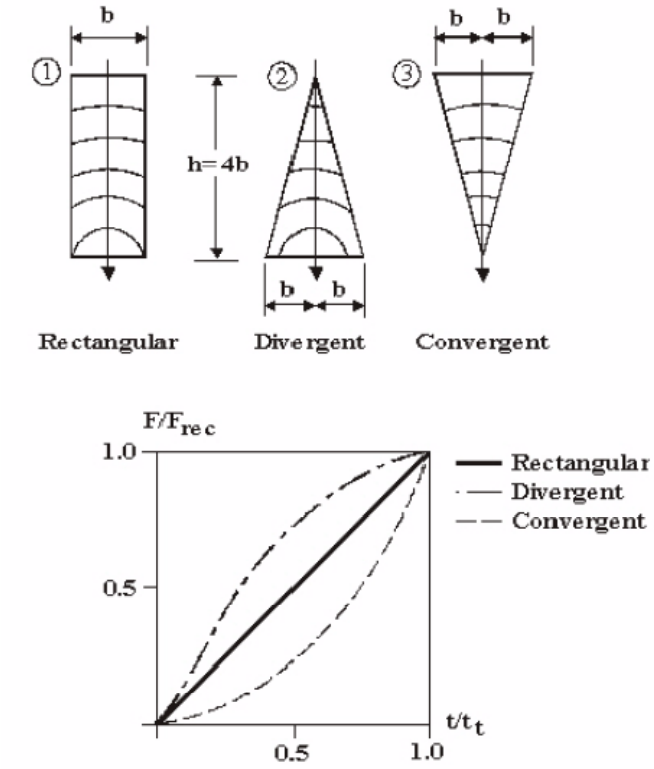

Figure 24: The three pre-defined time/area curves available in MOUSE (DHI, 2008)

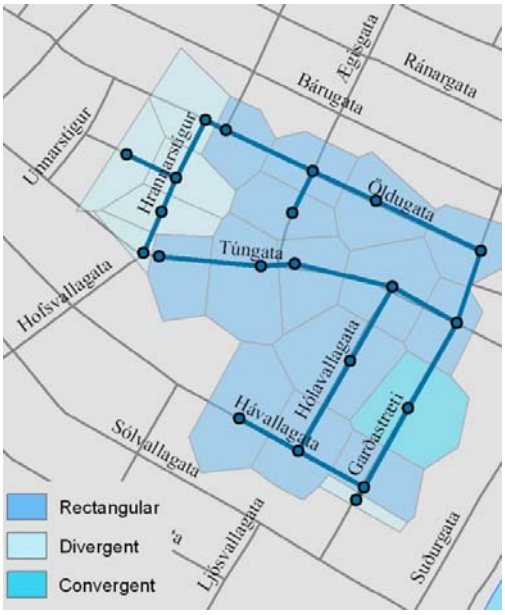

Figure 25: Example of how sub-catchments were classified into rectangular, divergent or convergent are as by Mike Urban

Figure 26: Example of how GIS layers of green areas, roads, sidewalks and houses were translated into runoff coefficients by Mike Urban

To account for wetting and filling of catchment depressions the default value for the on-off initial loss parameter of 0,6 mm was used (DHI, 2008).

The imperviousness of each sub-catchment was calculated based on the runoff coefficients shown in Table 1 using GIS layers of houses, sidewalks, roads and green areas. Figure 26 shows a small part of the system, the underlying GIS layers and the calculated runoff coefficients. To account for densification, runoff coefficients were scaled by 10 and 20% in a special analysis.

Table 10: Runoff Coefficients

Areas	Runoff Coefficient
Houses	0,9
Roads	0,9
Sidewalks and parking lots	0,8
Green areas	0,2

2.5.4 Pipe flow

The pipe flow calculations in Mike Urban simulate unsteady flow with alternating free surface and pressurised conditions using the Saint – Venant equations, or the continuity and momentum equations:

$$\frac{\partial Q}{\partial x} + \frac{\partial A}{\partial t} = 0 \tag{3.23}$$

$$\frac{\partial Q}{\partial t} + \frac{\partial \left(\alpha \frac{Q^2}{A}\right)}{\partial x} + gA\frac{\partial y}{\partial x} = gAI_0 - gAI_f \tag{3.24}$$

where Q is discharge (m^3/s), A is the flow area (m^2), y the flow depth, g gravity acceleration (m/s^2), x the distance in the flow direction (m), t is the time, α the velocity distribution coefficient, I_0 the bottom slope and I_f the friction slope.

The first two terms on the left side represent inertia forces, the third term pressure forces and on the right are gravity and friction forces. The Saint-Venant equations assume a small bottom slope, sub-critical flow, incompressible and homogeneous fluid and they are thus only valid for free surface flow. Mike Urban models pressurised flow by using the Preissmann slot method (see for example Cunge and Wegner (1964)).

The program offers three approaches to solve the equations; the dynamic; diffusive and kinematic wave. The kinematic wave approximation omits the inertia and pressure terms of the momentum equation and is independent of downstream conditions. That means that it cannot account for backwater flow. The diffusive wave includes the pressure, which makes it possible to implement downstream boundary conditions, but only relatively steady backwater phenomena can be simulated. The dynamic wave on the other hand includes all the terms, but is therefore has the most computational demand. The network modelled here is an old, relatively complicated system with negative slopes and complicated connections so the approximations could not be used here. Therefore the dynamic wave method was used, as is in general recommended (DHI, 2008).

2.5.5 Calibration

The parameters defined above, such as runoff coefficients, time area curves, initial loss etc. all help to make a realistic model. When designing a new wastewater system the parameters defined above are generally recommended to be used unchanged (see for example Kloakforsyningen(2004)), but when simulations are done for existing neighbourhoods it is preferable to calibrate the model with real data, to make it more realistic. The hydrological reduction factor parameter, which is used to account for water losses such as evapo-transpiration, imperfect imperviousness etc., can be adjusted so that model results coincide with real data. The default value for the hydrological reduction factor in Mike Urban is 0,90 and that was the first value used in the calibration process.

The optimal way to calibrate a model would be to use rainfall data combined with stream flow measurements. To carry out such measurements was not within the scope of this project. The only measurements available are from a pumping station in Ingólfsstræti

(Tómasson, 2010). There are no real-time measurements, only bi-monthly flow volume readings, which turned out to be faulty due to equipment malfunction. That pumping station does though record the time when there is overflow, so that could be used for calibration, although the measurements turned out to be faulty for the last years due to computer system update.

The pumping station has three pumps, each with a capacity of 160 l/s, i.e. the total capacity is 480 l/s. To find the constant dry weather flow, dry periods were found using IMO precipitation data from Bústaðavegur. These periods of the bimonthly flow volume reading at Ingólfsstræti were analyzed, and the dry water flow was found to be 140 l/s. For a selected number of years which had available overflow time data or the years 2000-2003 the total time when the pumps could not handle the flow (and overflow pumps would be activated) was calculated by simulating the drainage area of the Ingolfsstræti pumping station using IMO precipitation data. data.

As can be seen in Table 11 the overflow hours needed in the model correspond acceptably well to the overflow hours recorded at the pumping station. The measured overflow hours for 2001 are though suspiciously few, compared to the other years, which points to equipment malfunction also in that year.

Table 11: Hours when overflow was in use, in model and in real life for the years 2000-2003

Year	Overflow in Model [h]	Measured Overflow [h]
2000	77,2	**94,2**
2001	61,3	**33**
2002	96,0	**94,7**
2003	103,6	**108,9**

3 Results and Discussion

3.1 Trends and changes in extreme precipitation

To establish whether changes could be seen in extreme short duration precipitation in the available period, 1951-2008, the statistical tests outlined in chapter 2.4.1 were used. The Mann-Kendall (MK) test directly checks for trends, while the Mann-Whitney (MW) and Kolmogorov-Smirnov (KS) tests were used to compare the first half of the period (1951-1980) to the second half (1981-2008). Figure 27 shows the 1-p values from the MK, MW and KS tests for 10, 20, 30 and 60 minutes, for maximum precipitation of each month of the year and finally the annual maxima. As can be seen on the right side of the figures, the tests showed no significant trends on the annual basis. In wastewater system design in Iceland, only the annual values are used, and thus, since no significant trends are observed, for any of the durations (10, 20, 30 and 60 minutes) no significant changes should be expected to have occurred over this period of time.

As is described in chapter 1.1 changes in precipitation differ between seasons. For example in Germany, increases have been observed summer, and decreases in spring (Zolina, et al., 2008). Therefore the analysis was performed on the monthly data as well. The months where the most significant trends can be seen are August and November. For November all tests are significant on a 95% level for 10 and 20 minutes. For 30 minutes only the MW test is significant and none of the tests are significant for 60 minutes. In August for 10 minutes duration, the MK and KS tests are significant on a 95% level, but MW on a 90% level. For 60 minutes all tests area significant on a 95% level, but for 20 and 30 minutes only the MK is significant on a 95% level, while MW is significant on a 90% level and KS not significant at all. The tests show differing results as the MW and KS tests look for different distributions in the time series, while the MK test only looks at trends.

In Table 12 the Theil-Sen estimations of the slope can be seen on annual and monthly basis for the four short duration rainfall events (10, 20, 30 and 60 minutes). The slopes relevant according to the statistical trends are shown as bold. The 95% confidence intervals are also shown, which are found using the bootstrap method described in chapter 2.4.1. The confidence intervals can also be used as a test if the trend is significant; if the interval has both positive and negative values the trend is not significant. To give an indication what a trend means for specific month, the median of the maxima is as well shown in the table, but the median is more frequently used when dealing with extreme values, as it is not as sensitive as the mean (Helsel & Hirsch, 2002).

The most interesting months, or where the trend is significant are August and November. As can be seen on Figure 28, the trend in August is 0,012 mm/year for 10 minutes. This may look small, but if this trend continues for, say, 20 years, the total increase is 0,24mm. Adding that to the median (1,20 mm) gives an increase of 20%. Stated in mm/h/year, as in Table 2, that is 0,072mm/h/year, which is the close to the 0,08mm/h/year trend found for 10 minutes in Canada (Adamowski, et al., 2009). In contrast, Figure 29 shows that in November the trend is negative and considerably smaller than in August but since the median of the November rain is also smaller the decrease would be 16%.

Where the trend is not significant there are still interesting results. The direction of the annual trend is negative (although very small and insignificant) for all durations. Positive

trends are seen in the spring, save for April, for all durations, and negative trends in the autumn.

Careful consideration is needed when interpreting these results. The absence of significant trends over the past 60 years for the short duration annual precipitation maxima does not mean that there has not been any change in other statistical characteristics of precipitation. There may indeed be changes underway (as climate models seem to indicate, see chapter 1.2), but not yet showing significant impacts. The trends that were actually found significant also have to be used with care. That a trend of 0.012 mm/y for the past 60 years has been found for 10 minute duration in August, does not necessarily mean that the same trend will continue in the future.

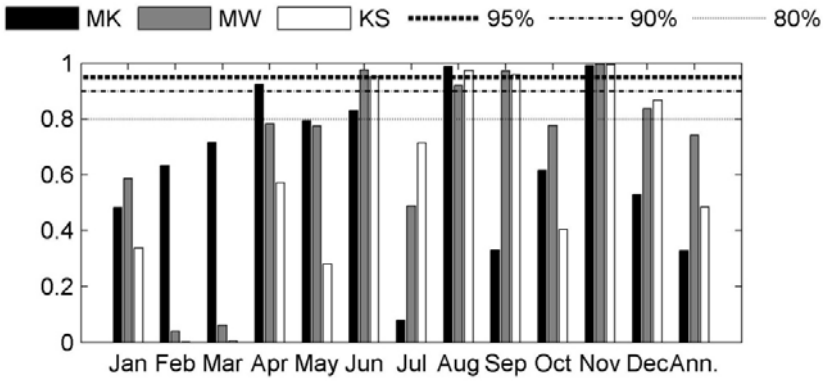

a) 10 minutes

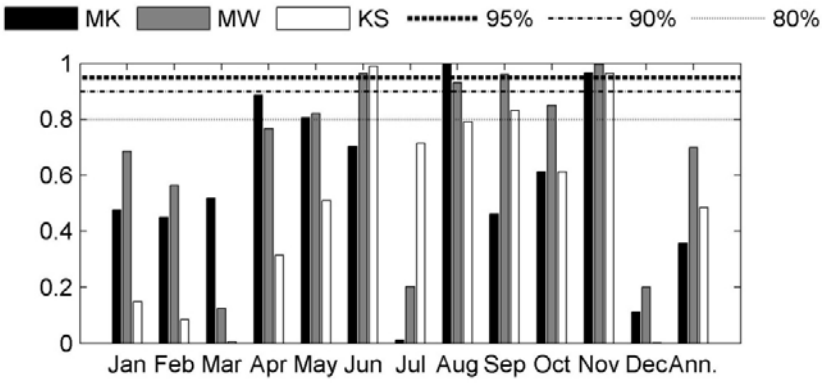

b) 20 minutes

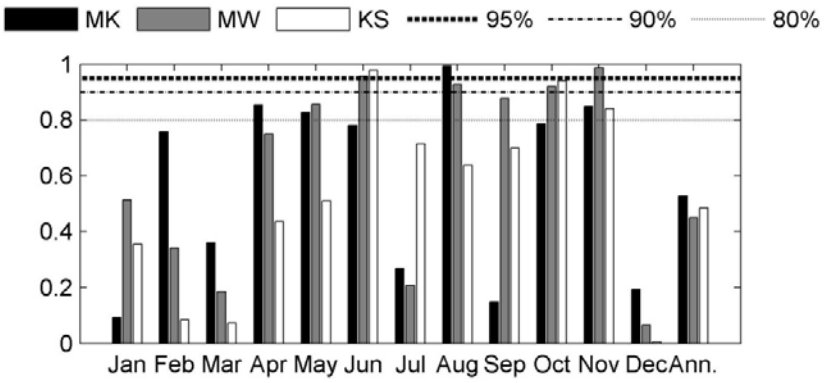

c) 30 minutes

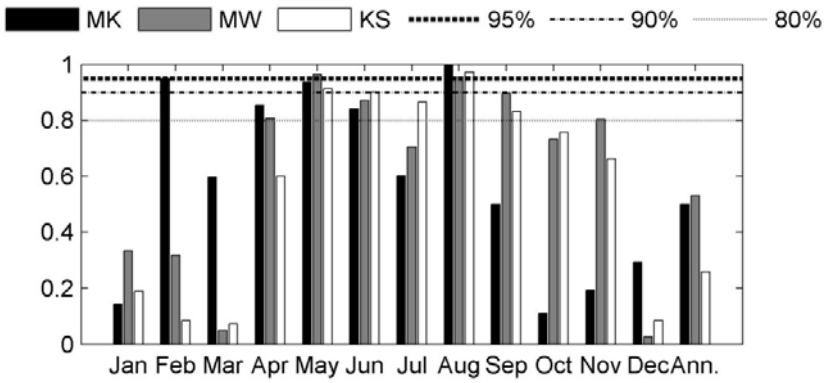

d) 60 minutes

Figure 27: 1-p values from Mann-Kendall, Mann-Whitney and Kolmogorov-Smirnov tests for extreme precipitation with different duration. Shown are the 95%, 90% and 80% 1-p values which mean that on the 5%, 10% and 15% levels the hypothesis of no trend/change is rejected.

Table 12: Slope [mm/year], confidence intervals based on bootstrapping, and median of the maxima [mm]. Bolded text indicates significant trends

	Slope [mm/y]	Conf. interv. [mm/y]		Median [mm]
Ann.	-0.002	[-0.015	0.009]	2.30
Jan	0.000	[-0.010	0.004]	1.10
Feb	0.002	[-0.003	0.008]	1.00
Mar	0.004	[-0.005	0.014]	0.90
Apr	-0.004	[-0.009	0.000]	0.90
May	0.003	[0.000	0.008]	0.90
Jun	-0.006	[-0.017	0.003]	1.00
Jul	0.000	[-0.009	0.008]	1.20
Aug	**0.012**	**[0.000**	**0.022]**	**1.20**
Sep	0.000	[-0.014	0.007]	1.40
Oct	-0.004	[-0.012	0.005]	1.20
Nov	**-0.008**	**[-0.015**	**-0.002]**	**1.00**
Dec	-0.002	[-0.009	0.004	1.20

a) 10 minutes

	Slope [mm/y]	Conf. interv. [mm/y]		Median [mm]
Ann.	-0.003	[-0.024	0.011]	3.50
Jan	-0.003	[-0.014	0.006]	1.70
Feb	0.003	[-0.008	0.014]	1.50
Mar	0.004	[-0.007	0.017]	1.60
Apr	-0.006	[-0.014	0.000]	1.40
May	0.005	[-0.002	0.014]	1.30
Jun	-0.008	[-0.027	0.007]	1.70
Jul	0.000	[-0.019	0.013]	1.70
Aug	**0.020**	**[0.006**	**0.031]**	**1.90**
Sep	-0.005	[-0.023	0.013]	2.10
Oct	-0.004	[-0.017	0.008]	2.00
Nov	**-0.011**	**[-0.021**	**-0.002]**	**1.80**
Dec	0.000	[-0.013	0.013]	2.00

b) 20 minutes

	Slope [mm/y]	Conf. interv. [mm/y]		Median [mm]
Ann.	-0.007	[-0.023	0.012]	4.30
Jan	0.000	[-0.015	0.012]	2.20
Feb	0.007	[-0.008	0.023]	2.00
Mar	0.002	[-0.010	0.018]	2.00
Apr	-0.007	[-0.018	0.004]	1.80
May	0.009	[-0.003	0.021]	1.80
Jun	-0.012	[-0.034	0.010]	2.10
Jul	0.000	[-0.028	0.014]	2.40
Aug	**0.023**	**[0.004**	**0.039]**	**2.40**
Sep	0.000	[-0.025	0.017]	2.40
Oct	-0.008	[-0.021	0.011]	2.50
Nov	-0.008	[-0.022	0.002]	2.30
Dec	0.000	[-0.015	0.019]	2.50

c) 30 minutes

	Slope [mm/y]	Conf. interv. [mm/y]		Median [mm]
Ann.	-0.009	[-0.034	0.018]	6.45
Jan	0.000	[-0.021	0.024]	3.30
Feb	0.019	[0.000	0.040]	3.10
Mar	0.010	[-0.013	0.035]	3.15
Apr	-0.013	[-0.033	0.009]	2.70
May	0.015	[0.000	0.032]	2.45
Jun	-0.017	[-0.040	0.009]	3.10
Jul	-0.011	[-0.041	0.017]	3.20
Aug	**0.033**	**[0.013**	**0.056]**	**3.70**
Sep	-0.011	[-0.046	0.017]	3.60
Oct	-0.001	[-0.036	0.029]	3.70
Nov	0.000	[-0.025	0.015]	3.50
Dec	0.004	[-0.018	0.031]	3.70

d) 60 minutes

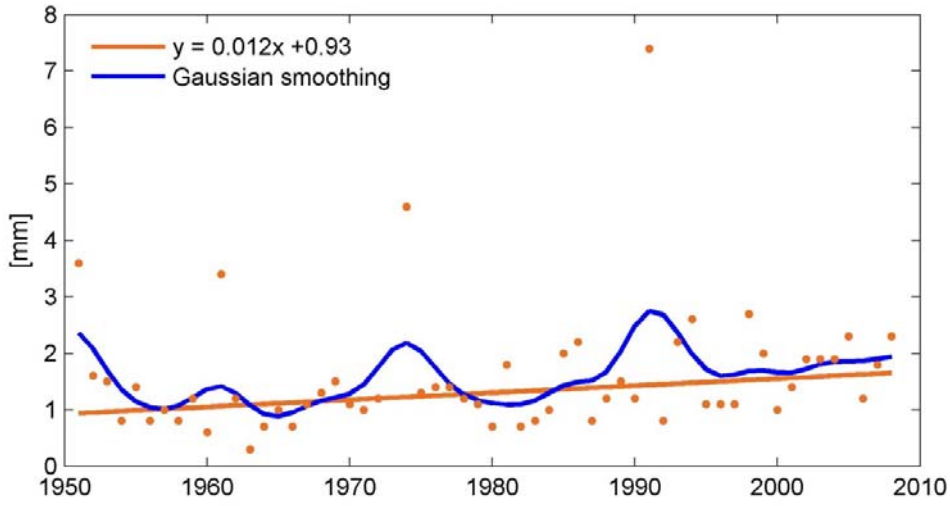

Figure 28: Theil-Sen trend estimation for 10 minutes in August (orange line), and a simplified Gaussian smoothing of the data, showing oscillations in the data (blue line).

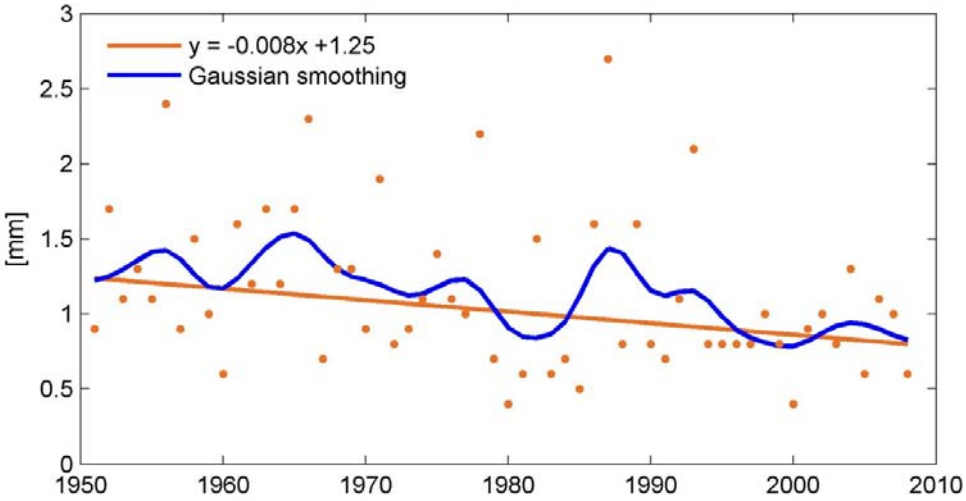

Figure 29: Theil-Sen trend estimation for 10 minutes in November (orange line), and a simplified Gaussian smoothing of the data, showing oscillations in the data (blue line).

3.1.1 Changes in precipitation with a return period of 5 years

For the purposes of wastewater management it may be even more interesting to analyze design parameters such as the event with 5 year return period (M5). The size of the M5 event is found using equation 3.15. When calculated for the entire period (1951-2008) for 10 minutes it is found to be 3.27 mm. To see how it has changed, the M5 (in 10 minutes) is calculated for the entire period over a 20 year moving window thus creating a new series ranging from 1971-2008.

Figure 30 shows this new series, its 95% confidence interval found using bootstrapping (blue lines), as well as the M5 event for the entire period, and its confidence interval (red

lines). What is especially interesting is to see how one measurement can change this design event. Before 1991 the M5 event is steady around 3mm, but jumps up to 3.5 with the downpour event in August 1991. By looking at Figure 31 this can be seen even clearer, as the August 1991 event has been removed (see chapter 2.2). This demonstrates the importance of having long sets of precipitation data when finding precipitation with a certain return period.

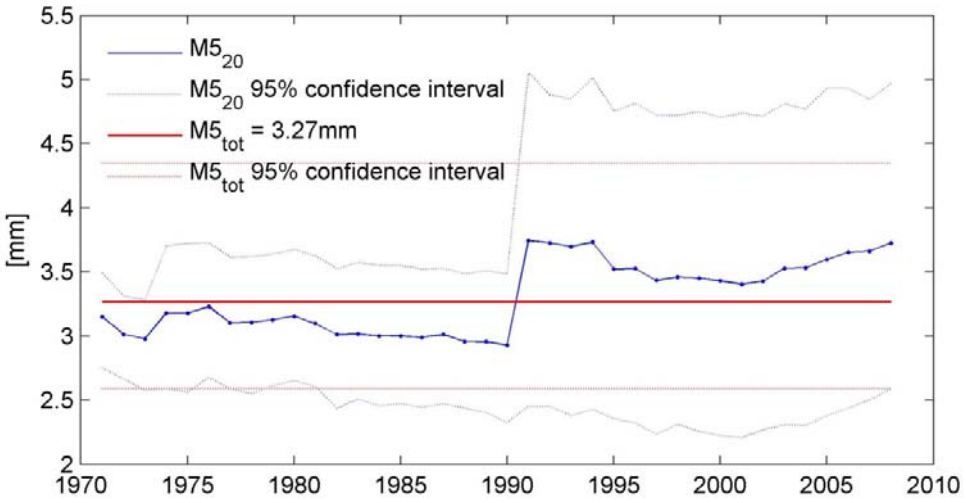

Figure 30: M5 values for 10 minutes calculated over a 20 year moving window (blue points), 95% confidence interval of the 20 year moving window M5 values (blue dotted line), the M5 event calculated for the entire period (red line) and the 95% confidence interval of the M5 event calculated for the entire period.

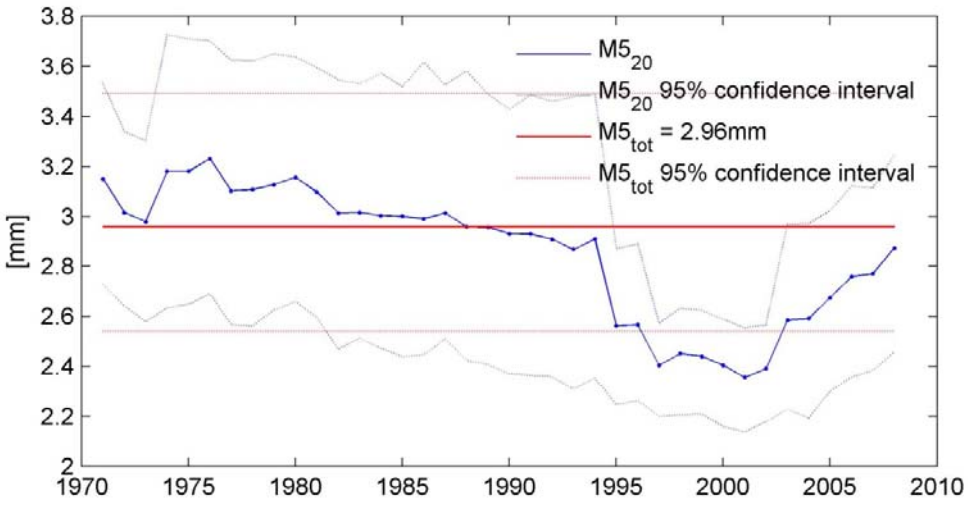

Figure 31: M5 values calculated over a 20 year moving window, as on Figure 30 without including the August event of 1991.

3.1.2 Comparison of IMO data with Breiðholt data

To compare the Breiðholt and the IMO data both scatter plots and a Kolmogorov-Smirnov (KS) test was used (see 2.4.1). If a relationship existed it should be shown by a pattern on the scatter plot shown in Figure 32. For example in March the data points are distributed quite randomly around the 1:1 line, while in November more points are above the line. To analyse further the Kolmogorov-Smirnov (KS) test was used. The null hypothesis is that the IMO data and the Breiðholt data are drawn from the same population. When the p-value (shown in

Table 13) is lower than the significance level the null-hypothesis is rejected, i.e. the samples are assumed to be drawn from different populations. By looking at the table it can be seen that it is accepted at the 5% significance level that both samples are drawn from the same distribution, except in November.

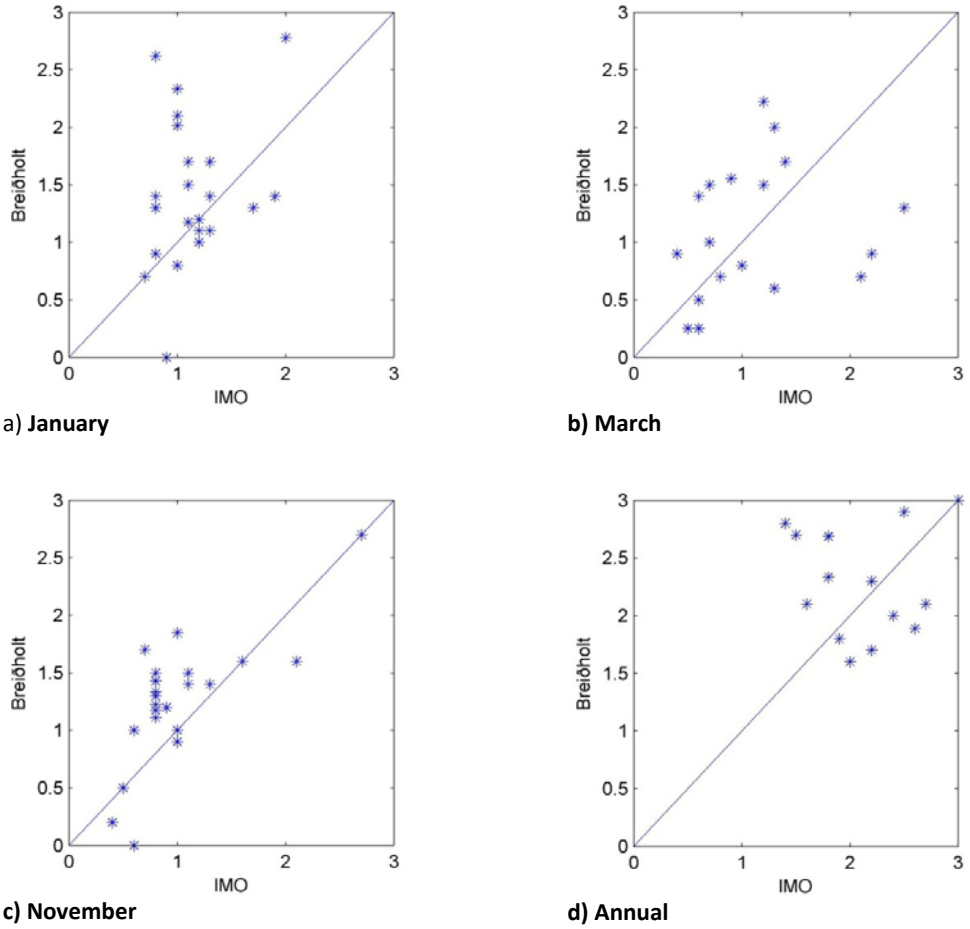

a) **January** **b) March**

c) November **d) Annual**

Figure 32: Scatter plots comparing 10 minutes IMO and Breiðholt precipitation (mm).

Table 13: P-values resulting from a Kolmogorov-Smirnov test comparing IMO and Breiðholt data.

Month	p-value (KS)
January	0,06
February	0,35
March	0,67
April	0,72
May	0,98
June	0,95
July	0,39
August	0,26
September	0,29
October	0,62
November	**0,001**
December	0,14
Annual	0,62

3.1.3 The 1M5 method

The IDF relationship that is currently used for most design in Iceland is described by equation 3.17 using constants derived from precipitation data from the years 1951- 1994 (Table 14). The precipitation data used by Elíasson and Thordarson (1996) to develop the 1M5 method is summarized in Table 14. P_{max} is the maximum precipitation over the 1951-1994 with respective duration; X_n and S_n are the mean and standard deviation of the precipitation series, M5 the precipitation with a 5 year return period calculated with equation 3.16 and C_i as defined in equation 3.19. Table 15 shows the same parameters as Table 14 but for the period 1951-2008 and with re-extracted data.

It can be clearly seen that for 10 minutes almost all the statistical parameters are higher, be it the biggest event, the mean value, the variance, and thus the M5 event or the C_i. The differences decrease for longer durations. It is important to point out that this does not necessarily mean that shorter durations are increasing more, but more likely it is due to the fact that only the 10 minutes data was completely re-extracted. Table 16 shows the values of the parameters as they should have looked in 1994, had the data been correctly extracted. It is almost identical to the current data, as it does include the big event in 1991.

Table 14: Statistical parameters describing the IMO precipitation data from the years 1951-1994 used by Elíasson and Thordarson (1996)

	P_{max}	X_n	S_n	M5	C_i
10 min	4.6	2.3	0.8	3.0	0.215
20 min	6.0	3.5	1.1	4.5	0.203
30 min	9.2	4.5	1.5	5.7	0.213
60 min	17.3	6.7	2.3	8.6	0.215

Table 15: Statistical parameters describing the IMO precipitation data from the years 1951-2000, using re-extracted data.

	P_{max}	X_n	S_n	M5	C_i
10 min	7.4	2.5	0.9	3.27	0.233
20 min	11.0	3.7	1.3	4.82	0.221
30 min	13.6	4.7	1.6	6.00	0.219
60 min	17.6	6.8	2.0	8.47	0.192

Table 16: Statistical parameters describing the IMO precipitation data from the years 1951-1994, using re-extracted data.

	P_{max}	X_n	S_n	M5	C_i
10 min	7.4	2.5	1.0	3.34	0.25
20 min	11.0	3.8	1.5	4.98	0.24
30 min	13.6	4.7	1.8	6.2	0.24
60 min	17.6	6.9	2.2	8.66	0.20

The 1M5 method was developed based in the data available in 1994. The R_a and R_b formulas (equations 3.21 and 3.22) are derived using a linear regression of M5 values as a function of duration on a logarithmic plot. The original R_a and R_b formulas derived by Elíasson and Thordarson (1996b) are shown as red in Figure 33. The R_b equation is derived using M5 values with short duration and R_b with duration of 1 day or longer. As it is not within the scope of this study to look at changes in precipitation with longer duration, the R_b formula is not analyzed here, but the original used. Jónsdóttir et al. (2008) did find a positive trend in maximum one day precipitation at some stations in Iceland so the Rb function should be updated using data from the past 15 years (it was derived using data from 1951-1994).

To find new constants for the R_a formula linear regression was used, which resulted in the following new R_a formula, which is shown as blue in Figure 33

$$R_a = 1{,}031\, t_r^{0{,}5265}$$

No attempt was made to find a confidence interval for these new constants, as this is based on only 4 data points, the M5 values for 10, 20, 30 and 60 minutes.

To see the effects of this new equation the 1M5 method was updated. Table 17 shows calculated precipitation in l/s/ha, based on 1M5 as 38mm and C_i as 0.21, before and after the method was updated. As can be seen the greatest increase is in 10 minutes, and slowly decreases to around 4% in 60 minutes. It is interesting to see that there seems to be a slightly more increase with greater return period. In these calculations the C_i has not been changed, but as was seen in Table 16 C_i seems to be increasing, which matters for return periods greater than 5 years increases the intensity (see chapter 2.4.3).

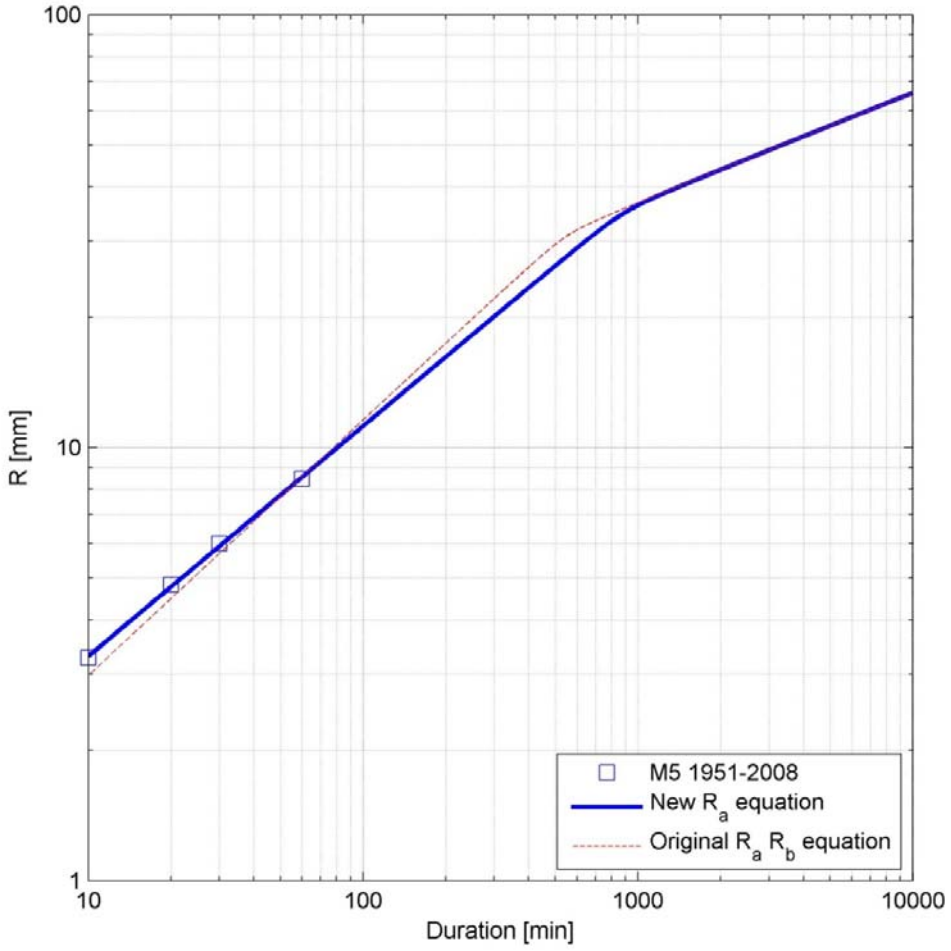

Figure 33: Log-log plot of M5 values. The blue line is based on R_a together with equation 3.22 and the red line on equations 3.21 and 3.22

Table 17: Precipitation intensity [l/s/ha] calculated a) using the original 1M5 method by Elíasson and Thordarson (1996b), b) using the 1M5 method updated using new and re-extracted data, for different duration and return period

	1 year			5 years			10 years		
t_r	a)	b)	Increase	a)	b)	Increase	a)	b)	Increase
10	32	37	15%	48	56	16%	54	63	17%
20	24	27	10%	36	40	11%	41	46	12%
30	21	22	7%	30	33	8%	35	38	9%
60	16	16	3%	23	24	4%	26	27	4%

3.1.4 Connections to other atmospheric variables

As precipitation is an integrated part of the atmospheric cycles, changes in other atmospheric variables may influence precipitation. Climate models are simulating temperature and average or total precipitation so if connection between these variables and short duration extreme precipitation can be found they could help predict future changes in short duration extreme precipitation

Before performing any other analysis a simplified Gaussian smoothing filter (see equation 3.12) was used on the 10 minutes maximum precipitation time series (1951-2008) to see if any underlying pattern could be found. Figure 34 shows the smoothed annual maxima and there seems to be around 15 year oscillation. As can be seen in Figure 35 decadal to multi-decadal oscillations are present in almost all months, although more pronounced in the winter time. The amplitude of these oscillations seems higher than any potential long-term trend, so they make it difficult to see if a long term trend is being found or only a part of multi-decadal oscillation.

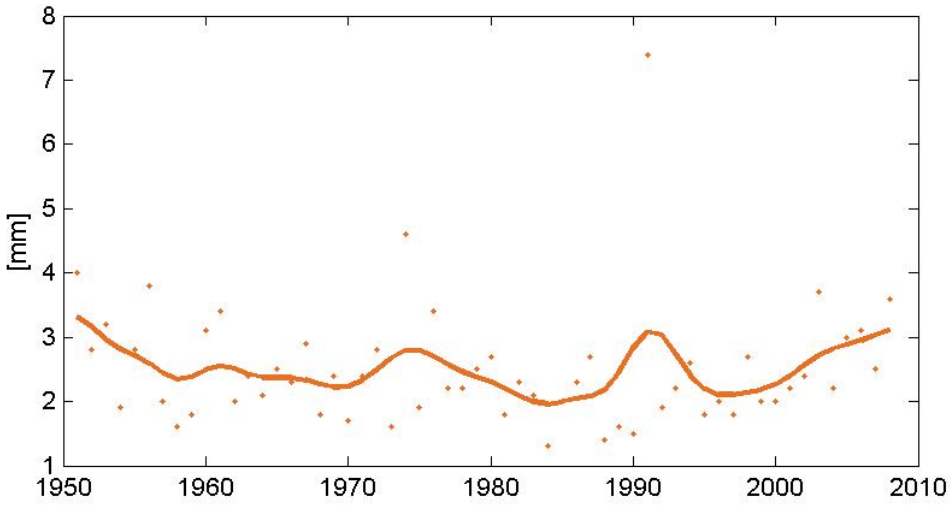

Figure 34: Smoothed 10 minutes annual maximum precipitation

The inconclusive results regarding trends discussed in chapter 3.1 and the oscillations seen in Figures 35 and 36 gave inspiration to analyze whether short duration extreme precipitation could be related to any other atmospheric variables, preferably variables with more available data, or variables that are being analysed in climate models. If such connections could be seen, it would be possible to make predictions about changes in the pattern of short duration precipitation as was for example done by Førland, et al (1998) for maximum 1 day precipitation.

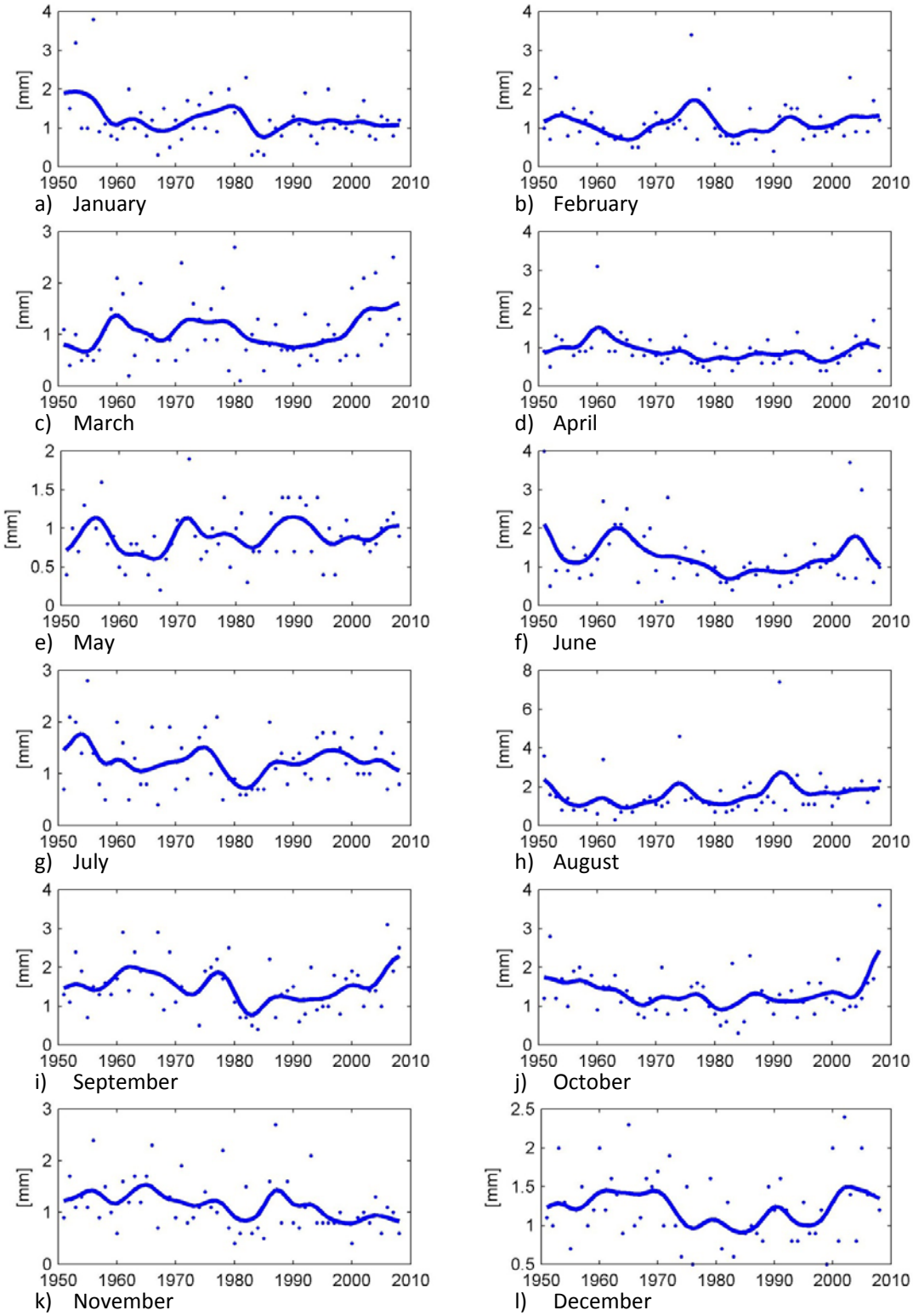

Figure 35: Smoothed lines showing decadal variations for 10 minutes

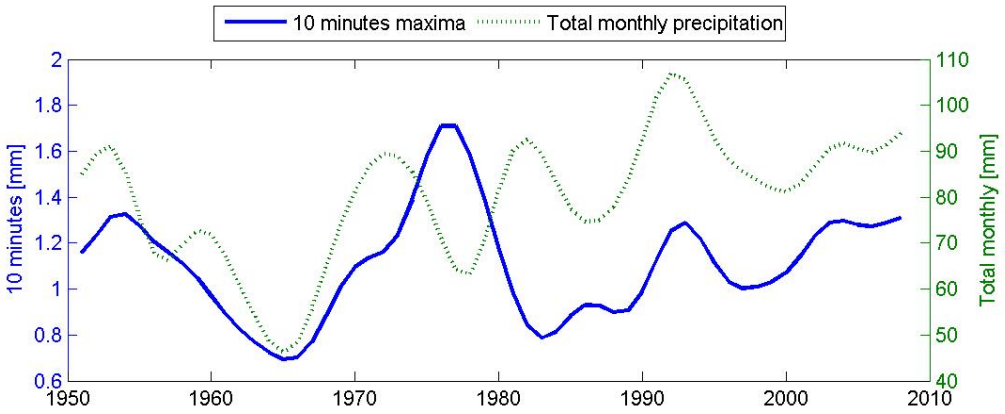

Figure 36: Gaussian smoothing of 10 minutes maximum precipitation and total precipitation in February

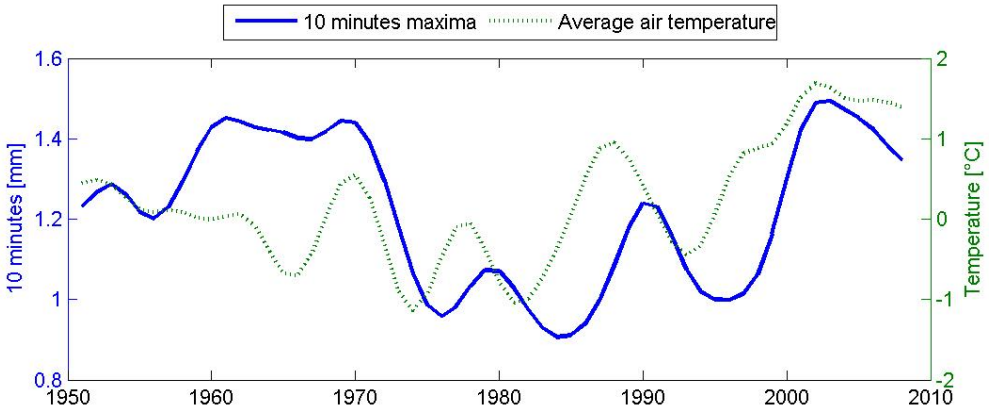

Figure 37: Gaussian smoothing of 10 minutes maximum precipitation and average temperature in December

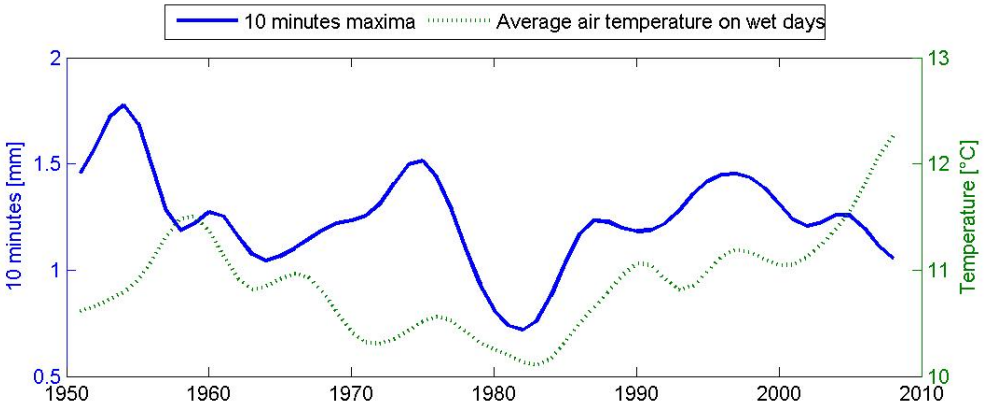

Figure 38: Gaussian smoothing of 10 minutes maximum precipitation and average temperature on wet days in July

The connection will be analyzed in a similar way as the trends were investigated earlier. By looking at Figure 36 it can be seen that in February most of the time when there is high total monthly precipitation, the 10 minutes precipitation is also high. Figure 37 shows both the 10 minutes maximum precipitation and average temperature in December. Both seem to have had 20 year oscillations, with 10 minutes maxima slightly lagged. Figure 38 shows 10 minutes maximum precipitation together with average temperature on wet days in July. Here the oscillations are not as clear, although interestingly wet day temperature seems to have been increasing the past 30 years, and the oscillations are on a 5 year timescale. In the case of Figure 36 the years where total precipitation was the highest would be compared to the lowest years. If there is a significant difference between these two samples from the 10 minutes precipitation series according to the statistical tests, then it is assumed that a connection exists between short duration monthly precipitation maxima and total monthly precipitation. This is done using the Kolmogorov-Smirnov and Mann-Whitney tests.

Total monthly precipitation, average temperature ($\bar{T}$), average temperature on wet days (T_{wet},), and temperature of the day of the maxima (T_d) for the years where dates were available (1986-2008) were analyzed. The full results from the statistical analysis can be seen in Annex I. Firstly, no significant relations were found on an annual basis. The results for each month are summarized in Table 18. Firstly the aforementioned total monthly precipitation was investigated, and, as may be expected this was the variable with the greatest connection, though not in the summer time. This indicates that in winter the greatest extreme precipitation events have a bigger chance to happen during the wettest months.

A limiting factor for checking the relation with temperature was that the exact dates of the maxima are not known before 1986. Thus the average temperature of all days, T, and wet days, T_{wet}, for each month for entire time series and then the temperature at the day of the event, T_d, were analyzed. When only looking at the average temperature, the winter months November – March show the greatest connection, while there is no connection in April and May. Warmer temperatures in winter could be related to more southerly flows, associated with storms bringing moist air and precipitation over Southern Iceland. There is not the same pattern when looking at the average wet day temperature and the temperature at the day of the event. There the strongest connection is found in July and August, possibly indicating more convective activity.

Table 18: Months where significant connection (Annex I) between 10, 20, 30 and 60 minutes extreme precipitation and R_{tot} , total monthly precipitation, , $\bar{T}$, average temperature, T_{wet}, average temperature on wet days, and T_d, temperature of the day of the maxima (1986-2008).

	Jan	Feb	Mar	Apr	May	Jun	Jul	Aug	Sep	Oct	Nov	Dec
R_{tot}	x	x	x	x	x				x	x	x	x
$\bar{T}$		x	x			x					x	x
T_{wet}							x	x	x			x
T_d	x						x	x				

3.2 Flood Modelling

As was outlined chapter 3.1, the updating of the data resulted in a 16% increase of 10 minutes design intensity in the 1M5 method. The trend analysis showed that in August an increase of 20% could be expected given that the same trend will continue for 20 years. According to climate models (see chapter 1.3) a 20 % increase is not a likely scenario, but using that increase should give a clear indication of the weaknesses of the system and locations of sensitive areas in the system. This scaling is of a similar magnitude as used in Table 6. Based on this, three main scenarios were modelled using Chicago Design Storms (CDS) with precipitation intensity with a 5 year return period, and IMO digital data from 1998-2008, firstly current design requirements, meaning the original 1M5 method (CDS_1) developed by Elíasson and Thordarson (1996b), shown here to give 16% lower values than the updated 1M5 method, correspondingly the IMO precipitation series for 1998 to 2008 scaled down by 16% (IMO_1); secondly the updated 1M5 method (CDS_2) and correspondingly the IMO precipitation series (IMO_2) and thirdly a 20% scaling of both the IMO series (IMO_3) and the updated 1M5 method (CDS_3).

Table 19: Precipitation scenarios analyzed

	Current design requirements	Current situation	20% upscaling
CDS	CDS_1	CDS_2	CDS_3
IMO (1998-2008)	IMO_1 (84% of IMO_2)	IMO_2	IMO_3 (120% of IMO_2)

To determine the difference between these 6 cases a number of indicators were defined. Three levels of flooding can be defined, based on the potential damages. Firstly, according to design requirements set forth by Reykjavík Energy (Orkuveita Reykjavíkur, 2008) pipes should not be running more than full, i.e. under pressure, with 5 year return period precipitation. Therefore the number of full flowing pipes is defined as an indicator, i.e. where the water level in a pipe divided by the diameter is equal to one (P). The P indicator was only calculated for CDS. Secondly, the pressure increase when water rises in manholes can cause flooding in low lying cellars, although no flooding is seen on the surface. Therefore the number of manholes where water level reaches 1 m below ground is defined as an indicator (M_{-1m}). Thirdly, to count in how many places surface flooding occurs the number of flooded manholes (M) is defined as an indicator. Lastly, to quantify the magnitude of surface flooding the volume of water flowing out of the system, up from manholes, is defined as an indicator (V).

The number of full flowing pipes (P) and the number of flooded manholes (M) are the indicators that are critical in terms of design, as Reykjavík Energy requires that during an event with a return period of 5 years (or 20 years for sensitive areas) that pipes are not under pressure, and that the hydraulic grade line never reaches the surface, i.e. manholes are never flooded (Orkuveita Reykjavíkur, 2008).

To sum up, these four indicators were defined for the system:

1. Number of flooded manholes (M)
2. Number of manholes with water level 1 m below ground (M_{-1m})
3. Number of full flowing pipes (P)
4. Volume of water flowing up from manholes (V)

Mike Urban has its own main indicators; water level in pipes and in manholes. It is possible to calculate other indicators using Mike Urban, but because of the length of the IMO series and the complexity of the system the amount of data was on the high end for Mike Urban to handle. It was therefore decided to use the more robust calculation program MATLAB for all further calculations. Although the entire area shown in Figure 14 was modelled in Mike Urban, only the pipes and corresponding manholes shown in Figure 39 were analysed. The area selected represents the drainage area of the pumping station in Ingólfsstræti without problematic boundary points. This area has 487 pipes and 444 manholes compared to 949 and 862 in the total model, so calculations were considerably faster than if the entire model had been analysed. This area does contain the oldest part of the system, and the most sensitive area, where for example the parliamentary buildings are situated.

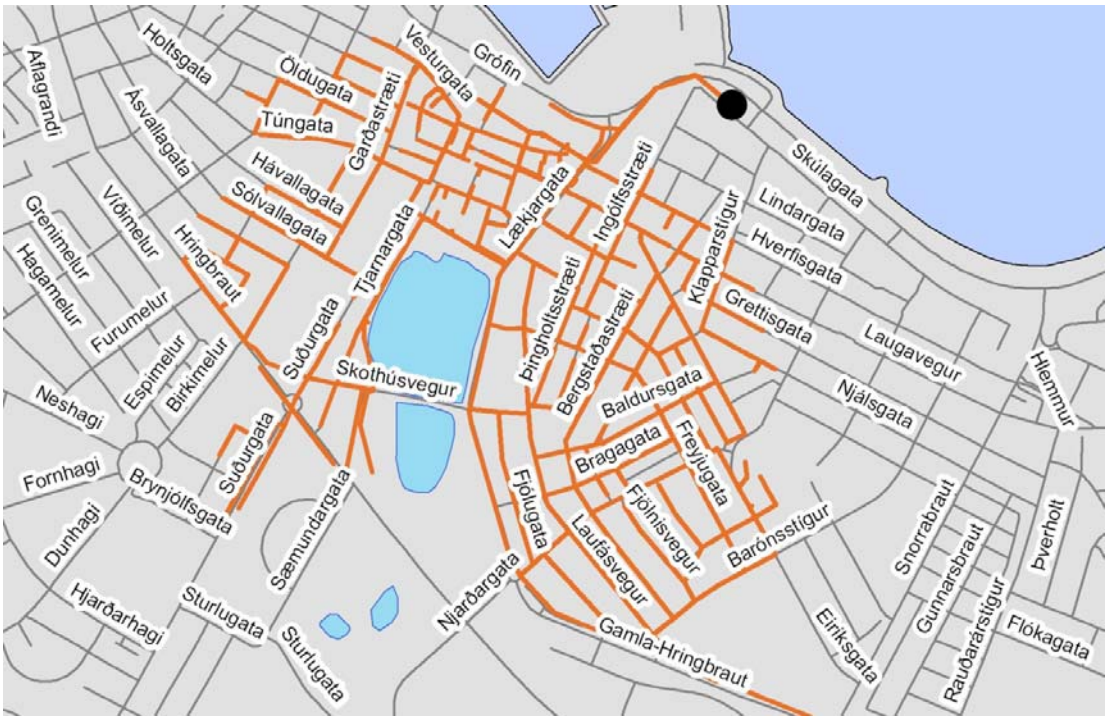

Figure 39: The part of the system analysed. Represent the drainage area of the pumping station in Ingólfsstræti (shown with a black point) without problematic boundary points.

3.2.1 Chicago Design Storms

As shown in Table 19 three sets of Chicago Design Storms were analysed. Firstly the CDS that have been in use for the past 15 years (CDS_1), secondly the CDS based on the updated 1M5 method (CDS_2) and thirdly a 20% scaling of CDS_3 (CDS_3). Figure 40 shows the Chicago Design Storm for CDS_2.

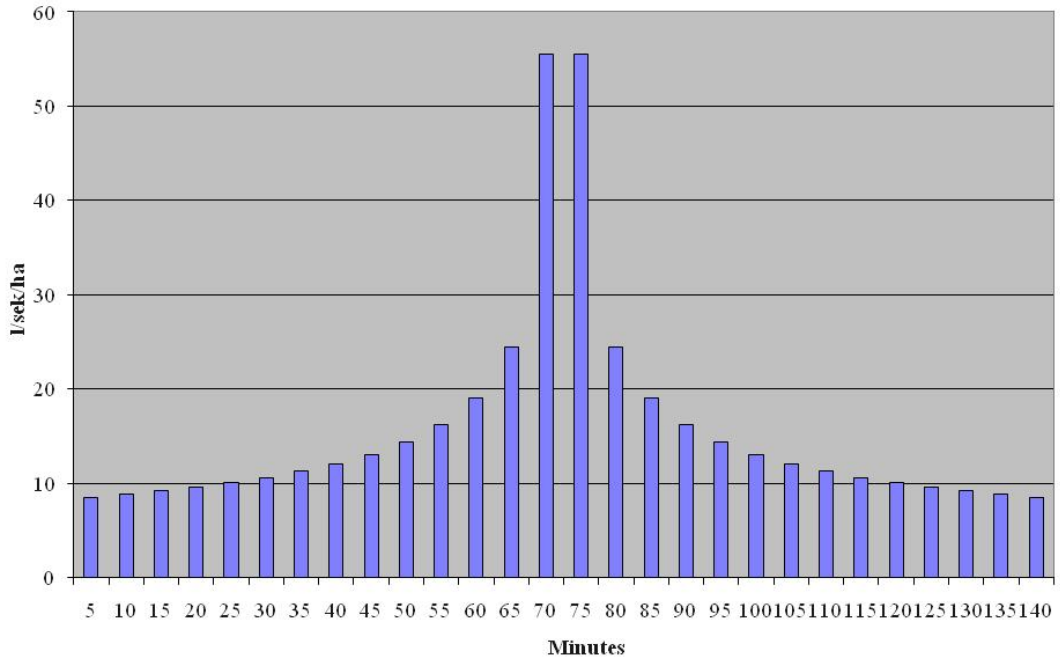

Figure 40: CDS_2: Chicago Design Storm from 1M5 method with updated precipitation data. Return period of 5 years and duration of 10 minutes

When using Chicago Design Storms the least favourable duration should be selected. The updated 1M5 was used to generate 10, 20 and 30 minutes CDS_2, and the three manhole related indicators calculated. As can be seen in Table 20 duration of 10 minutes is the least favourable duration, as the three indicators are all greatest with 10 minutes CDS. This area is therefore the most sensitive to very short rain showers, which is typical for small systems. Larger capacity pipes far down the system are more sensitive to longer duration precipitation but still problems are not observed for example close to Ingólfsstræti pumping station.

Table 20: Comparison of Mike Urban model indicators for CDS_2 simulations assuming variable rainfall duration of 10, 20 and 30 minutes with a return period of 5 years.

Duration [minutes]	M	M_{-1m}	V [m^3]
10	26	135	469
20	9	88	159
30	6	74	52

To see what return period was the most sensitive to the update of the 1M5 method, the 2 indicators that are used in design for Reykjavík Energy, M, P, were calculated for 2, 5, 20 and 50 year return periods. Table 21 shows these indicators for CDS_1 and CDS_2 and how much increase was seen from the original CDS_1 to CDS_2. As expected, more floods are seen with higher return period, but interestingly the greatest change for these indicators is for the 5 year return period. For most of the analysis below, a 5 year return period is used,

as this is the most commonly used return period for regular wastewater systems, although this is central area and should therefore be design for 20 year return period events. Using 5 year return period also enables comparison to the 11 year IMO time series.

Table 21: The M and P indicators for CDS1 and CDS2, and their percentage increase, for different rainfall return periods.

	M			P		
	CDS_1	CDS_2	Increase	CDS_1	CDS_2	Increase
2 yr	14	18	29%	81	109	35%
5 yr	**19**	**26**	**37%**	**94**	**136**	**45%**
10 yr	27	37	37%	119	160	34%
20 yr	37	49	32%	146	185	27%
50 yr	50	65	30%	169	224	33%

Table 22 provides an overview of the four indicators for the three analysed cases with a return period of 5 years. In the table it can be seen that the number of incidents has considerably increased compared to the current design practice. Interestingly, for CDS_3 that was scaled 20% from CDS_2 the number of flooded manholes and volume increases a great deal more than 20%.

Table 22: Overview of the four indicators for the three analysed CDS cases with return period of 5 years. Lower line shows a percentage increase from CDS_1.

	CDS_1	CDS_2	CDS_3
M	19	26	43
	-	37%	126%
M_{-1m}	120	135	164
	-	13%	37%
P	94	136	175
	-	45%	86%
V	337	469	852
	-	39%	153%

Figures 41-43 show both all the locations of flooded manholes (M), as well as the volume flowing from each manhole (V) represented by varying size red circles. These figures show clearly that there are specific areas which become more problematic with greater precipitation; where for CDS_1 (Figure 41) there are none or little problems, i.e. the most problematic areas consist of only 1-2 manholes with a small volume of surface flow, but for CDS_2 (Figure 42) and CDS_3 (Figure 43) the problems escalate, more surface water volume and neighbouring manholes start filling up as well. Firstly already for CDS_1 a considerable flooding seems to be happening at Tjarnargata, by the pond (see Figure 39 for street names). This is a residential street close to the pond so immediate surface flooding threat (property damage) is lowered as the pond can be the receiving body, although as it is an important recreational area, untreated wastewater should not enter into the pond. Flooding property damages have already been in Tjarnargata as can be seen in Figure 12 on page 19.

Another location were a model flood coincides with a reported flood is by Hringbraut (the left side of the maps were a cellar flood was reported in 2007. For CDS_1 only minor floods can be seen in Hringbraut, but for CDS_2 the floods have reached up to Ljósvallagata where the actual flood was reported. For CDS3 the volume on the street has increased greatly and the flood spread further up the street. Hringbraut is a high traffic road, but rather narrow in the area where the flooding seems to be taking place. This flooding could therefore be a danger to traffic.

Other escalating problematic areas are the intersections of Gamla-Hringbraut/Laufásvegur (lower right corner) and Lækjargata/Skothúsvegur (right side of the pond). Both these areas show problems already for CDS_1, but no damages have been reported to Sjóvá. Possible explanitions for these as well as other areas is that not all rainwater ends up in the wastewater systems, as gullies are generally small and far between them. Close to both of these areas are open, green areas that are potentially taking some of this rainwater.

At Vesturgata (top of Figures 42-43), no problems can be seen for CDS_1 but in CDS_2 water is briefly seen at the surface for one manholes, while for CDS_3 5 manholes are flooded. This shows the sensitivity of the area.

In Figure 44-47 the relative water level can be seen, i.e. the depth of water in the pipe (y) divided by the diameter (D). Where the pipes are red, i.e. y/D is equal to 1 the figures show the indicator P. Already for CDS_1 there is a considerable amount of pipes already full or under pressure, or 20%. Although such large part of the system is full for CDS_1 there is still some capacity left in the system in CDS_3 or in 64% of the system the pipes are not under pressure. 40% of the pipes are less than 75% full. Interestingly, no problems are observed in the old Lækur, mention in chapter 1.5 (Figure 10, which now is a sewer with diameter of 1,6m).

Figures 47-49 show where the water level in manholes reached 1 m below ground (M_{-1}), and for how long time. Here it can be seen that in the sensitive area between the pond and the sea, the water level is already quite high in manholes. This is for example where the parliamentary buildings are located. This is also geographically the lowest area in the model, meaning that coupled with an increase in sea level, floods might become likely.

Figure 41: Location of flooded manholes (M) and volume (m^3) of water flowing up from manholes (V) for CDS_1 with a 5 year return period

Figure 42: Location of flooded manholes (M) and volume (m^3) of water flowing up from manholes for CDS_2 with a 5 year return period

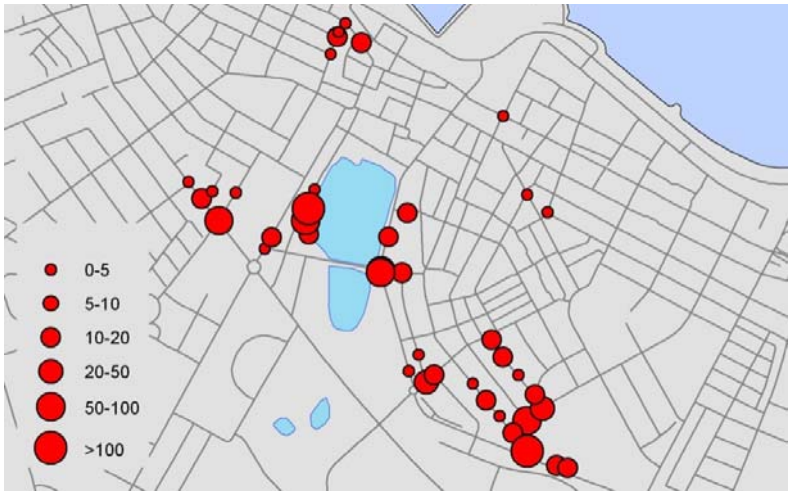

Figure 43: Location of flooded manholes (M) and volume (m^3) of water flowing up from manholes for CDS_3 with a 5 year return period

Figure 44: Relative water level (y/D) in pipes for CDS_1 with a 5 year return period

Figure 45: Relative water level (y/D) in pipes for CDS_2 with a 5 year return period

Figure 46: Relative water level (y/D) in pipes for CDS_3 with a 5 year return period

f 

Figure 47: Manholes with water level 1m below ground (M_{-1}) and the duration of that water level for CDS_1 with a 5 year return period.

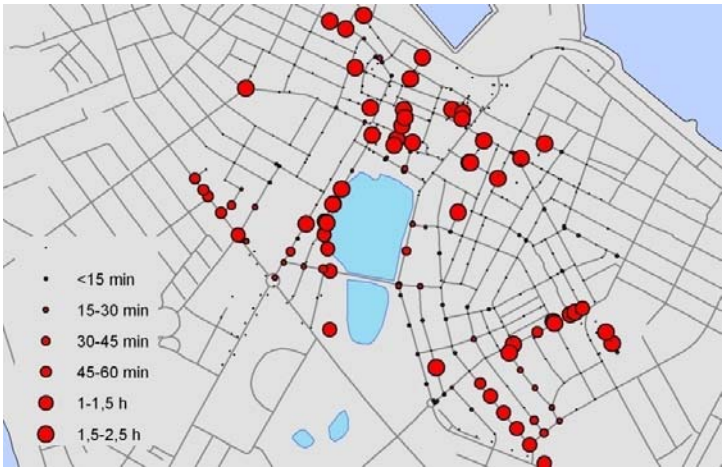

Figure 48: Manholes with water level 1m below ground (M_{-1}) and the duration of that water level for CDS_1 with a 5 year return period.

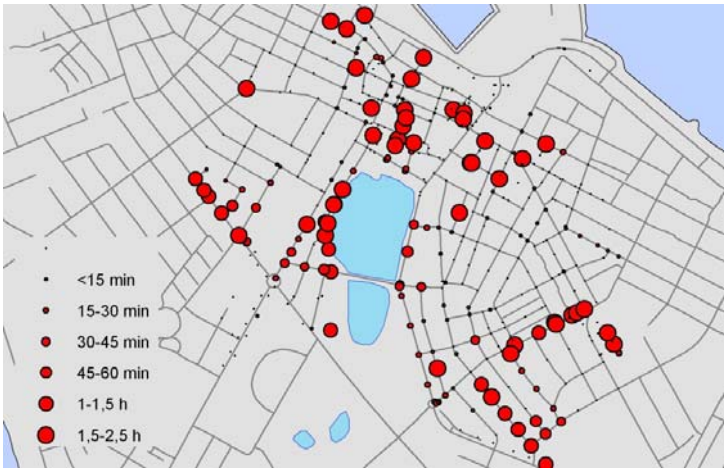

Figure 49: Manholes with water level 1m below ground (M_{-1}) and the duration of that water level for CDS_1 with a 5 year return period.

3.2.2 IMO precipitation time series

The IMO has had a digital rain gauge with a 10 minutes resolution since 1998 at its premises. As can be seen on Figure 14 on page 21 the rain gauge is about 2-3 km from the analysed area, and is on a hill, about 50 m above sea level while the highest point in the model is 38 m above sea level, and most of the drainage area is between 10 and 20 m above sea level.

Table 23: Overview of the three indicators, M, M_{-1m} and V for the three analysed cases IMO_1, IMO_2 and IMO_3.

	IMO_1	IMO_2	IMO_3
M	0	12	25
M_{-1m}	40	100	140
V [m^3]	0	271	852

One of the most interesting results from this analysis is that no flooding is seen using IMO_1 (the downscaled series), and the water rises up to 1 m below ground level for only 40 manholes (M_{-1m}), while for IMO_2 (the actual time series), 12 manholes are flooded and M_{-1m} more than doubles. IMO_1 as scaled down by 16% to imitate the current design practice (1M5 method by Elíasson and Thordarson (1996b)) which gives 16% lower design intensity. This clearly shows the significance of the update.

As this is a series with 11 years it may be expected that a CDS with a 5 year return period would be seen at some point, and indeed both in 2008 and 2003 events with 10 minutes precipitation higher than the M5 event, 3.27mm, but the indicators indicate no comparable heavy events during this time. This indicates that the 1M5 method together with CDS is a conservative one.

For the IMO series, the indicators M and M_{-1m} were not only used to count the number of manholes flooded, but also the number of flooding events (flooding event here refers both to M and M_{-1m}). Flooding events are delimited by 6 hours of no flooding, i.e. a new flooding event is counted if 6 hours pass from the last flood, which is comparable to how precipitation events are defined in Hrafnsdóttir (2005). The CDS analysis in chapter 3.2.1 only accounts for the magnitude and location of possible flooding events, not the frequency of their occurrence. As pointed out in chapters 1.1 and 1.2 the frequency of extreme events has already been observed to increase and an increase is projected. Table 24 shows the number of flooding events for M and $M_{-1m.}$ Figures 50- 52 show firstly all flooded manholes (M) and the associated volume (V) with blue dots, and secondly the M_{-1} flooding events with red dots (M_{-1}). The increasing size of the red dots in Figures 47- 49 show that the number of cellar flooding events may increase, indeed there are 35% more M_{-1} events for IMO_2 than IMO_1 and 40% more for IMO_3, a development which could be escalated by more frequent storms.

Table 24: Overview of the number of flooding events for M and M_{-1m} for the three analysed cases IMO_1, IMO_2 and IMO_3.

	IMO_1	IMO_2	IMO_3
M	0	38	98
M_{-1m}	42572	57819	59211

By comparing Figures 50-52 and Figures 47-49 it can be seen that although the amount of manholes that have flooded (M) is a lot lower for IMO than CDS, water is rising up in manholes at the same places (M_{-1}). The sensitivity of the central parliament area is clearly seen for all the IMO cases; same applies to Tjarnargata and Hringbraut.

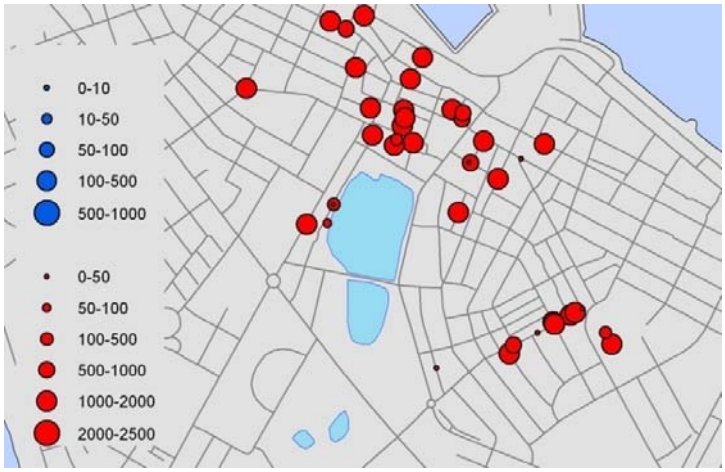

Figure 50: Volume (blue dots, m^3) of water flowing up from manholes, and M_{-1}, the number of times the water level is 1m below ground (red dots) for IMO_1 (1998-2008).

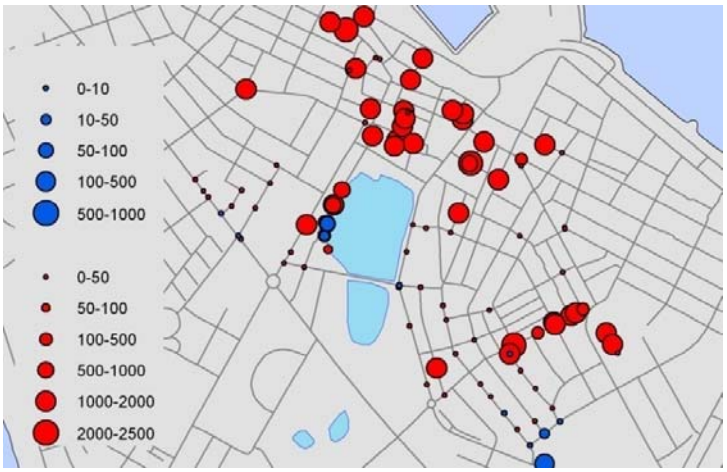

Figure 51: V, volume (blue dots, m^3) of water flowing up from manholes, and M_{-1}, the number of times the water level is 1m below ground (red dots) for IMO_2 (1998-2008).

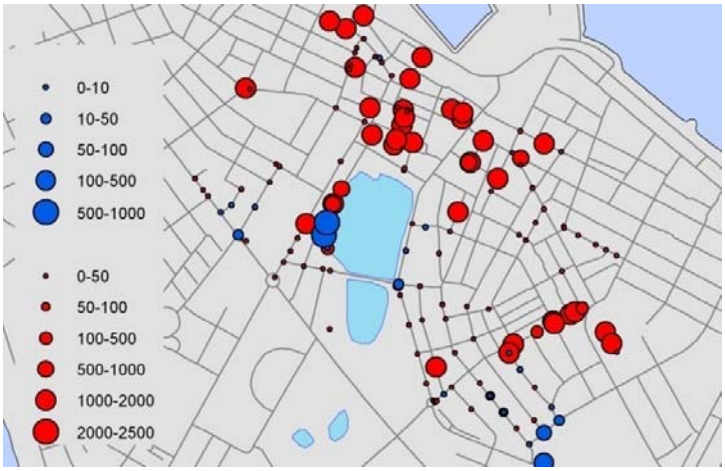

Figure 52: Volume (blue dots, m^3) of water flowing up from manholes, and M_{-1}, the number of times the water level is 1m below ground (red dots) for IMO_3 (1998-2008).

3.2.3 Densification

As was outlined in chapter 2.1.1, increased density is planned in the city before 2024 (Skipulags- og byggingarsvið, 2008). This increased density will increase the runoff coefficients. If planned buildings and constructions were known these could be implemented in the GIS layers used to assess the runoff coefficients in Mike Urban, but as they are not, the simplification was made that the density increased uniformly in the entire drainage area. All runoff coefficients of the model were thus scaled by 10% and 20%, both for the updated CDS_2 and the possible future scenario of CDS_3.

Table 25 provides an overview of all four indicators for the four cases, i.e. both CDS_2 and CDS_3 with runoff coefficient scaled by 10 and 20%. By comparing the last line in CDS_2, the 20% density increase, and the first line in CDS_3, the hypothetical 20% increase in precipitation, it can be seen that planned increase in densification may influence flooding way more than illustrational extreme increase in precipitation, as the indicators for 20% increase in densification are higher than for 20% increase in precipitation (CDS_3).

Table 26 compares the results in Table 25 with the indicator results for CDS_2 from the original model shown in Table 20. As can be seen for CDS_2 the indicators increase from 15% to 39% with only 10% densification. The combined effects of densification and a 20% increase in precipitation (CDS_3) are shown in the lower part of Table 25. With a 10% increase in density the number of flooded manholes (M) and volume of water flowing from them (V) more than doubles, and for the 20% increase the volume (V) more than triples.

Table 25: Effect of densification on wastewater system flooding indicators assuming a 10 and 20% increased density for CDS_2 and CDS_3 with a 5 year return period. For comparison the zero alternative, no densification, is shown as well.

	C	M	M_{-1m}	V [m^3]	P
CDS_2	0%	26	135	469	136
	10%	35	155	645	158
	20%	45	164	903	177
CDS_3	0%	43	164	852	175
	10%	54	178	1220	190
	20%	62	205	1558	217

Table 26: Values of flooding indicators with increased density (Table 25) compared to original normalized with CDS_2 (Table 20).

	C	M	M_{-1m}	V [m^3]	P
CDS_2	10%	35%	15%	38%	16%
	20%	73%	21%	93%	30%
CDS_3	10%	108%	32%	160%	40%
	20%	138%	52%	232%	60%

Figure 53 shows the most extreme case which could be the scenario after 20 years, if the trend continues, and the current plan for a denser city will have come true.

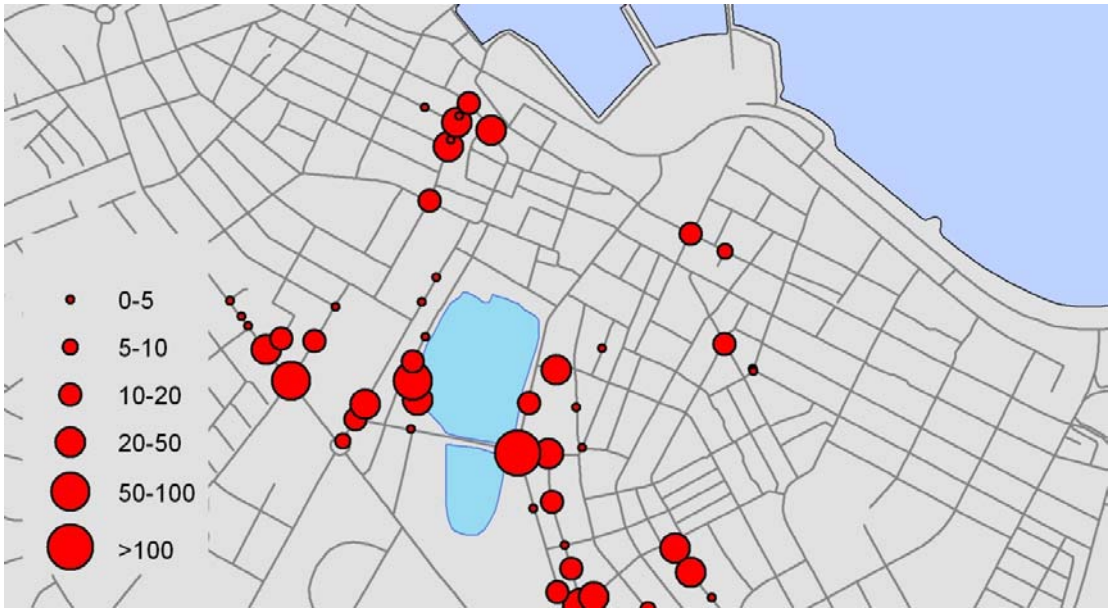

Figure 53: Volume (m^3) of water flowing up from manholes for CDS_3 with a 20% higher runoff coefficient.

3.2.4 Sections

Here above it has been described how the frequency of floods changes with increased precipitation and densification. The maps in figures 42 to 54 show clearly where problems are to be expected with large precipitation events. All these points warrant further analysis, to see how these problems can be avoided, and what solutions would be best for each case. By using data from insurance companies, such as shown in Figure 12, page 19, damages could be assessed and priorities made. This is outside of the scope of this study, but Figures 55–57 are examples of sections from Mike Urban where flooding occurs. These are all places mentioned in the previous sections, chosen as examples because each represents special potential problems.

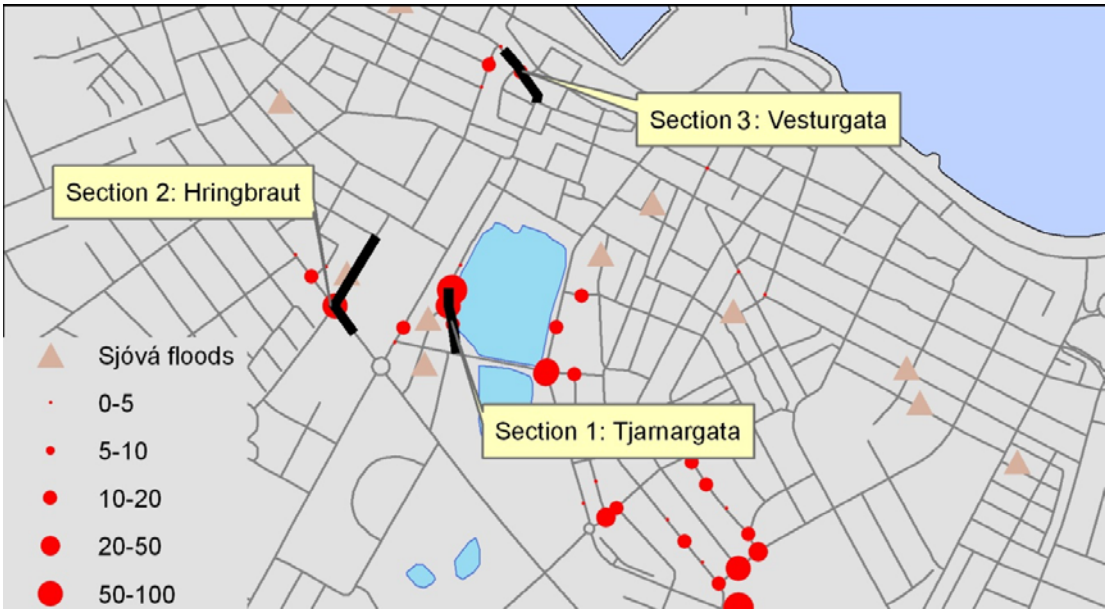

Figure 54: Location of sections of problematic areas. Red dots are volume of water flowing up from manholes (V) for CDS_3 and the triangles are flooding incidents registered by the Sjóvá insurance company.

As pointed out before, Tjarnargata is one of the streets where property damage has been reported due to flooding, and all CDS show this as a problematic spot. As the section in Figure 55 shows the pipes are relatively large, compared to this system (Figure 18) but there is barely any slope, and even a negative slope for the last section, which increases the effect of a narrower pipe downstream.

Section 2, in Figure 56, displays another case of a pipe being connected to narrower downstream pipe. Where Ljósvallagata meets Hringbraut the 250mm pipe in Ljósvallagata connects to a 229 mm pipe in Hringbraut, causing flooding and backup problems. As Figure 54 shows problems have already been observed in Ljósvallagata. When a pipe is connected to a narrower one, that not only decreases the hydraulic capacity, but at the connection there is an increased risk of sedimentation and in general that floating matter will get stuck there.

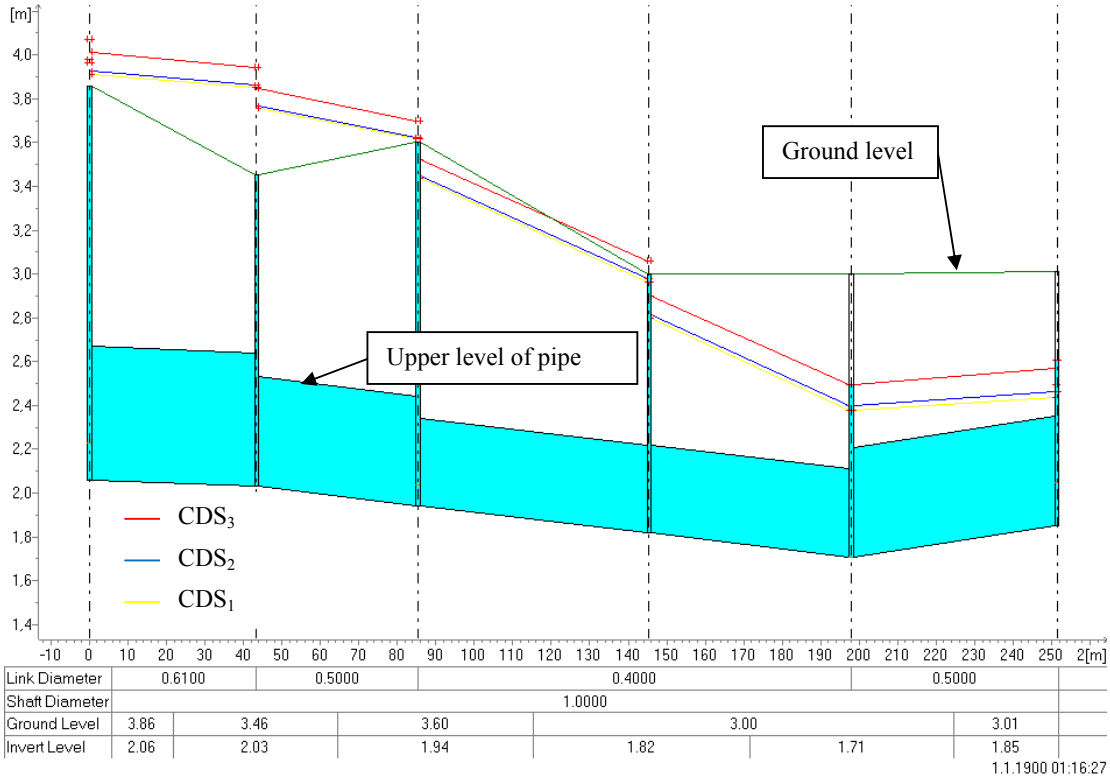

Figure 55: Weak section 1 – Tjarnargata

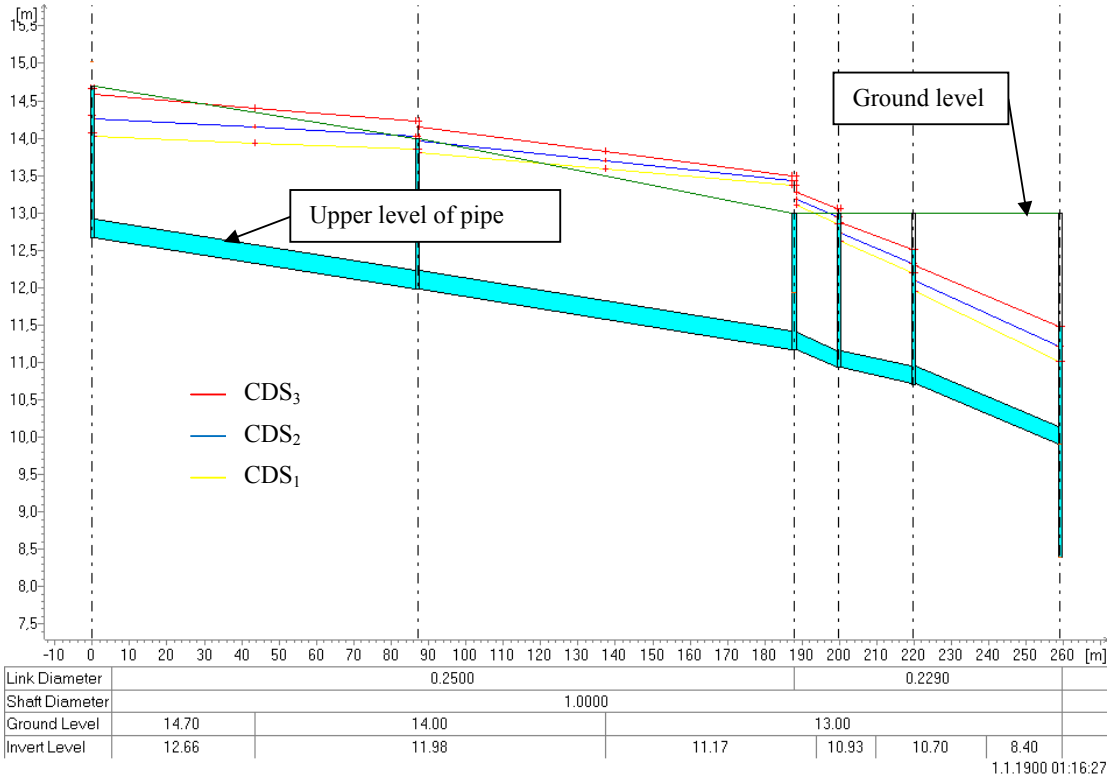

Figure 56: Weak section 2 – Ljósvallagata/Hringbraut

Vesturgata, shown in Figure 57 is not as obviously problematic as Tjarnargata; according to the current design criteria no floods should be seen on the surface for the 5 year CDS_1, but already with the updating the problems can be noticed (CDS_2), and the whole area around becomes problematic if the CDS is scaled up (CDS_3). As can be seen, the first pipe has a high slope, or around 50‰, while the receiving pipe, of the same size has a lot lower slope or around 7‰, and therefore a lower capacity.

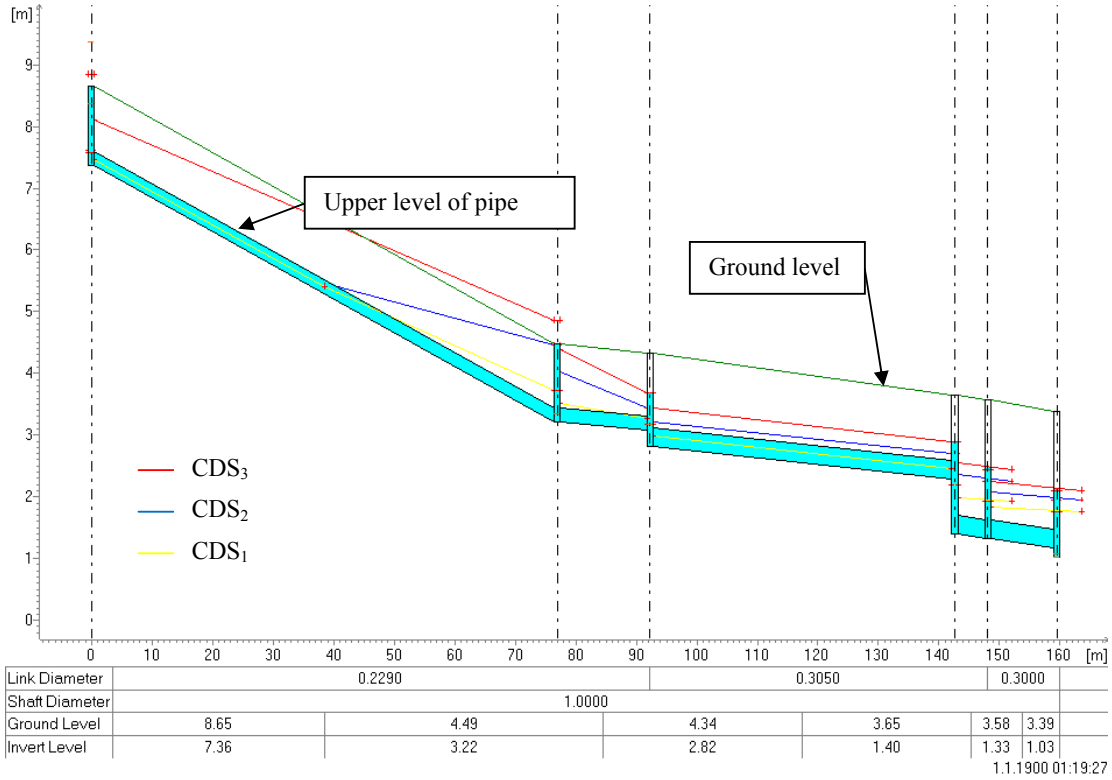

Figure 57: Weak section 3 - Vesturgata

4 Conclusions

The objectives of this study were twofold; firstly to investigate changes in short duration extreme precipitation in Reykjavík, and secondly to analyse impacts of precipitation changes on wastewater systems in Reykjavík and its design requirements.

Analyzes of precipitation changes showed mixed results. Robust statistical tests showed that no long term trends could be detected in the data in the past 60 years, but decadal to multi-decadal oscillations were observed which may hinder the detection of long-term trends. A positive significant trend of 0.12mm/decade or 0.072 mm/h/year, was found in August (10 minutes duration) and a negative trend of -0.08 mm/decade or -0.048mm/h/year was found in November. The trend magnitude in August is comparable to the 0.08 mm/h/year trend that Adamowski et al. (2009) found in Northern Ontario.

Extreme values are more challenging to describe and predict than average values. The possible connections identified to temperature and total precipitation may therefore be a stepping stone into better understanding short duration precipitation by exploring further these connections.

For practical purposes an interesting outcome is the updated 1M5 program, which now, using the updated data, gives up to 16% higher outcomes than before. As Table 16 shows, this is not due to changes in the climate, but due to re-extraction of the data. This shows the importance of taking good care of data, and for a country that has so few high resolution precipitation gauges this is even more important.

Flooding in downtown Reykjavík was analysed using two types of rainfall data (IMO and CDS) each with three scenarios and four indicators. CDS with precipitation intensity from the current design method in Reykjavík, the 1M5 method developed by Elíasson and Thordarson (1996b), showed that 20% of pipes are full or under pressure, and that surface floods are seen at 19 manholes. Using the updated 1M5 method the indicators increase by around 40%. To see the effects of the 1M5 method update even clearer, the 11 year IMO series was scaled down by 16%. The simulation with that downscaled time series showed no surface flooding, while the actual original series showed surface floods at 12 manholes.

It may not be possible to make any general assumptions about flooding in other areas in Reykjavík, if their capacity is as full as this old system, but at least it can be seen that for systems that are sensitive to precipitation with duration of 10 minutes, the increase in design intensity due to the updated 1M5 method greatly influences the capacity of the system.

The CDS analysed were with a return period of 5 years. Within the 11 year IMO series there are 2 events with a return period equal or greater to 5 years. Despite that many more manholes were flooded in the CDS analysis than the IMO analysis, which suggests that the 1M5 method coupled with Chicago Design Storms, is a conservative method.

Three sensitive areas were especially analysed, by Tjarnargata, Vesturgata and Hringbraut, where it was seen that problems arose and escalated. Issues found were for examples pipes connected to narrower downstream pipes, equal size pipes but decreased slope, or simply insufficient pipe capacity.

Increased densification as planned by the city, could multiply the problems in the area. For example it was found that if the density increases by 10%, the number of flooded manholes would increase by 35%, and if the increase were 20%, the number would increase by 73% and volume of surface water would increase by 93%.

The 20% precipitation increase that has been used as a hypothetical future, for illustrative purposes to highlight system weaknesses, based on a trend found only in August, may be an unlikely possibility. With a higher temporal and spatial resolution of climate models, it may in the future become feasible to carry out a study like this on actual future projection data. Precipitation intensity is not the only variable important for storm water systems that is subject to change due to climate change. Changes in precipitation patterns and frequency, temperature and more frequent melting periods could have just as big impacts.

References

Adamowski, J., Adamowski, K., & Bougadis, J. (2009). Influence of Trend on Short Duration Storms. *Water Resources Management* .

Alfnes, E., & Førland, E. J. (2006). *Trends in extreme precipitation and return values in Norway 1900 - 2004.* Norwegian Meteorological Institute.

Arisz, H., & Burell, B. C. (2006). Urban drainage infrastructure planning and design considering climate change. *EIC Climate Change Technology* (pp. 1-9). IEEE .

Arnbjerg-Nielsen, K. (2006). Significant climate change of extreme rainfall in Denmark. *Water Science and Technology , 54* (6-7), 1-8.

Ashley, R. M., Balmforth, D., Saul, A., & Blanskby, J. (2005). Flooding in the future - predicting climate change, risks and responses in urban areas. *Water Science and Technology , 52* (5), 265-273.

Bates, B., Kundzewicz, Z. W., Wu, S., & Palutikof, J. (Eds.). (2008). *Climate Change and Water. Technical Paper of the Intergovernmental Panel on Climate Change.* Geneva: IPCC Secretariat.

Berggren, K. (2007). *Urban Drainage and Climate Change - Impact Assessment.* Licentiate Thesis, Luleå University of Technology.

Berggren, K., Olofsson, M., Viklander, M., & Svensson, G. (2007). Tools for measuring climate change impacts on urban drainage systems. *Sustainable techniques and strategies in urban water management : Novatech 2007* (pp. 239-246). Lyon: Graie.

Bergþórsson, P. (1977). Aftaka úrkoma á Íslandi. *Veðrið , 2*.

Björnsson, H., Sveinbjörnsdóttir, Á. E., Daníelsdóttir, A. K., Snorrason, Á., Sigurðsson, B. D., Sveinbjörnsson, E., et al. (2008). *Hnattrænar loftslagsbreytingar og áhrif þeirra á Íslandi – Skýrsla vísindanefndar um loftslagsbreytingar.* Umhverfisráðuneytið.

Bonaccorso, B., Canceliere, A., & Rossi, G. (2005). Detecting trends of extreme rainfall series in Sicily. *Advances in Geosciences , 2*, 7-11.

Christensen, J. H., Carter, T. R., Rummukainen, M., & Amanatidis, G. (2007). Evaluating the performance and utility of regional climate models: the PRUDENCE project. *Climatic Change , 81* (1-6).

Christensen, J. H., Hewitson, B., Busuioc, A., Chen, A., Gao, X., Held, I., et al. (2007). Regional Climate Projections. In S. Solomon, D. Qin, M. Manning, Z. Chen, M. Marquis, K. Averyt, et al. (Eds.), *Climate Change 2007: The Physical Science Basis. Contribution of Working Group I to the Fourth Assessment Report of the Intergovernmental Panel on Climate Change.* Cambridge University Press.

Crochet, P. (2007). A Study of Regional Precipitation Trends in Iceland Using a High Quality Gauge Network and ERA 40. *Journal of Climate , 20*, 4659-4677.

Cunge, J. A., & Wegner, M. (1964). Integration numeriques des equations d'ecoulement de Barre de Saint-Venant par un schema implicite de differences finies: Application au cas d'une galerie tantot en charge, tantot a surface libre. *La Houille Blance , 1*, 33-39.

DANVA. (2007). *En kogbog for analyser af klimaændringers effekter på afløbssystemer - med fokus på oversvømmelser.*

Denault, C., Millar, R. G., & Lence, B. J. (2006, June). Assessment of possible impacts of climate change in an urban catchment. *Journal of the American Water Resources Association* , 685-697.

DHI. (2008). *MOUSE Pipe flow: Reference manual.* Mike by DHI.

DHI. (2008). *MOUSE: Runoff reference manual.* MIKE by DHI.

Elíasson, D. J. (2009, October). UOOR Meeting.

Elíasson, J., & Thordarson, S. (1996a). *Útreikningar á skúrum.* Reykjavík: Verkfræðistofnun Háskóla Íslands - Vatnaverkfræðistofa.

Elíasson, J., & Thordarson, S. (1996b). *Vatnafræðilegar forsendur fráveituhönnunar.* Reykjavík: Verkfræðistofnun Háskóla Íslands - Vatnaverkfræðistofa.

Førland, E. J., Alexandersson, H., Drebs, A., Hanssen-Bauer, I., Vedin, H., & Tveita, O. E. (1998). *Trends in maximum 1-day precipitation in the Nordic region.* DNMI - Det norske meteorologiske institutt.

Grum, M., Jørgensen, A., Johansen, R. M., & Linde, J. (2006). The effect of climate change on urban drainage: an evaluation based on regional climate model simulation. *Water Science and Technology , 54* (6-7), 9-15.

Guðmundsdóttir, A. L., & Gylfadóttir, H. M. (2007). *Lækurinn, fyrr og nú.* Reykjavík: Minjasafn Reykjavíkur.

Hanna, E., Jónsson, T., & Box, J. E. (2004). An analysis of Icelandic climate since the nineteenth century. *Internationl Journal of Climatology , 24*, 1193-1210.

Hay, L. E., Wilby, R. L., & Leavesley, G. H. (2000). A comparison of the delta change and downscaled GCM scenarios for three mountainous basins in the United States. *Journal of the American Water Resources Association , 36* (2), 387-397.

Helsel, D., & Hirsch, R. (2002). Statistical Methods in Water Resources. In *Hydrologic Analysis and Interpretation.* U.S. Geological Survey.

Hjartarson, Á. (2010). *Básendar - Básendaflóð*. Retrieved 8 20, 2010, from ÍSOR: http://isor.is/efni/1-basendar-basendaflod

Hrafnsdóttir, H. (2005). *Úrvinnsla regngagna úr veðurstöðvum við Staldrið og Breiðholtslaug - Hönnunargildi fyrir settjarnir.* Reykjavík: Almenna verkfræðistofan.

IPCC. (2007). *Climate Change 2007: The Physical Science Basis. Contribution of Working Group I to the Fourth Assessment.* (S. Solomon, D. Qin, M. Manning, M. Marquis, K. Averyt, M. M. Tignor, et al., Eds.) Cambridge University Press.

Jónas Elíasson og Sigvaldi Thordarson. (1996). *Vatnafræðilegar forsendur fráveituhönnunar.* Reykjavík: Verkfræðistofnun - Vatnaverkfræðistofa.

Jónsdóttir, J. F. (2006). Afrennsliskort og mat á áhrifum veðurfarsbreytinga á vatnafar. *Orkuþing 2006: Orkan og samfélagið - vistvæn lífsgæði*, (pp. 209-217). Reykjavík.

Jónsdóttir, J. F., Jónsson, P., & Uvo, C. B. (2006). Trend analysis of Icelandic discharge, precipitation and temperature series. *Nordic Hydrology , 37* (4-5), 365-376.

Jónsdóttir, J. F., Uvo, C. B., & Clarke, R. T. (2008). Trend analysis in Icelandic discharge, temperature and precipitation series by parametric methods. *Hydrology Research , 39* (5-6), 425-436.

Karl, T. R., & Knight, R. W. (1998). Secular Trends of Precipitation Amount, Frequency, and Inensity in the United States. *Bulletin of the American Meteorological Society , 79* (2), 231-241.

Keifer, C. J., & Chu, H. H. (1957). Synthetic Storm Pattern for Drainage Design. *Journal of the Hydraulics Division of the American Society of Civil Engineers* .

Kloakforsyningen. (2004). Kapitel 8: Planlægning. In *Projecthåndbog for kloakker.* Aalborg: Aalborg Kommune.

Kundzeqicz et al., Z. (2005). Summer floods in central Europe - Climate change track? *Natural Hazards , 36*, 165-189.

Kunkel, K. E. (2003). North American Trends in Extreme Precipitation. *Natural Hazards , 29*, 291-305.

Kyselý, J. (2008). Trends in heavy precipitation in the Czech Republic over 1961 - 2005. *International journal of climatology* .

Lane, S. N. (2008). Climate change and the summer 2007 floods in the UK. *Geography , 93* (2), 91-98.

Lupikasza, E. (2009). Spatial and temporal variability of extreme precipitation in Poland in the period 1951-2006. *International Journal of climatology* .

Morgunblaðið. (1991, August 18). Úrkomumet í úrfellinu á föstudagskvöldið: Milljónatjón í vatnsflóðinu. *Morgunblaðið* , p. 2.

Nakićenović, N., & Swart, E. R. (2000). *Special Report on Emissions Scenarios.* Cambridge University Press.

Ólafsson, M. *City scape, Hafnarstræti, seen from east to west.* Reykjavík Museum of Photography, Reykjavík.

Ólafsson, M. *Lækurinn og Lækjargata, Lækjargata 2-14.* Reykjavík Museum of Photography, Reykjavík.

Olofsson, M., Berggren, K., Viklander, M., & Svensson, G. (2007). *Hydraulic impact on urban drainage systems due to climate change.* Luleå: Division of Architecture and Infrastructure.

Olsson, J., Berggren, K., Olofsson, M., & Viklander, M. (2009). Applying climate model precipitation scenarios for urban hydrological assessment: A case study in Kalmar City, Sweden. *Atmospheric Research , 92* (3), 364-375.

Olsson, J., Olofsson, M., Berggren, K., & Viklander, M. (2006). Adaption of RCA3 Climate Model Data for the specific needs of urban hydrology simulations. *Extreme precipitation, Multisource Data Measurement and Uncertainty.*

Orkuveita Reykjavíkur. (2009). *Almennar hönnunarforsendur veitukerfa OR.* Orkuveita Reykjavíkur.

Orkuveita Reykjavíkur. (2007). *Fráveita - Fullkomið kerfi sem verndar umhverfið og náttúruna.*

Orkuveita Reykjavíkur. (2008). *Leiðbeiningar um hönnunarrennsli skólps og ofanvatns.* Reykjavík: Orkuveita Reykjavíkur.

Osborn, T. J., Hulme, M., Jones, P. D., & Basnett, T. A. (2000). Observed trends in the daily intensity of United Kingdom Precipitation. *International Journal of Climatology , 20*, 347-364.

Pagliara, S., Viti, C., B. Gozzini, F. M., & Crisci, A. (1998). Uncertainties and trends in extreme rainfall series in Tuscany, Italy: Effects on urban drainage networks design. *Water Science Technology , 37* (11), 195-202.

Peng, H., Wang, S., & Wang, X. (2008). Consistency and asymptotic distribution of the Theil-Sen estimator. *Journal of Statistical Planning and Inference , 138* (6).

Plósz, B. G., Liltved, H., & Ratnaweera, H. (2006). Climate Change Factors Influencing Wastewater Treatment In Oslo, Norway – A Case Study On Winter Operation. *10th Nordic/NORDIWA Wastewater Conference.*

Ponce, V. M. (1989). *Engineering Hydrology. Principles and Practices.* Prentice Hall.

Semadeni-Davies, A., Hernebring, C., Svensson, G., & Gustafsson, L.-G. (2008). The impacts of climate change and urbanisation on drainage in Helsingborg, Sweden: Combined Sewer system. *Journal of Hydrology* , 100-113.

Shaw, H., Reisinger, A., Larsen, H., & Stumbles, C. (2005). *Incorporating climate change into stormwater design - why and how?* Ministry for the Environment.

Sjóvá. (2010). Skýfalls og asahlákutjón. Reykjavík.

Skipulags- og byggingarsvið. (2008). *Aðalskipulag Reykjavíkur 2001-2024: Greinargerð I.* Reykjavíkurborg.

Spildevandskomiteens Regnudvalg. (2008). *Regneark til bestemmelse af Regnkurver, CDS regn og bassinvoluminer.* DHI.

STARDEX. (2005). *STARDEX Final Report: Downscaling climatic extremes.*

Straub, T. D., Melching, C. S., & Kocher, K. E. (2000). *Equations for Estimating Clark Unit-Hydrograph Parameters for Small Rural Watersheds in Illinois.* Urbana: U.S. Department of the Interior and U.S. Geological Survey.

Svenskt Vatten. (2007). *Klimatförändringarnas inverkan på allmänna avloppssystem.*

Tómasson, K. H. (2010, June 9). Interview at Ingólfsstræti pumping station. Reykjavík.

Trenberth, K. E. (1999). Conceptual framework for changes of extremes of the hydrological cycle with climate change. *Climatic Change , 42*, 327-339.

Trenberth, K.E., Jones, P., Ambenje, P., Bojariu, R., Easterling, D., et al. (2007). Observations: Surface and Atmospheric Climate Change. In Solomon, S., D. Qin, M. Manning, Z. Chen, M. Marquis, et al. (Eds.), *Climate Change 2007: The Physical Science Basis. Contribution of Working Group I to the Fourth Assessment Report of the Intergovernmental Panel on Climate Change.* Cambridge University Press.

Ulbrich et al., U. (2003). The central Europen floods of August 2002. Part I: Rainfall periods and flood development. *Weather , 58*, 371-377.

Vaes, G., Willems, P., & Berlamont, J. (2002). 100 years of Belgian rainfall: are there trends? *Water Science and Technology , 45* (2), 55-61.

Vatnaskil. (1995). *Úrvinnsla regnmælinga í Breiðholti.* . Gatnamálastjórinn í Reykjavík.

Wang, W., Chen, X., Shi, P., & Gelder, P. H. (2008). Detecting changes in extreme precipitation and extreme streamflow in the Dongjiang River Basin in Southern China. *Hydrology and Earth System Sciences , 12*, 207-221.

Waters, D., W. Edgar Watt, J. M., & Andersson, B. C. (2003). Adaption of a Storm Drainage System to Accommodate Increased Rainfall Resulting from Climate Change. *Journal of Environmental Planning and Management , 46* (5), 755-770.

Wilby, R. L., & Wigley, T. M. (1997). Downscaling general circulation model output: a review of methods and limitations. *Progress in Physical Geography , 21* (4), 530-548.

Wilcox, R. R. (2009). *Basic statistics: Understanding conventional methods and modern insights.* Oxford University Press.

Wilcox, R. R. (2010). *Fundamentals of Modern Statistical Methods: Substantially Improving Power and Accuracy.* Springer.

Zhang, X., Hogg, W. D., & Mekis, É. (2001). Spatial and Temporal Characteristics of Heavy Precipitation Events over Canada. *Journal of Climate , 14*, 1923-1936.

Zolina, O., Simmer, C., Kapala, A., Bachner, S., Gulev, S., & Maechel, H. (2008). Seasonally dependent changes of precipitation extremes over Germany since 1950 from a very dense obervational network. *Journal of Geophisical research , 113*.

Annex I: Connection to other atmospheric variables

Table 27: MW and KS tests comparing extreme events in months with lower temperature in Reykjavík (S1) with months (years) with higher temperature (S2)

		January	February	March	April	May	June	July	August	September	October	November	December	Annual
10 minutes	S1	-2,0 °C 1,2mm	-1,3 °C 1,0mm	-0,7 °C 0,8mm	2,0 °C 0,9mm	5,7 °C 0,9mm	8,6 °C 1,1mm	10,3 °C 1,2mm	10,0 °C 1,4mm	6,9 °C 1,4mm	3,6 °C 1,3mm	0,4 °C 1,1mm	-1,1 °C 1,1mm	-1,1 °C 2,4mm
	S2	1,3 °C 1,3mm	1,6 °C 1,3mm	2,3 °C 1,3mm	4,3 °C 1,0mm	7,3 °C 0,9mm	10,0 °C 1,4mm	11,6 °C 1,3mm	11,1 °C 1,7mm	9,0 °C 1,6mm	5,5 °C 1,4mm	3,1 °C 1,2mm	1,5 °C 1,4mm	1,5 °C 2,6mm
	MW	0,2484	0,1280	0,0079	0,8597	0,7047	0,2615	0,2801	0,2003	0,2677	0,4472	0,1204	0,0133	0,8517
	KS	0,2698	0,1687	0,0094	0,9989	0,9950	0,3213	0,2400	0,6371	0,7198	0,9066	0,1844	0,0291	0,9270
20 minutes	S1	-2,0 °C 1,8mm	-1,3 °C 1,4mm	-0,7 °C 1,4mm	2,0 °C 1,4mm	5,7 °C 1,4mm	8,6 °C 1,7mm	10,3 °C 2,0mm	10,0 °C 1,9mm	6,9 °C 2,1mm	3,6 °C 2,0mm	0,4 °C 1,7mm	-1,1 °C 1,8mm	-1,1 °C 3,5mm
	S2	1,3 °C 1,9mm	1,6 °C 1,9mm	2,3 °C 2,0mm	4,3 °C 1,6mm	7,3 °C 1,4mm	10,0 °C 2,1mm	11,6 °C 2,0mm	11,1 °C 2,7mm	9,0 °C 2,5mm	5,5 °C 2,1mm	3,1 °C 2,0mm	1,5 °C 2,2mm	1,5 °C 4,0mm
	MW	0,4472	0,0488	0,0085	0,5863	0,8433	0,1390	0,4102	0,0363	0,2343	0,5700	0,0720	0,0504	0,2555
	KS	0,6371	0,1687	0,0037	0,9556	1,0000	0,0980	0,2353	0,2085	0,3003	0,9784	0,2646	0,1048	0,3213
30 minutes	S1	-2,0 °C 2,3mm	-1,3 °C 1,8mm	-0,7 °C 1,8mm	2,0 °C 1,7mm	5,7 °C 1,9mm	8,6 °C 2,1mm	10,3 °C 2,5mm	10,0 °C 2,3mm	6,9 °C 2,7mm	3,6 °C 2,4mm	0,4 °C 2,1mm	-1,1 °C 2,4mm	-1,1 °C 4,4mm
	S2	1,3 °C 2,6mm	1,6 °C 2,4mm	2,3 °C 2,5mm	4,3 °C 2,0mm	7,3 °C 1,8mm	10,0 °C 2,7mm	11,6 °C 2,6mm	11,1 °C 3,3mm	9,0 °C 3,2mm	5,5 °C 2,7mm	3,1 °C 2,6mm	1,5 °C 2,8mm	1,5 °C 4,9mm
	MW	0,2668	0,0603	0,0084	0,3284	0,5877	0,1542	0,6953	0,0871	0,2862	0,3139	0,0232	0,0924	0,3961
	KS	0,4080	0,0876	0,0094	0,7959	0,9168	0,0483	0,4149	0,2001	0,7198	0,4574	0,1388	0,4515	0,3213
60 minutes	S1	-2,0 °C 3,4mm	-1,3 °C 3,0mm	-0,7 °C 2,8mm	2,0 °C 2,5mm	5,7 °C 2,8mm	8,6 °C 3,0mm	10,3 °C 3,4mm	10,0 °C 3,3mm	6,9 °C 3,9mm	3,6 °C 3,7mm	0,4 °C 3,1mm	-1,1 °C 3,7mm	-1,1 °C 6,6mm
	S2	1,3 °C 4,0mm	1,6 °C 3,7mm	2,3 °C 3,9mm	4,3 °C 3,1mm	7,3 °C 2,8mm	10,0 °C 4,0mm	11,6 °C 3,9mm	11,1 °C 4,8mm	9,0 °C 4,6mm	5,5 °C 4,2mm	3,1 °C 4,1mm	1,5 °C 4,1mm	1,5 °C 7,0mm
	MW	0,0983	0,0851	0,0035	0,3297	0,6755	0,0661	0,3884	0,0119	0,1422	0,1313	0,0056	0,2542	0,9071
	KS	0,0648	0,1687	0,0094	0,4430	0,4903	0,0980	0,6290	0,0128	0,0876	0,0158	0,0308	0,1252	0,9270

Table 28: MW and KS tests comparing extreme events in months with lower average temperature on wet days in Reykjavík (S1) with months (years) with higher average temperature on wet days (S2)

		January	February	March	April	May	June	July	August	September	October	November	December	Annual
10 minutes	S1	-0,9 °C 1,2mm	-0,5 °C 1,1mm	-0,2 °C 0,9mm	2,5 °C 0,9mm	5,9 °C 0,9mm	8,6 °C 1,1mm	10,2 °C 1,1mm	10,0 °C 1,4mm	7,3 °C 1,4mm	4,1 °C 1,3mm	1,3 °C 1,1mm	-0,2 °C 1,1mm	-0,2 °C 2,4mm
	S2	2,2 °C 1,2mm	2,3 °C 1,1mm	2,8 °C 1,2mm	4,7 °C 1,0mm	7,5 °C 0,9mm	9,9 °C 1,4mm	11,5 °C 1,3mm	11,2 °C 1,7mm	9,2 °C 1,7mm	6,2 °C 1,3mm	3,8 °C 1,2mm	2,3 °C 1,3mm	2,3 °C 2,6mm
	MW	0,6136	0,5104	0,1800	0,6880	0,7731	0,3182	0,0719	0,1224	0,1416	0,5484	0,3992	0,0480	0,9193
	KS	0,9876	0,9168	0,1844	0,7884	0,9168	0,7406	0,2400	0,2497	0,4903	0,7732	0,5141	0,2011	0,7406
20 minutes	S1	-0,9 °C 1,8mm	-0,5 °C 1,6mm	-0,2 °C 1,6mm	2,5 °C 1,4mm	5,9 °C 1,5mm	8,6 °C 1,7mm	10,2 °C 1,9mm	10,0 °C 1,9mm	7,3 °C 2,1mm	4,1 °C 2,0mm	1,3 °C 1,7mm	-0,2 °C 1,8mm	-0,2 °C 3,5mm
	S2	2,2 °C 1,9mm	2,3 °C 1,7mm	2,8 °C 1,8mm	4,7 °C 1,6mm	7,5 °C 1,4mm	9,9 °C 2,1mm	11,5 °C 2,1mm	11,2 °C 2,7mm	9,2 °C 2,5mm	6,2 °C 2,1mm	3,8 °C 1,9mm	2,3 °C 2,2mm	2,3 °C 4,0mm
	MW	0,5700	0,3049	0,2184	0,6773	0,3606	0,2588	0,0901	0,0113	0,1191	0,4715	0,2152	0,0439	0,2555
	KS	0,8779	0,4903	0,0980	0,9556	0,1687	0,3213	0,1328	0,0699	0,0876	0,5724	0,6371	0,0576	0,3213
30 minutes	S1	-0,9 °C 2,3mm	-0,5 °C 2,1mm	-0,2 °C 2,1mm	2,5 °C 1,7mm	5,9 °C 1,9mm	8,6 °C 2,1mm	10,2 °C 2,4mm	10,0 °C 2,3mm	7,3 °C 2,6mm	4,1 °C 2,4mm	1,3 °C 2,2mm	-0,2 °C 2,3mm	-0,2 °C 4,4mm
	S2	2,2 °C 2,5mm	2,3 °C 2,2mm	2,8 °C 2,3mm	4,7 °C 2,0mm	7,5 °C 1,7mm	9,9 °C 2,7mm	11,5 °C 2,7mm	11,2 °C 3,4mm	9,2 °C 3,2mm	6,2 °C 2,7mm	3,8 °C 2,5mm	2,3 °C 2,8mm	2,3 °C 4,9mm
	MW	0,4197	0,4907	0,2651	0,4324	0,1676	0,2589	0,2244	0,0247	0,0926	0,1548	0,0995	0,0549	0,3961
	KS	0,8179	0,9168	0,5141	0,7102	0,1687	0,0980	0,1420	0,1080	0,3003	0,1080	0,2497	0,3003	0,3213
60 minutes	S1	-0,9 °C 3,5mm	-0,5 °C 3,2mm	-0,2 °C 3,1mm	2,5 °C 2,5mm	5,9 °C 3,0mm	8,6 °C 3,1mm	10,2 °C 3,3mm	10,0 °C 3,3mm	7,3 °C 3,6mm	4,1 °C 3,7mm	1,3 °C 3,2mm	-0,2 °C 3,6mm	-0,2 °C 6,6mm
	S2	2,2 °C 3,9mm	2,3 °C 3,5mm	2,8 °C 3,5mm	4,7 °C 3,1mm	7,5 °C 2,5mm	9,9 °C 3,9mm	11,5 °C 3,9mm	11,2 °C 4,9mm	9,2 °C 4,8mm	6,2 °C 4,2mm	3,8 °C 3,9mm	2,3 °C 4,2mm	2,3 °C 7,0mm
	MW	0,1903	0,4029	0,1414	0,3257	0,1462	0,1634	0,1720	0,0036	0,0133	0,0711	0,0522	0,1561	0,9690
	KS	0,4358	0,4903	0,1844	0,4218	0,3003	0,3213	0,4218	0,0128	0,0187	0,0044	0,1420	0,0876	0,9270

Table 29: MW and KS tests comparing extreme events from 1986-2008 on cold days (S1) to those on warm days (S2)

		January	February	March	April	May	June	July	August	September	October	November	December	Annual
10 minutes	S1	-0,3 °C 0,9mm	1,8 °C 1,1mm	0,8 °C 1,2mm	1,3 °C 0,8mm	5,3 °C 1,0mm	8,2 °C 1,0mm	9,7 °C 1,2mm	10,0 °C 1,5mm	6,0 °C 1,4mm	4,8 °C 1,3mm	2,4 °C 1,0mm	1,4 °C 1,1mm	1,4 °C 2,2mm
	S2	3,8 °C 1,3mm	4,6 °C 1,2mm	4,0 °C 1,0mm	5,1 °C 0,9mm	8,0 °C 1,0mm	10,6 °C 1,3mm	12,2 °C 1,4mm	11,8 °C 2,2mm	10,1 °C 1,5mm	8,2 °C 1,5mm	6,4 °C 1,1mm	4,9 °C 1,3mm	4,9 °C 2,8mm
	MW	0,0184	0,6198	0,5997	0,4571	0,9505	0,7566	0,1295	0,3081	0,9016	0,6208	0,8011	0,3354	0,3877
	KS	0,1006	0,9094	0,8067	0,9094	0,8870	0,9933	0,2604	0,5833	0,9293	0,8870	1,0000	0,8353	0,5199
20 minutes	S1	-0,3 °C 1,5mm	1,8 °C 1,7mm	0,8 °C 1,8mm	1,3 °C 1,3mm	5,3 °C 1,5mm	8,2 °C 1,7mm	9,7 °C 1,8mm	10,0 °C 2,2mm	6,0 °C 2,2mm	4,8 °C 1,8mm	2,4 °C 1,6mm	1,4 °C 2,0mm	1,4 °C 3,4mm
	S2	3,8 °C 2,0mm	4,6 °C 1,7mm	4,0 °C 1,6mm	5,1 °C 1,5mm	8,0 °C 1,6mm	10,6 °C 2,1mm	12,2 °C 2,1mm	11,8 °C 3,4mm	10,1 °C 2,3mm	8,2 °C 2,2mm	6,4 °C 1,8mm	4,9 °C 2,1mm	4,9 °C 4,1mm
	MW	0,0147	0,5577	0,5997	0,8289	0,7100	0,4573	0,0828	0,0601	0,9509	0,4040	0,8289	0,7811	0,4971
	KS	0,0067	0,6157	0,9727	0,9818	0,8067	0,8622	0,0361	0,0258	0,5833	0,4595	0,8353	0,9610	0,5833
30 minutes	S1	-0,3 °C 2,0mm	1,8 °C 2,4mm	0,8 °C 2,4mm	1,3 °C 1,7mm	5,3 °C 2,0mm	8,2 °C 2,0mm	9,7 °C 2,2mm	10,0 °C 2,7mm	6,0 °C 2,8mm	4,8 °C 2,3mm	2,4 °C 2,2mm	1,4 °C 2,7mm	1,4 °C 4,3mm
	S2	3,8 °C 2,9mm	4,6 °C 2,2mm	4,0 °C 2,1mm	5,1 °C 1,9mm	8,0 °C 2,1mm	10,6 °C 2,6mm	12,2 °C 2,7mm	11,8 °C 4,2mm	10,1 °C 3,0mm	8,2 °C 2,9mm	6,4 °C 2,4mm	4,9 °C 2,8mm	4,9 °C 5,3mm
	MW	0,0363	0,6216	0,5576	0,8527	0,6657	0,4218	0,0598	0,0899	0,8291	0,2533	0,9017	0,7811	0,4406
	KS	0,0258	0,6157	0,9610	0,9727	0,8067	0,8622	0,0403	0,0258	0,9818	0,4595	0,9999	0,9992	0,9727
60 minutes	S1	-0,3 °C 3,3mm	1,8 °C 3,8mm	0,8 °C 3,9mm	1,3 °C 2,6mm	5,3 °C 3,2mm	8,2 °C 2,8mm	9,7 °C 3,2mm	10,0 °C 4,1mm	6,0 °C 4,0mm	4,8 °C 3,4mm	2,4 °C 3,6mm	1,4 °C 4,0mm	1,4 °C 6,7mm
	S2	3,8 °C 4,6mm	4,6 °C 3,7mm	4,0 °C 3,3mm	5,1 °C 2,8mm	8,0 °C 3,4mm	10,6 °C 3,8mm	12,2 °C 3,7mm	11,8 °C 5,6mm	10,1 °C 4,2mm	8,2 °C 4,6mm	6,4 °C 3,7mm	4,9 °C 4,0mm	4,9 °C 7,2mm
	MW	0,1308	0,6222	0,8051	0,8775	0,6437	0,1156	0,1851	0,4598	0,7579	0,0640	1,0000	0,6664	0,7347
	KS	0,0915	0,6157	0,6811	0,9293	0,6157	0,2604	0,2812	0,0752	0,9465	0,3032	0,9465	0,8622	0,4892

Table 30: MW and KS tests comparing extreme events in months with lowest total amount (S1) of precipitation with months (years) the highest total precipitation (S2).

		January	February	March	April	May	June	July	August	September	October	November	December	Annual
10 minutes	S1	52mm 1,1mm	49mm 0,9mm	46mm 0,9mm	35mm 0,8mm	25mm 0,7mm	29mm 1,3mm	35mm 1,2mm	37mm 1,4mm	44mm 1,2mm	56mm 1,2mm	51mm 0,9mm	56mm 1,1mm	56mm 2,5mm
	S2	104mm 1,3mm	110mm 1,3mm	110mm 1,2mm	77mm 1,1mm	68mm 1,0mm	63mm 1,2mm	67mm 1,3mm	86mm 1,8mm	96mm 1,8mm	115mm 1,5mm	109mm 1,3mm	117mm 1,4mm	117mm 2,5mm
	MW	0,0096	0,0053	0,0178	0,0065	0,0009	0,4541	0,2627	0,0928	0,0013	0,0125	0,0047	0,0080	0,8823
	KS	0,0308	0,0916	0,0980	0,0043	0,0079	0,5141	0,9314	0,2001	0,0029	0,0616	0,0483	0,0114	0,9270
20 minutes	S1	52mm 1,6mm	49mm 1,4mm	46mm 1,4mm	35mm 1,3mm	25mm 1,2mm	29mm 1,9mm	35mm 1,8mm	37mm 2,1mm	44mm 1,8mm	56mm 1,8mm	51mm 1,5mm	56mm 1,8mm	56mm 3,8mm
	S2	104mm 2,1mm	110mm 1,9mm	110mm 2,0mm	77mm 1,7mm	68mm 1,6mm	63mm 2,0mm	67mm 2,3mm	86mm 2,5mm	96mm 2,8mm	115mm 2,2mm	109mm 2,2mm	117mm 2,2mm	117mm 3,7mm
	MW	0,0058	0,0106	0,0015	0,0600	0,0064	0,2335	0,0520	0,2246	0,0003	0,0054	0,0004	0,0083	0,1519
	KS	0,0140	0,0830	0,0014	0,0585	0,0534	0,0483	0,4358	0,3556	0,0010	0,0050	0,0047	0,0017	0,0980
30 minutes	S1	52mm 2,1mm	49mm 1,8mm	46mm 1,8mm	35mm 1,6mm	25mm 1,6mm	29mm 2,3mm	35mm 2,2mm	37mm 2,6mm	44mm 2,3mm	56mm 2,2mm	51mm 2,0mm	56mm 2,3mm	56mm 4,6mm
	S2	104mm 2,8mm	110mm 2,5mm	110mm 2,6mm	77mm 2,1mm	68mm 2,0mm	63mm 2,6mm	67mm 3,0mm	86mm 3,1mm	96mm 3,6mm	115mm 2,9mm	109mm 2,8mm	117mm 2,9mm	117mm 4,8mm
	MW	0,0053	0,0120	0,0007	0,0305	0,0175	0,1329	0,0067	0,2734	0,0001	0,0004	0,0011	0,0129	0,9318
	KS	0,0052	0,0175	0,0005	0,1185	0,0830	0,1844	0,0153	0,3747	0,0001	0,0002	0,0153	0,0010	0,9961
60 minutes	S1	52mm 3,2mm	49mm 2,9mm	46mm 2,6mm	35mm 2,4mm	25mm 2,3mm	29mm 3,1mm	35mm 3,0mm	37mm 3,6mm	44mm 3,3mm	56mm 3,3mm	51mm 3,0mm	56mm 3,4mm	56mm 6,3mm
	S2	104mm 4,2mm	110mm 3,7mm	110mm 4,0mm	77mm 3,2mm	68mm 3,2mm	63mm 4,0mm	67mm 4,2mm	86mm 4,6mm	96mm 5,1mm	115mm 4,6mm	109mm 4,2mm	117mm 4,4mm	117mm 7,3mm
	MW	0,0114	0,0267	0,0003	0,0638	0,0029	0,0097	0,0041	0,0584	0,0006	0,0008	0,0014	0,0136	0,0324
	KS	0,0132	0,1719	0,0001	0,1158	0,0079	0,0037	0,0018	0,1132	0,0029	0,0021	0,0238	0,0187	0,0980